

NOVEL INTRAOCULAR DRUG DELIVERY SYSTEM
FOR THE PREVENTION OF POSTERIOR
CAPSULE OPACIFICATION

by

BRETT EDWIN THOMES

Presented to the Faculty of the Graduate School of
The University of Texas at Arlington in Partial Fulfillment
of the Requirements
for the Degree of

DOCTOR OF PHILOSOPHY

THE UNIVERSITY OF TEXAS AT ARLINGTON

December 2006

Copyright © by Brett E. Thomes 2006

All Rights Reserved

ACKNOWLEDGEMENTS

I would like thank the Lord for this opportunity to study under a great group of faculty and committee members. I would like to give my sincere thankfulness to my doctoral advisor, Dr. Liping Tang. I would also like to thank Dr. Robert Eberhart and Dr. Richard Timmons for their guidance and inspiration over the years. It was truly a blessing to be given the opportunity to work with each of you and learn from your experience and knowledge first hand.

I also want to thank my wife, Julie. She always encouraged and supported me in continuing my studies. She sacrificed for our family so that I could complete this research and I am forever grateful. I thank my whole family for being there for me and for helping out during those long hours of research.

I would like to acknowledge those who assisted in completing this work including Dr. Qun Peng, Dr. Zou Ling, and Pam Neill.

October 6, 2006

ABSTRACT

NOVEL INTRAOCULAR DRUG DELIVERY SYSTEM
FOR THE PREVENTION OF POSTERIOR
CAPSULE OPACIFICATION

Publication No. _____

Brett E. Thomes, Ph.D.

The University of Texas at Arlington, 2006

Supervising Professor: Liping Tang

Posterior capsule opacification (PCO) is a major complication associated with the implantation of intraocular lens (IOLs). Evidence suggests that PCO formation is caused by abnormal lens epithelial cell (LEC) migration/proliferation. We hypothesize that pharmacologic agents must target inflammatory cells in addition to LECs to inhibit PCO formation. To successfully target both inflammatory cells and LECs, a novel intraocular drug delivery system (DDS) was developed for implantation in the lens capsular bag. Such a system permits direct delivery of anti-inflammatory and anti-proliferative drugs in the lens capsule for extended periods of time resulting in reduced PCO formation.

A lubricious polyurethane coating was selected as the drug delivery platform for this study based on a series of tests including lubricity, adhesion, leachable, stability, toxicity, and biocompatibility testing. In vitro studies were used to identify specific drugs that were capable of inhibiting inflammatory cell activation, LEC migration, and/or LEC proliferation at low concentrations (<0.01 mg/mL), including diclofenac (DI), colchicine (COL), mitomycin-C (MMC), 5-fluorouracil (5-FU), RGD-peptide, dexamethasone, and heparin (HEP). Results also demonstrated that these drugs were released from the coating at minimum effective levels past 10 days by varying coating properties.

In vivo studies (New Zealand white rabbit) demonstrated that the intraocular DDS using single drug and drug combinations including DI, COL, and MMC reduced IOL-associated foreign body reactions. Histological analysis provided evidence that cell adhesion to the IOL was significantly reduced compared to the control IOL. Histology also showed the effects of various drugs on ocular tissue and verified that optimal concentrations for each drug exist. When concentrations were not optimal, cellular responses were uninhibited and other side effects occurred including chronic inflammation.

Within the scope of this study, DI, COL, and MMC demonstrated the ability to inhibit inflammation and LEC migration/proliferation at low concentrations in vitro and in a rabbit model. The intraocular DDS demonstrated that it was capable of releasing drugs for prolonged periods of time and effectively reduced IOL-associated foreign body reactions and subsequent PCO formation processes.

TABLE OF CONTENTS

ACKNOWLEDGEMENTS.....	iii
ABSTRACT	iv
LIST OF ILLUSTRATIONS.....	xi
LIST OF TABLES.....	xvi
Chapter	
1. INTRODUCTION	1
1.1 Mechanism of IOL-induced PCO Formation	3
1.1.1 The Potential Role of LECs in PCO Formation.....	4
1.1.2 The Role of Inflammatory Cells & Blood Components in PCO Formation	5
1.1.3 The Link between Fibrin Deposition & PCO Formation	6
1.2 Concepts for PCO Preventive Drug Delivery.....	8
1.2.1 IOL Coatings as a Drug Delivery Platform	11
1.2.2 Potential PCO Preventative Pharmacologic Agents	13
1.2.2.1 Pharmacologic Agents: Anti-Inflammatory	14
1.2.2.2 Pharmacologic Agents: LEC Programmed Death.....	18
1.2.2.3 Pharmacologic Agents: LEC Adhesion Blocker	19
1.2.2.4 Pharmacologic Agents: Integrin Blocker for LEC Migration.....	20
2. OVERVIEW OF SPECIFIC AIMS.....	22

3. AIM 1: LUBRICIOUS COATING DEVELOPMENT.....	24
3.1 Coating Lubricity Testing.....	29
3.1.1 Introduction.....	29
3.1.2 Experimental Design	29
3.1.3 Results.....	30
3.1.4 Conclusion – Select Coating for Drug Delivery Platform.....	32
3.2 Coating Adhesion Testing	33
3.2.1 Introduction.....	33
3.2.2 Experimental Design	33
3.2.3 Results.....	34
3.3 Extractable Test Method – Leachable Impurities from Coating	35
3.3.1 Introduction.....	35
3.3.2 Experimental Design	35
3.3.3 Results.....	36
3.4 Toxicity Testing – MEM Cytotoxicity Test Method.....	36
3.4.1 Introduction.....	36
3.4.2 Experimental Design	37
3.4.3 Results.....	38
3.5 Accelerated Aging - Coating Stability Test Method	39
3.5.1 Introduction.....	39
3.5.2 Experimental Design	39
3.5.3 Results.....	40

3.6 Biocompatibility Testing – Acute Intracutaneous Reactivity Test Method.....	40
3.6.1 Introduction.....	40
3.6.2 Experimental Design	40
3.6.3 Results.....	41
3.7 Overall Discussion – Physical Properties of Lubricious Coating.....	42
4. AIM 2: DETERMINE MOST EFFECTIVE PHARMACOLOGIC AGENTS.....	44
4.1 LEC Growth Inhibition Assay.....	46
4.1.1 Introduction.....	46
4.1.2 Experimental Design	46
4.1.3 Results.....	48
4.2 LEC Migration Assay	56
4.2.1 Introduction.....	56
4.2.2 Experimental Design	56
4.2.3 Results.....	57
4.3 Inflammatory Activity Assay	62
4.3.1 Introduction.....	62
4.3.2 Experimental Design	62
4.3.3 Results.....	63
4.4 Overall Discussion.....	65
5. AIM 3: OPTIMIZE COATING FOR DRUG LOADING & RELEASE.....	69
5.1 To establish spectrophotometric measurements of drug concentrations in vitro	72

5.1.1 Introduction.....	72
5.1.2 Experimental Design	72
5.1.3 Results.....	72
5.2 Maximize Drug Loading.....	79
5.2.1 Introduction.....	79
5.2.2 Experimental Design	80
5.2.3 Results.....	81
5.3 Optimize Coating to Improve Drug Loading & Release Properties.....	84
5.3.1 Introduction.....	84
5.3.2 Experimental Design	84
5.3.3 Results.....	87
5.3.3.1 Study #1: Varying PVP Content of Coating.	87
5.3.3.2 Study #2: Drug Release Optimization.	88
5.3.3.3 Study #3: Optimization of PVP Content in Coating.	90
5.3.3.4 Study #4: Determine Drug Release Properties for Each Drug.....	91
5.4 Overall Discussion on Drug Loading and Release.....	100
6. AIM 4: IN VIVO TESTING OF DRUG DELIVERY SYSTEM	100
6.1 Phase I – Animal Implantation of Multiple Drug System	106
6.1.1 Introduction.....	106
6.1.2 Experimental Design	106
6.1.2.1 Test Implants.....	106

6.1.2.2 Surgical Procedure	107
6.1.2.3 Histology	108
6.1.2.4 Surface Analysis.....	108
6.1.3 Results - Animal Study Phase I	109
6.2 Phase II – Animal Implantation of Diclofenac Drug System	121
6.2.1 Introduction.....	121
6.2.2 Experimental Design	121
6.2.3 Results - Animal Study Phase II.....	121
6.3 Phase III – Animal Implantation of Colchicine Drug System	127
6.3.1 Introduction.....	127
6.3.2 Experimental Design	127
6.3.3 Results - Animal Study Phase III.....	127
7. CONCLUSIONS AND PERSPECTIVE	134
Appendix	
A. DESIGNED EXPERIMENT #1 – 24 HOUR DRUG LOADING	137
B. DESIGNED EXPERIMENT #1 – 48 HOUR DRUG LOADING	139
C. DESIGNED EXPERIMENT #2 – DRUG RELEASE	141
REFERENCES	143
BIOGRAPHICAL INFORMATION.....	149

LIST OF ILLUSTRATIONS

Figure	Page
1.1 Schematic drawing of adult human lens.	2
1.2 Factors responsible for IOL-induced PCO formation.	3
1.3 Role of LECs in PCO formation.	4
1.4 PCO formation on PMMA IOL (A) and cibacron blue-coated (B) IOL after 8 weeks implantation in rabbits.....	7
1.5 LEC accumulation on PMMA and cibacron blue-coated IOLs after 8 weeks implantation in rabbits.....	8
1.6 Pharmacological diagrams to depict the concentrations of drugs delivered via multiple injections vs. controlled release device.....	10
2.1 Experimental design for developing a coating that incorporates therapeutic regimens to combat IOL-mediated PCO formation.....	23
3.1 Experimental design for developing lubricious coating on an IOL	28
3.2 Maximum forces for selected lubricious coatings required to deliver an IOL through a lens delivery system.....	31
3.3 Mean lens delivery forces for lubricious polyurethane coatings, aqueous based and organic solvent	32
3.4 Classification chart for rating coating adhesion strength.....	34
3.5 Tape test results for aqueous based PU/PVP coated lens.....	35

4.1	Experimental design for Aim 2.....	45
4.2	Percentage of LEC growth inhibition for various concentrations of MMC versus the saline control.....	48
4.3	Percentage of LEC growth inhibition for various concentrations of colchicine versus the saline control.....	49
4.4	Percentage of LEC growth inhibition for various concentrations of 5-fluorouracil.....	50
4.5	Percentage of LEC growth inhibition for various concentrations of EDTA.....	51
4.6	Percentage of LEC growth inhibition for various concentrations of RGD-peptide.....	52
4.7	Percentage of LEC growth inhibition for various concentrations of dexamethasone.....	53
4.8	Percentage of LEC growth inhibition for various concentrations of diclofenac.....	54
4.9	Percentage of LEC growth inhibition for various concentrations of heparin.....	55
4.10	The percentage of LEC confluency following the treatment of various concentration of EDTA after 14 days.....	58
4.11	The percentage of LEC confluency following the treatment of various concentration of RGD-peptide after 14 days.....	59
4.12	The percentage of LEC confluency following the treatment of various concentration of heparin after 14 days.....	60
4.13	The percentage of LEC confluency following the treatment of various concentration of 5-FU after 14 days.....	61
4.14	Inflammatory cell responses to pharmacologic agents.....	64
5.1	Drug loading methods to incorporate drugs into the lens hydrogel coating.....	70
5.2	Flow chart of experimental design sequence for Aim 3.....	71

5.3	Molecular structure of the congo red drug model.....	73
5.4	Chemical structure of diclofenac.....	73
5.5	Standard curve for diclofenac.....	74
5.6	Molecular structure of colchicine.....	75
5.7	Standard curve for colchicine.....	76
5.8	Chemical structure of MMC.....	76
5.9	Standard curve for MMC.....	77
5.10	Molecular structure of heparin.....	78
5.11	Standard curve for heparin.....	79
5.12	Main factors effecting drug loading after 24 hours.....	82
5.13	Factorial analysis for determining the critical factors effecting drug loading after 48 hours.....	83
5.14	Effect of PVP content on daily release of diclofenac.....	87
5.15	The effect of coating PVP content on drug release duration.....	88
5.16	Main factors effecting drug release properties.....	89
5.17	Effect of eliminating PVP from coating on release rates.....	90
5.18	Diclofenac release rates (mg/mL) under physiologic conditions.....	92
5.19	Diclofenac cumulative release rates (total mg) under physiologic conditions..	93
5.20	Diclofenac cumulative percent release under physiologic condition.....	94
5.21	Colchicine release under physiologic conditions.....	96
5.22	Colchicine cumulative release under physiologic conditions.....	97
5.23	Colchicine cumulative percent release under physiologic conditions.....	98

5.24	MMC daily release rates under physiologic conditions.....	99
5.25	MMC cumulative percent release under physiologic conditions.....	100
6.1	Overall experimental design for Aim 4.....	105
6.2	Effect of drug eluting coatings on fibrotic cell adhesion to posterior surface of lens.	105
6.3	Effect of multi-drug regimen on fibrotic cell adhesion to posterior side on lens.....	112
6.4	Fibrotic cell colonization on lens surfaces following 14 days of implantation in New Zealand White rabbits.....	113
6.5	Cross section of posterior capsule of control lenses	114
6.6	Cross section of posterior capsule for drug eluting lenses	115
6.7	SEM micrographs of the surface of coated lenses... ..	116
6.8	The size distribution of particles present in BSS... ..	118
6.9	The size distribution of particles released from lenses loaded with diclofenac + colchicine... ..	118
6.10	The size distribution of particles released from lenses loaded with heparin + colchicine.....	119
6.11	The size distribution of particles released from lenses loaded with diclofenac + MMC.....	119
6.12	The size distribution of particles released from lenses loaded with colchicine only.....	120
6.13	SEM micrographs of hydrated diclofenac coated lenses	122
6.14	The size distribution of particles released from lenses loaded with diclofenac from 5 to 40 mg/mL coating solution.....	123
6.15	The loading concentrations of diclofenac (DI) considerably affected fibrotic cell accumulation on the posterior capsule.....	124

6.16	Adherent fibrotic cells on the surface of the lens after 14 days implantation.....	125
6.17	Cross section of posterior capsule for diclofenac loaded lenses.....	126
6.18	SEM micrograph of hydrated colchicine coated lenses.....	128
6.19	The size distribution of particles released from lenses loaded with colchicine from 2.6 to 30.3 mg/mL coating solution.....	129
6.20	The loading concentration of colchicine (COL) affected the degree of fibrotic cell adherence on the posterior capsule.....	131
6.21	Adherent fibrotic cells on the surface of the lens after 14 days of implantation in New Zealand White rabbits.....	132
6.22	Cross section of posterior capsule for colchicine loaded lenses.....	133

LIST OF TABLES

Table	Page
3.1 Lubricious surface coatings selected for drug delivery platform on an intraocular lens.....	25
3.2 Leachable levels (PU & PVP) for aqueous based PU/PVP coating.....	36
3.3 Grading scale for evaluating cellular characteristics and percent lyses.	37
3.4 Grading scale for determining the percent lysis for cell cultures.....	38
3.5 Cytotoxicity results of aqueous based PU/PVP coating extracts.	39
3.6 Biocompatibility results for aqueous based PU/PVP coating extracts.	41
4.1 Summary of minimum concentrations to effectively inhibit LEC growth, LEC migration, and inflammatory cell activation as determined by in vitro testing.....	68
5.1 Key factors and testing conditions included in drug loading designed experiment.	80
5.2 Key factors included in the fractional factorial designed experiment.....	85

CHAPTER 1

INTRODUCTION

The development of cataracts is the leading cause of blindness worldwide (7). For much of the world's population, cataract induced visual impairment is treated effectively by surgical removal of the cataractous lens and implantation of an artificial intraocular lens (IOL). Unfortunately, patients with IOL implantation may suffer long term complications such as posterior capsule opacification (PCO) or secondary cataract. The estimated incidence of PCO five years after surgery is 14-50% in adults and nearly 100% in children (5, 6). Despite intensive research efforts, the pathogenesis of PCO formation is not totally understood and the lack of such knowledge hinders the development of an IOL with improved safety and biocompatibility. It is imperative that a better understanding of the pathogenesis of PCO is attained so that an improved IOL may be developed for reducing PCO formation.

To restore clear vision, cataract surgery involves the removal of the natural lens, known as the lens epithelium. In order to reach the lens epithelium, an opening, or capsulorhexis, is created on the anterior side of the lens capsule or capsular bag. An instrument is then inserted through this opening to remove lens tissue and lens epithelial cells (LECs). However, histology has shown that LECs are typically left behind in the

capsular bag (Figure 1.1) after this procedure. Finally, an IOL is placed inside the lens capsule and clear vision is restored.

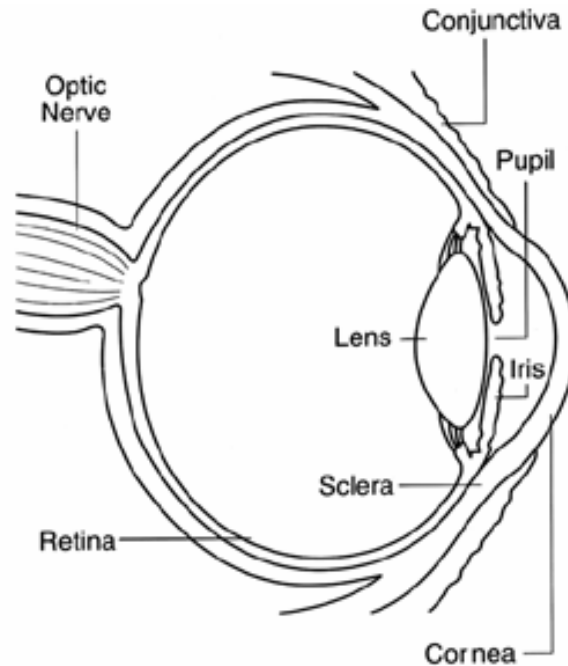


Figure 1.1 Schematic drawing of adult human lens. The lens is enclosed in a basement membrane called the lens capsular bag (approx. $4\mu\text{m}$ thick). The lens is made up of a central core of primary lens fibers which is surrounded by layers of secondary lens fibers. The anterior surface of the lens is lined by a single layer of LECs. (National Eye Institute, NIH)

It is generally believed that PCO is formed due to, at least partially, extensive migration and proliferation of residual LECs on the posterior capsule. IOL implantation has also been shown to trigger the recruitment of inflammatory cells (8, 9, 14) due to the injury associated with surgical incision. The results from many recent studies support that residual LECs in conjunction with the inflammatory response initiate cellular activity that are responsible for PCO formation (8, 11).

1.1 Mechanism of IOL-induced PCO Formation

Recent research efforts have uncovered more detailed information regarding the mechanism of IOL-associated PCO formation. The most well known cause of PCO is the migration and proliferation of residual LECs into the visual axis on the posterior capsule (8, 9, 10). In addition to LECs migration and proliferation (12, 13), recent studies have also demonstrated that foreign body reactions play an important role of PCO formation (Figure 1.2) (8, 14). Inflammatory cells release products that induce LEC proliferation and cause phenotypic changes in LECs ultimately resulting in PCO. In order to effectively reduce or inhibit PCO formation, it is imperative to target both types of cells. The following sections discuss the potential role of LECs (1.1.1), inflammatory cells (1.1.2) and their products (1.1.3) on PCO formation.

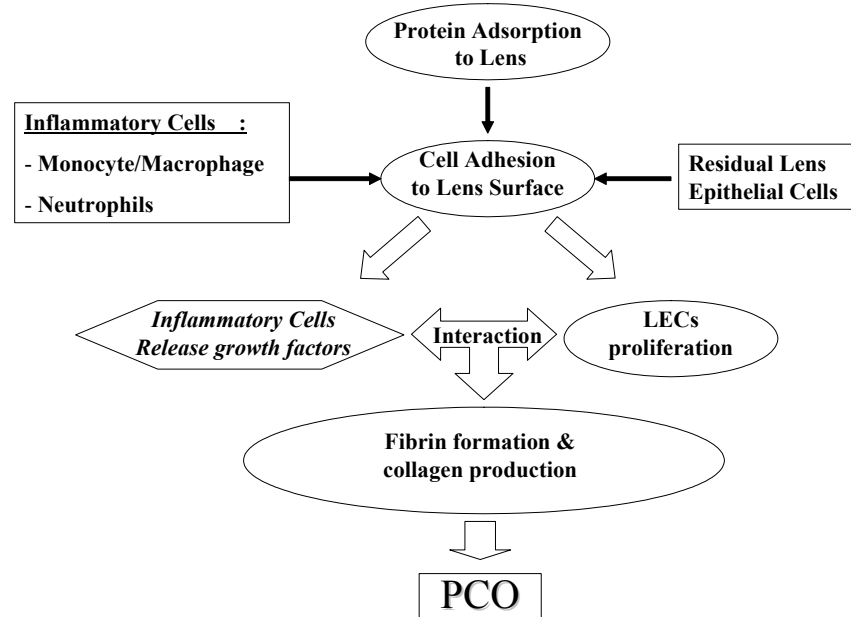


Figure 1.2 Factors responsible for IOL-induced PCO formation. Within minutes of implantation, the lens is covered with a layer of host proteins. Within hours, both LECs and inflammatory cells attach to the surface of the lens. Products of inflammatory cells induce fibrin formation, collagen production, and LECs proliferation and differentiation into fibroblast like cells leading to fibrous tissue formation leading to PCO.

1.1.1 The Potential Role of LECs in PCO Formation

After cataract surgery, residual LECs are left in the capsule which interacts with growth factors and other molecules present in the lens capsule. Residual LECs migrate from the equatorial region of the capsule and proliferate onto the posterior capsule. The LECs may undergo phenotypic changes in response to a variety of stimuli to form contractile fibroblast-like cells such as epithelial pearls and contractile smooth muscle-like cells (α -SMA) with contractile properties (Figure 1.3) (15, 13, 16).

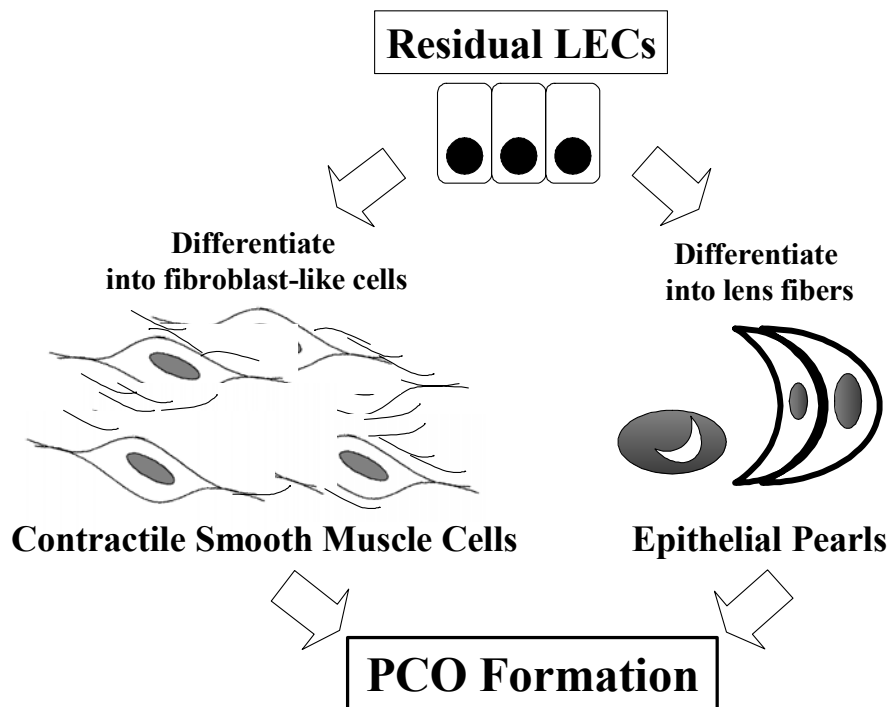


Figure 1.3 Role of LECs in PCO formation. Following cataract surgery, residual LECs differentiate into lens fibers and also transform into fibroblast-like cells such as contractile smooth muscle-like cells. These events initiate collagen synthesis, tissue contraction, and fiber formation leading to PCO (18).

The smooth muscle-like cells are believed to initiate fibrotic tissue formation over the posterior capsule. The fibrous tissues are composed of multiple layers of cells on the posterior capsule. This fibrotic tissue also possesses contractile properties that can cause extensive wrinkling of the posterior capsule and which, in addition, secretes extracellular matrix (ECM). ECM proteins have been shown to play an essential role in LEC cell attachment and migration via adhesion molecules (17).

It is well documented that LEC migration and proliferation processes occur within weeks of cataract surgery. Studies have shown that LEC growth begins within 24 hours. Within a few days, dividing cells can be detected throughout the anterior epithelium. Cells have also been observed growing from the capsulorhexis onto the posterior capsule and across the anterior surface of the IOL (19, 20). Rapid growth of LECs, observed up to one week after surgery, may eventually cover the posterior capsule with a confluent monolayer of cells. Collagen deposition and LEC proliferation onto the IOL and onto the capsule cause wrinkling of the posterior capsule. As time progressed, capsular wrinkles became increasingly apparent and cause a marked rise in light scatter indicative of PCO (21).

1.1.2 The Role of Inflammatory Cells & Blood Components in PCO Formation

Along with LECs from the lens capsule, inflammatory cells are recruited from circulation and colonize on the IOL surface immediately after cataract surgery (1, 3, 22, 23, 24, 25, 26, 27). Inflammation associated with cataract surgery results from trauma caused by surgical procedure, foreign-body reaction to the IOL, and/or immunological reactions involving numerous inflammatory mediators (28, 29). The inflammatory

response often starts at the cut edge of the sclera and also at the cut edge of the lens capsule initiating cellular proliferation and laying down of ECM (28). The severity of the inflammatory response is exacerbated by the IOL implant, a foreign body. This foreign body elicits a three-stage immune response that involves many different cell types, including polymorphonuclear leukocytes, monocytes, and fibroblasts. In general, inflammation is believed to be induced by chemical mediators. These mediators exist locally and fluctuate in number according to the severity of the inflammatory reaction (induced by the mediators). Furthermore, when the inflammatory inhibitors are administered, the local inflammatory reactions can be substantially diminished (4).

1.1.3 The Link between Fibrin Deposition & PCO Formation

During the past 6 years, our laboratory has investigated the processes governing PCO formation and foreign body reactions to IOL implants. Using rabbit implantation model, we have observed the sequence of the events following IOL implantation. First, minutes after implantation, the IOL is covered with a layer of host proteins. Several hours after implantation, a thick layer of fibrin is often found to precipitate on IOL implants (Figure 1.4A). Two weeks later, a substantial number of foreign body cells and LECs are found on implant surfaces. PCO formation becomes apparent a few weeks later. Based on the sequence of events, we have thus assumed that the deposition of fibrin clot and the activation of inflammatory cells are essential to the pathogenesis of PCO formation. We found that the depletion of fibrinogen substantially reduced fibrin deposition and subsequent PCO formation on IOL (Figure 1.4).

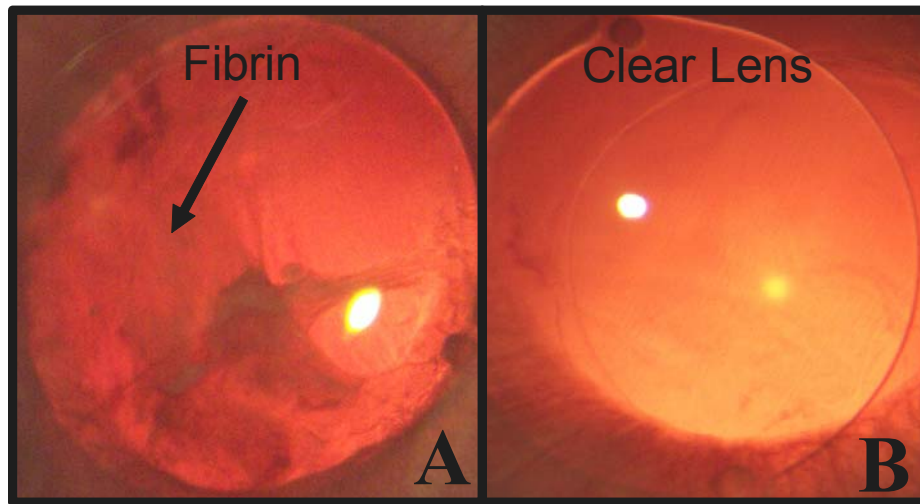


Figure 1.4 PCO formation on PMMA IOL (A) and cibacron blue-coated (B) IOL after 8 weeks implantation in rabbits. Cibacron blue-coated IOLs have been shown to be able to specifically, selectively and reversibly adsorbed albumin. Results indicate that by increasing the concentration of surface-bound albumin, cibacron blue coating (B) significantly reduced (>90%) PCO formation. Uncoated PMMA IOLs (A) resulted in fibrin formation and PCO formation.

Since the reduction of fibrin deposition diminishes PCO formation, we assumed that surface fibrin is responsible to inflammatory cells (Figure 1.5A) and foreign body giant cell (Figure 1.5B) accumulation on IOL surfaces. On the other hand, fibrin-repelling coating should substantially improve the tissue compatibility of IOLs. To test this hypothesis, we used cibacron blue-coated IOLs which have been shown to be able to specifically, selectively, and reversibly adsorbed albumin. Results indicated that increasing the concentration of surface-bound albumin (Figure 1.5 C&D) significantly reduced (>90%) the amount of deposited fibrin compared to uncoated PMMA (Figure 1.5 A&B). Most importantly, cibacron blue IOLs trigger significantly less (<20%) PCO formation and inflammatory cell accumulation on IOL implants. These results provide a

potential link between fibrin deposition and coagulation, inflammation, and PCO formation and suggest that by inhibiting the initial coagulation processes may inhibit the progression to PCO.

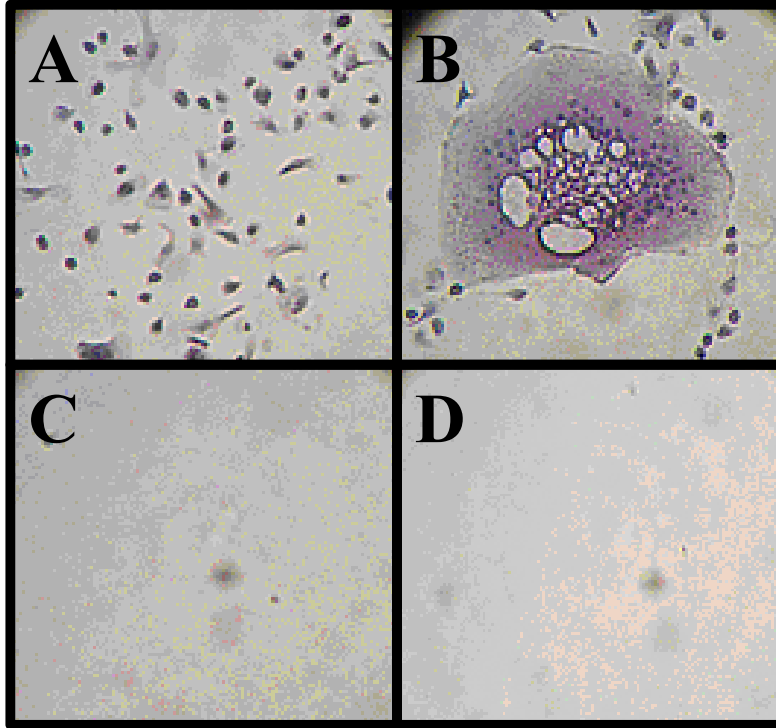


Figure 1.5 LEC accumulation on PMMA and cibacron blue-coated IOLs after 8 weeks implantation in rabbits. PMMA controls absorbed fibrinogen resulting in increased levels of (A) inflammatory cells and epithelial cells accumulation and (B) foreign body giant cell formation. Cibacron blue-coated IOLs (C, D) significantly reduced (>90%) the amount of fibrin deposition which resulted in less cell accumulation.

1.2 Concepts for PCO Preventive Drug Delivery

Many approaches have been developed to reduce the incidence of IOL-induced PCO formation. The most popular approaches are aimed at reducing the incision size and eliminating residual LECs during the operation. Pharmacological approaches have

also been tested. In traditional drug delivery methods, drugs are delivered to the eye exclusively via eye drops, topical ointments, or intravenous means. These delivery methods, though still the most common ones, have various disadvantages associated with them. Traditional drug delivery designs often represent a nonspecific chemical approach to mask undesirable drug properties such as limited bioavailability, lack of site specificity, and chemical instability. Many drugs delivered via eye drops poorly penetrate through the cornea into the eye and therefore limit the number of medications available for the treatment of ocular diseases, but also limit the extent to which those available can be used without incurring serious systemic side effects. Drugs can be also delivered by injection, however, depending on the rate of clearance from the vitreous of a particular medication, large boluses and frequent administrations are required to ensure therapeutic levels over an extended period of time (30). Since only a very small percentage of the injected drug reaches the affected area in the body, multiple injections are often required for treatment to be effective (31) (Figure 1.6). Frequent injections in clinical practice are not practical for chronic diseases that most often require multiple administrations over weeks, months, or years. Since drugs rarely penetrate to the back of the eye, high concentration of drugs are required that can lead to toxicity issues. Topical delivery is another relatively easy method of drug administration and carries little risk but penetration of the drug is poor in the retina or choroids (30). It is due to these various limitations that controlled drug delivery systems are required to inhibit ocular diseases, specifically those located in the back of the eye. It is conceivable that a

continuous, controlled, local drug delivery system can effectively reduce PCO formation or treat other ocular diseases located in or near the back of the eye.

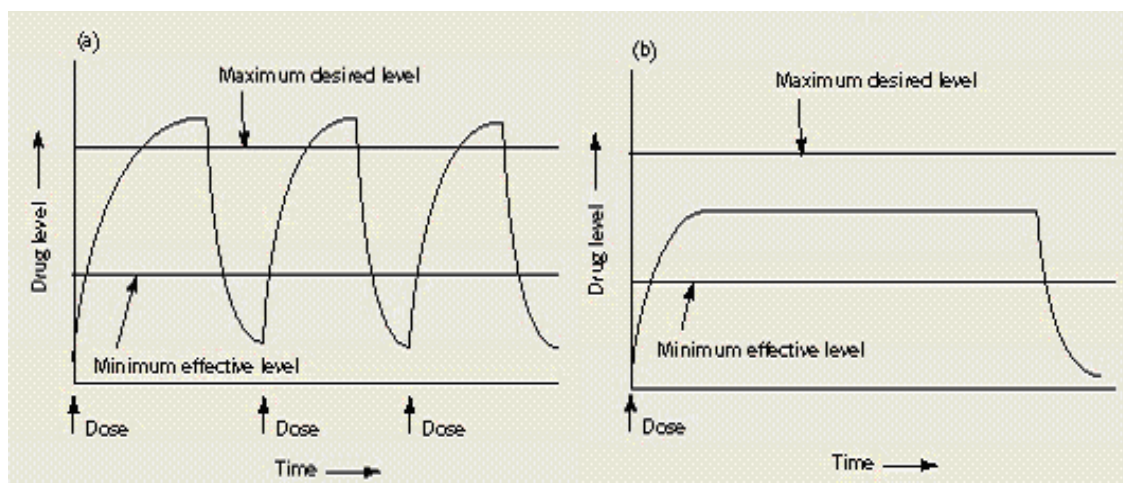


Figure 1.6 Pharmacological diagrams to depict the concentrations of drugs delivered via multiple injections vs. controlled release device. Drug levels in the blood with (a) traditional drug delivery (i.e. injection) require multiple injections while (b) controlled drug delivery via drug delivery system release drug directly to the site for extended periods of time (Peppas, 32).

Controlled drug delivery designs represent a new strategy for directed, localized, and efficient drug delivery. Targeting drugs to specific proteins or cells, or both, have potential as a selective drug delivery system for many diseases, particularly ocular diseases. There are many advantages to controlled drug delivery systems for the eye (32). In an ideal drug delivery system, the drug profile in the desired tissue were maintained at optimum therapeutic concentrations with minimum fluctuation, predictable and reproducible release rates for extended durations. For ocular diseases continuous drug delivery enables the sustained release of drugs to the back of the eye,

which offers flexibility and versatility for drug formulation and pharmacokinetics control that was not available with other methods such as eye drops and topical ointments. These improvements in delivery methods lead to the elimination of side effects, infrequent dosing, minimizing the dependence on patient compliance, and most importantly optimized drug therapy. Thus, controlled drug delivery appears to be a viable option to reduce PCO formation following cataract surgery which is the focus of this proposed investigation.

1.2.1 IOL Coatings as a Drug Delivery Platform

IOLs used in the cataract surgery are often constructed of polymers that are often hydrophobic, non-slippery, and often non-biocompatible. However, to facilitate insertion into the eye during cataract procedures, IOLs should exhibit low friction surfaces. As technology advances, surgical incision will decrease further exerting significant forces on IOLs during implantation. It is therefore necessary to coat these surfaces with a lubricious coating to assist in lens delivery. Studies have demonstrated that the interaction of corneal tissue to IOLs relative to surface adhesiveness and endothelial damage are lessened by hydrophilic and lubricious coatings (36). As a result, hydrophilic coatings will provide protection not only to the IOL but also the surrounding tissue. We have also uncovered that such hydrophilic coatings possess slow drug release properties and could also serve as a platform for a drug delivery system to combat PCO formation.

Hydrophilic coatings have been shown to improve the biocompatibility of medical devices. In addition to lubricity, flexible coatings are often needed to allow for

easy manipulation upon implantation. Many low friction coating materials are available. These include polytetrafluoroethylene (PTFE), glycerin, and silicone fluid. Unfortunately, the use of some hydrophobic coatings is restricted due to coating stiffness, poor bonding and a limited supply of medical grade raw materials. Furthermore, most of these hydrophobic coatings suffer from the limitation of not being able to incorporate drugs or other bioactive agents. Alternatively, a hydrogel-like surface provides a lubricious surface and also offers flexibility in terms of drug incorporation and in drug release. (37) However, challenges involving durability and adhesion exist for hydrophilic polymer coatings due to low physical integrity associated with high water content. Several approaches exist to overcome these limitations of hydrophilic coatings such as limited wet strength, poor adhesion, and fragility. However, these coating techniques have many weaknesses. (77)

One approach to improve hydrophilic coating adhesion is to graft one end of a functionalized hydrophilic polymer to the substrate. This is often accomplished via a reactive bridge between the inert substrate surface and a functional group on the hydrophilic polymer. This results in a very thin hydrophilic layer that is chemically linked to the surface. This approach overcomes many of the inherent limitations of hydrophilic coatings such as limited wet strength, poor adhesion, and fragility. However, this process relies on cumbersome processing techniques and in some cases organic solvent handling. (37, 77)

Another approach is to physically anchor a long-chain hydrophilic polymer in a supporting polymer network that is hydrophobic and does not swell in water. The long

hydrophilic polymer becomes entangled within the supporting polymer and allows the polymer to become hydrated. This is known as an interpenetrating network and is characteristic of many commercially available lubricious coatings. This approach utilizes either an organic or an aqueous based solvent. When utilizing an organic solvent the hydrophilic polymer is dissolved in the organic solvent along with the polymer that will form the supporting matrix. The device is then coated with the coating solution and the organic solvent is allowed to dry. (77) As a result, this process relies on cumbersome processing techniques and organic solvent handling. Organic solvents introduce significant risk, since residual solvent present in the coating after drying may lead to toxicity and adverse tissue reactions.

Fortunately, aqueous based coatings have been developed to overcome many of the physical and processing limitations of these types of hydrophilic coatings. First, organic solvents are eliminated which allows the ability to incorporate pharmacologic agents or drugs that are incompatible with organic solvents or that could be degraded upon exposure to them. Furthermore, using an aqueous based solvent eliminates potential organic solvent residual and improves the safety of the device. (37, 77) Aqueous based coatings overcome many of the inherent limitations of hydrophilic coatings by providing improved strength and adhesion and offer an ideal platform for controlled drug delivery.

1.2.2 Potential PCO Preventative Pharmacologic Agents

Evidence suggests that if the early inflammatory response and the early stages of LEC migration and proliferation are halted or significantly minimized, then PCO

formation will be reduced. Many pharmacological agents have been reported to significantly reduce the incidence of PCO in the experimental settings (41). However, almost all of these agents can cause significant ocular toxicity due to the method of delivery, i.e. eye drops, topical ointments, injections, etc. Such toxicity would be significantly reduced if these anti-proliferative and anti-adhesive agents are delivered directly to the lens capsule via hydrophilic IOL coating. To test the efficacy of the drug delivery system, this study will focus on pharmacologic agents that have been shown to significantly reduce the incidence of PCO by different means, including anti-inflammatory, LEC inhibitor drugs, and integrin blockers.

1.2.2.1 Pharmacologic Agents: Anti-Inflammatory

By reducing the degree of inflammatory responses, the incidence of PCO formation can be substantially diminished (5, 12). Along with LECs, monocytes, macrophages, and other inflammatory cells were found on the IOL surface immediately after cataract surgery. The inflammatory response in a rodent model for PCO appeared to be at its maximum at 3 days after cataract surgery, coinciding with maximum proliferation and migration of LECs in the capsular bag and capsular wrinkling. Many IOL-associated macrophages were found to synthesize transforming growth factor- β (TGF- β) 14 days after surgery, when lens fiber differentiation was evident. The release of TGF- β and other cytokines/chemokines, such as basic fibroblast growth factor (b-FGF), hepatocyte growth factors, and interleukins, by activated macrophages prompt LECs proliferation, ECM production, collagen contraction, capsular wrinkling, and cell differentiation (46, 47, 48, 49, 50).

Steroids, including dexamethasone, are commonly used as a routine treatment to reduce the inflammatory reaction for several weeks postoperatively. Dexamethasone increases the production of the protein lipocortin 1. Lipocortin 1 is a phospholipid binding protein, which inhibits phospholipase A, a key enzyme in the synthesis of inflammatory prostaglandins and leukotrenes from arachidonic acid. Inhibiting phospholipase A decreases the production of prostaglandins and leukotrenes thereby suppressing inflammation. Dexamethasone also blocks the production and release of cytokines by down-regulating mRNA expression of several key inflammatory enzymes, which also suppresses the inflammatory process. However, adverse effects are experienced with steroids including elevation of intraocular pressure, inhibition of wound healing, and facilitation of infections.

Non-steroidal anti-inflammatory drugs (NSAID), on the other hand, reduce inflammation by inhibiting the production of prostaglandins without major side effects. Diclofenac is one such drug that belongs to the class of NSAIDs and has recently been investigated to reduce PCO formation. Diclofenac has been shown to inhibit leukocyte migration and regulate arachidonic acid metabolism by inhibiting the enzyme cyclooxygenase (COX). The cyclooxygenase enzymes metabolize arachidonic acid following stimulation of phospholipase A2 on the cell membrane with immune and inflammatory mediators. By inhibiting the COX enzymes, diclofenac suppresses cytokine production thereby inhibiting prostaglandin synthesis, which promote inflammation produced in response to tissue injury (51). Prostaglandins are known to increase local blood flow and potentiate the effects of mediators such as bradykinin that

induce vasopermeability. Prostaglandins are also known to exert diverse effects on cellular functions. Evidence also indicates that diclofenac inhibits the lipooxygenase pathways, thus reducing formation of the leukotrenes, which also mediate the inflammatory response. Diclofenac has been shown to decrease blood aqueous barrier breakdown in eyes indicating that diclofenac was effective in the treatment of postoperative inflammation in otherwise normal eyes after phacoemulsification and IOL implantation with no other disease than cataract (4). Diclofenac was also shown to reduce PCO formation and LEC multi-layering by a single dose injection into the capsular bag after phacoemulsification in rabbits (52).

Recent studies have also identified giant cells on the anterior surface of intraocular lenses indicating an intraocular lens induced inflammatory response. Heparin is known to have inhibitory effects on multiple components of the inflammation cascade, including integrins, cytokines, neutrophil-derived elastases, complement activation, and platelet-activating factor and TNF- α -induced lung edema. The inflammatory cascade is first inhibited by P-selectin and L-selectin based interactions with heparin, occurring before the recruitment of integrins, cytokines, and proteases. Heparin also affects downstream steps in the inflammatory cascade by inhibiting the interaction of chemokines. Heparin consists of repeating disaccharide units containing D-glucuronic acid or L-iduronic acid and a glucosamine residue that is either *N*-sulfated, *N*-acetylated, or, occasionally, unsubstituted. Its molecular weight (MW) ranges from 3,000 to 30,000 daltons. Low MW heparin is depolymerized which destroys approximately 30% of the active penta-saccharide sequences. Unfractionated,

high MW heparin may produce drastically different in vitro or in vivo results due to difference in potency associated with the molecular weight of these molecules. However, low MW heparin has reduced non-specific binding compared to high MW heparin which results in higher bioavailability that may also affect in vivo performance. Heparin surface modified IOLs have been shown to reduce the inflammatory response by decreasing the amount of cellular deposits and giant cells following cataract surgery (53). In addition, heparin surface modification has been tested on various devices for the purpose of reducing bacterial adhesion and thereby reducing the risk of infection. The heparin surface modification is thus hypothesized to work in 3 ways to prevent foreign body reaction: 1) a constant molecular surface motion prevents proteins, bacteria, and white blood cells from adhering to the IOL helps minimize the foreign body response; 2) a negative charge of the heparin surface repels bacteria and white blood cells; and 3) a hydrophilic surface, which resembles the body's tissues, helps minimize cell adhesion. Studies have shown that heparin surface modified IOLs reduced postoperative inflammation and delayed the incidence of PCO in children. Results indicated that heparin immobilized IOLs contained less cellular and pigment deposits on the IOL surface within first month after operation when compared to PMMA IOLs (53). Others have found similar results with heparin-eluting drug delivery systems. Xie et al. (54) implanted a heparin drug delivery system into the posterior capsule which inhibited cell proliferation. With this drug delivery system, the cornea, iris, ciliary body and retina remained intact, and no significant toxic reactions were observed (54). No intraocular hemorrhage occurred during follow-up. Results

demonstrated that implantation of a heparin drug delivery system in the posterior chamber of experimental animals significantly maintained a higher heparin level in aqueous humor for a relatively long period of time with minimum toxic and side effects (54).

1.2.2.2 Pharmacologic Agents: LEC Programmed Death

Inhibition of LECs proliferation has been shown to effectively reduce PCO formation (55). Mitomycin-C, 5-fluorouracil, and colchicine are such pharmacologic agent that affects LECs responses.

Mitomycin-C is an alkylating agent which acts by inhibiting DNA synthesis and produces cell death by apoptosis and necrosis (52, 56). The drug has a preferential action for rapidly dividing cells such as residual LECs (55). Results indicate that mitomycin-C effectively inhibits LEC proliferation after a single dose injection into the capsular bag after phacoemulsification in rabbits (52) and effectively reduces PCO in rabbit eyes without causing ocular toxicity (55). Mitomycin-C has also been demonstrated to inhibit secondary cataract formation via blockage of LEC proliferation and fibrosis formation when used in solution during lens extraction (56).

5-Fluorouracil (5-FU) prevents cells from making DNA and RNA by interfering with the synthesis of nucleic acids, thus disrupting the growth of cells. Specifically, 5-FU, a pyrimidine analogue, is transformed inside the cell into different cytotoxic metabolites which are then incorporated into DNA and RNA. Upon incorporation into DNA and RNA, these cytotoxic metabolites finally induce cell cycle arrest and apoptosis by inhibiting the cell's ability to synthesize DNA.

Colchicine inhibits microtubule assembly in various cells, including LECs and inflammatory cells. Microtubule dynamics play a critical role in the assembly and function of the mitotic spindle and, thus, in cell proliferation. Colchicine inhibits microtubule assembly by binding directly to microtubules and interfering with polymerization of the microtubule subunit tubulin and thereby inhibiting cell proliferation and activation.

1.2.2.3 Pharmacologic Agents: LEC Adhesion Blocker

Another approach to inhibit PCO formation includes the inhibition of LEC attachment or migration to the posterior capsule by blocking cell adhesion receptors or targeting LECs directly (45, 57, 58, 59). Calcium and magnesium ions are required for cell adhesion. Thus, calcium and/or magnesium ion chelators, such as ethylene diamine tetraacetic acid (EDTA) have been shown to reduce cell adhesion (60, 61). Calcium also activates phospholipase-A2 in cells, which cleaves arachadonic acid from membrane phospholipids and thus may also reduce inflammation. EDTA inhibits LEC attachment/migration by rapidly and reversibly attracting, chelating and redistributing metal ions, or removing them from the body. Data indicates that treatment with a single dose treatment with EDTA results in significantly less LECs adhered to the IOL surface and reduced LEC proliferation on the posterior capsule resulting in reduced PCO formation (52). Others have shown that an implanted drug delivery disc inhibits LEC migration by blocking adhesion molecule integrins on the posterior capsule by controllably releasing EDTA and other drugs (60). In summary, EDTA along with other drugs has demonstrated the ability to effectively reduce PCO by blocking adhesion

molecule receptors responsible for cell adhesion and migration (61).

1.2.2.4 Pharmacologic Agents: Integrin Blocker for LEC Migration

Another pharmacological approach aimed at reducing PCO targets processes involved in LEC migration, thus inhibiting LEC proliferation (62). It has been shown that LECs adhere and migrate via adhesion molecules such as integrins. Generally, the tripeptide sequence Arginin-Glycine-Aspartic Acid (Arg-Gly-Asp or RGD-peptide) is the recognition motif for these receptors. Many adhesive proteins present in extracellular matrices contain the RGD-peptide as their cell recognition site. These proteins include fibronectin, vitronectin, osteopontin, collagens, thrombospondin, fibrinogen, and von Willebrand factor. Together, adhesion proteins and their receptors constitute a versatile recognition system providing cells with anchorage, traction for migration, and signals for polarity, position, differentiation, and possibly growth. RGD-peptide will be utilized to occupy cell receptors thereby inhibiting cell migration. Studies have shown that the addition of RGD-peptide inhibits LEC adhesion on a culture plate (63), ECM, and lens capsule (17, 59) in vitro. RGD-peptide containing cell-binding domains of fibronectin has also shown 100% inhibition of the attachment of cultured LECs (64, 65). In each of these studies, inhibition of LEC migration and adhesion prevented capsular wrinkling and folds typically seen in PCO (59). These findings provide further evidence that pharmacologic agents can prevent LEC migration and adhesion, potentially making it suitable for inhibiting PCO.

It should be noted that others have shown that a combination treatment of EDTA and RGD-peptide inhibits LEC migration by inhibiting the integrins expressed

on LECs. Blocking adhesion molecules expressed on LECs as in this study may further reduce PCO (60, 66). A similar study indicated that treatment with a single dose treatment with EDTA and RGD resulted in significantly less LECs adhered to the IOL surface and reduced LEC proliferation on the posterior capsule resulting in reduced PCO formation indicating that this combination may have the potential to prevent PCO by inhibiting cell migration and adhesion (52).

CHAPTER 2

OVERVIEW OF SPECIFIC AIMS

This series of experiments emphasized the development of an IOL drug delivery system not only to assist lens delivery but also to significantly reduce PCO formation in acute responses following IOL implantation. Overall, this work was aimed at developing a coating that incorporates therapeutic regimens to combat IOL-mediated PCO formation. The overall experimental design is listed below in Figure 2.1. The sequence of this investigation is listed below.

Aim 1. To develop a lubricious coating as a drug delivery platform and to assist in IOL small incision lens delivery.

Aim 2. To investigate the effects of pharmacologic agents on LEC proliferation, LEC migration, and inflammatory cell activation through in vitro testing.

Aim 3. To engineer the coating material for maximal drug loading and controlled drug release in vitro for selected pharmacologic agents.

Aim 4. To evaluate the effectiveness of a multi-drug drug delivery system to combat PCO formation in vivo.

The overall goal of this work is to improve the present understanding of the processes underlying PCO formation and response to implanted IOLs and to develop a novel approach to significantly reduce IOL-induced PCO formation.

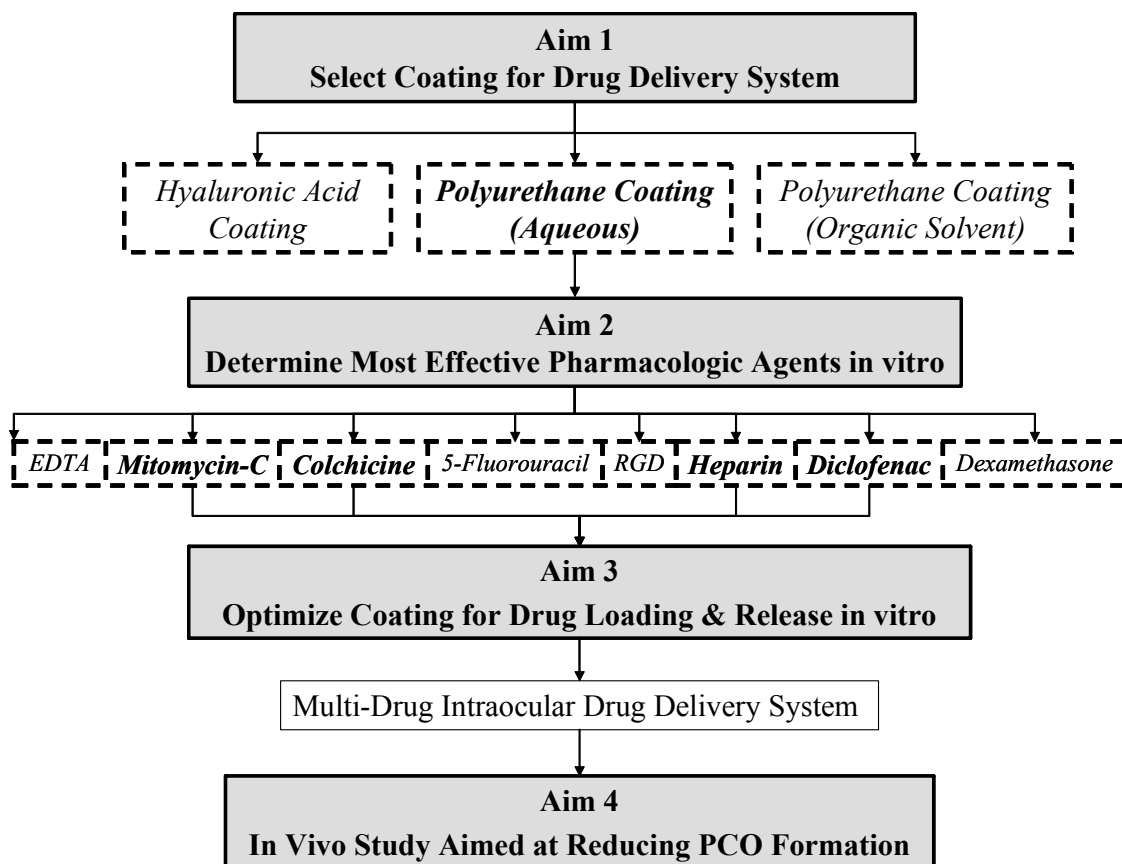


Figure 2.1 Experimental design for developing a coating that incorporates therapeutic regimens to combat IOL-mediated PCO formation.

CHAPTER 3

AIM 1: LUBRICIOUS COATING DEVELOPMENT

The objective of Aim 1 was to develop a lubricious coating as a drug delivery platform that also assisted in IOL small incision lens delivery. The first aim consisted of selecting a lubricious and stable coating that is capable of serving as a platform for drug delivery. The overall experimental design for Aim 1 is listed below in Figure 3.1. In order to meet the requirement for a lubricious and stable coating, selection criteria were identified. First, the coating must provide a lubricious surface when wet while still providing superior cohesive properties and superior adhesion properties to an IOL. The coating must also be easily processed and not rely on cumbersome processing techniques, such as UV curing, or involve solvents that degrade pharmacologic agents.

Numerous coatings were evaluated but only three (3) coatings were chosen for final testing to reduce friction and resultant damage on delivered IOLs. The coatings possessed (Table 3.1) superior cohesive and lubricious properties and included: 1) a solvent based polyurethane/ polyvinylpyrrolidone coating (PU/PVP organic solvent), 2) aqueous based polyurethane/ polyvinylpyrrolidone coating (aqueous PU/PVP), and 3) aqueous based hyaluronic acid (HA) coating.

Table 3.1. Lubricious surface coatings selected for drug delivery platform on intraocular lens.

Chemical Composition	Abbreviation	Coating Name	Solvent	Manufacturer
Polyurethane + Polyvinylpyrrolidone	PU/PVP Aqueous	LubriLAST	Aqueous	AST Products
Polyurethane + Polyvinylpyrrolidone	PU/PVP Organic Solvent	Hydromer Coatings	Organic	Hydromer
Hyaluronic Acid	HA Coating	Hydak	Aqueous	BioCoat

The aqueous based coating consists of a chemically cross-linked supporting polymer network with long-chain hydrophilic molecules intertwined within it. The polymer network is an aliphatic polyester urethane (PU). The hydrophilic molecule is polyvinylpyrrolidone (PVP) which is blended with the PU dispersion. The PVP hydrophilic component is incorporated into the coating and becomes entangled with the supporting network. In the presence of water or body fluids, the hydrophilic polymer adsorbs water molecules to create a watery interface at the surface of the device. A cross-linking agent that cross-links the supporting polymer matrix is added to enhance coating integrity (77, 79).

The polyurethane and polyvinylpyrrolidone in an organic solvent consists of polyisocyanate and polyurethane in methylethylketone (MEK). The hydrophilic polymer, PVP, is dissolved in the organic solvent along with polyurethane that will form the supporting matrix (78).

The hyaluronic acid coating consists of hyaluronan, a polysaccharide of the glycosaminoglycans class. Hyaluronan is a unique biopolymer that is found in all

tissues. Hyaluronan lends itself to cross-linking and immobilizing in various ways to produce hydrophilic, lubricious, and biocompatible surfaces which the body perceives as inert when implanted (80).

The three coatings were evaluated by lubricity testing as described in Section 3.1. This test provided critical information on the physical characteristics of each coating. Thus, results from lubricity testing were used to select the coating to be used as a platform for drug delivery. The selected coating was then subjected to additional tests for full characterization and proof of stability, safety, and biocompatibility as described in sections 3.2 to 3.6. The experimental plan for Aim 1 includes the following tests.

- Coating lubricity testing (3.1) (All 3 coatings)
 - 3.1.1 Introduction
 - 3.1.2 Experimental design
 - 3.1.3 Results
 - 3.1.4 Conclusion – Selection of Aqueous Based PU/PVP Coating for use as Drug Delivery Platform
- Coating adhesion testing (3.2) (selected coating only)
 - 3.2.1 Introduction
 - 3.2.2 Experimental design
 - 3.2.3 Results
- Extractable test method (3.3) (selected coating only)
 - 3.3.1 Introduction
 - 3.3.2 Experimental design

- 3.3.3 Results
- Toxicity testing (3.4) (selected coating only)
 - 3.4.1 Introduction
 - 3.4.2 Experimental design
 - 3.4.3 Results
- Accelerated aging stability test method (3.5) (selected coating only)
 - 3.5.1 Introduction
 - 3.5.2 Experimental design, and
 - 3.5.3 Results
- Biocompatibility testing (3.6) (selected coating only)
 - 3.6.1 Introduction
 - 3.6.2 Experimental design
 - 3.6.3 Results
- Overall discussion (3.7)

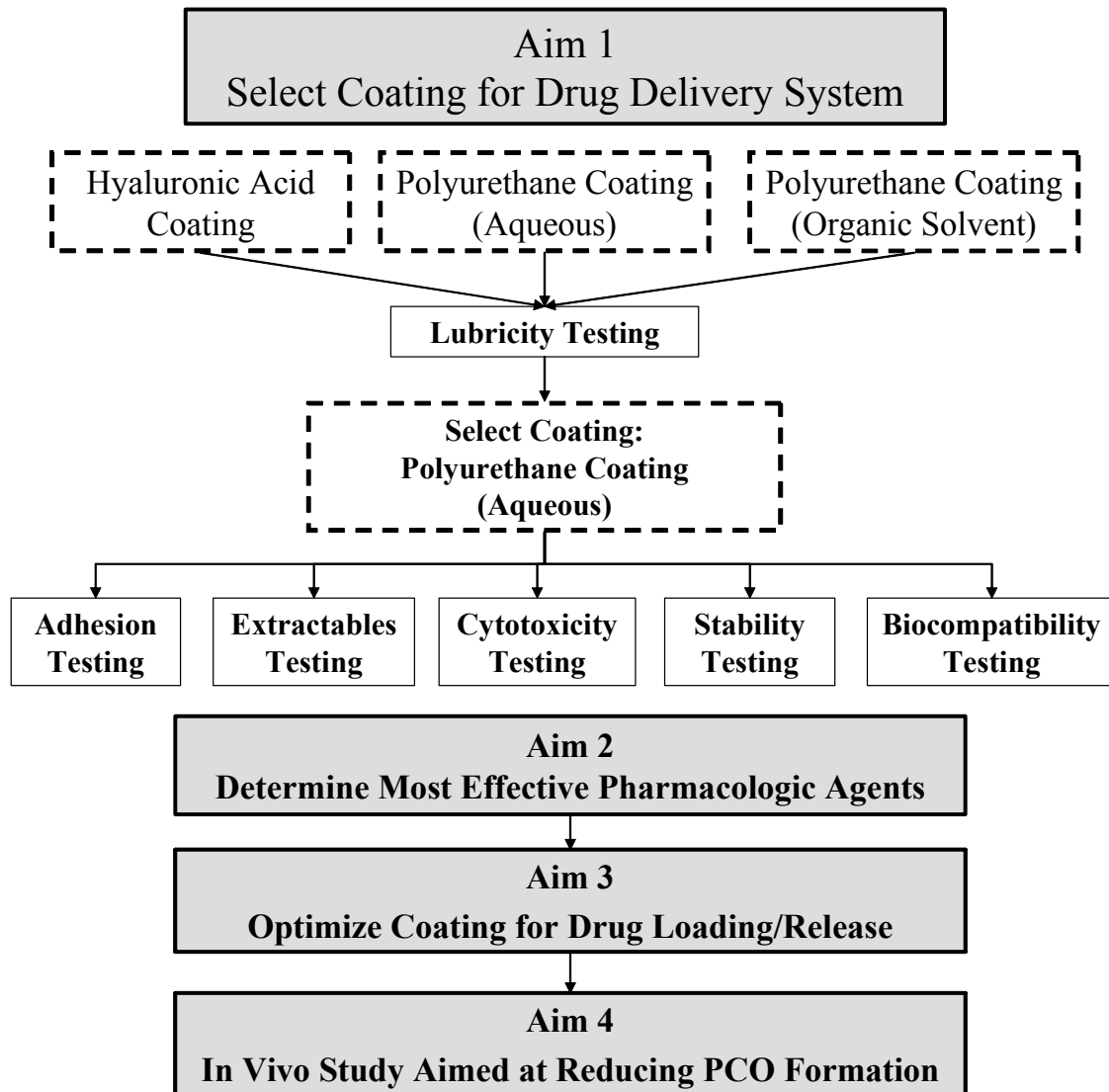


Figure 3.1 Experimental design for developing lubricious coating on an IOL.

3.1 Coating Lubricity Testing

3.1.1 Introduction

To reduce friction and resultant damage on delivered IOLs, three polymeric materials with superior cohesive and lubricious properties were identified and tested. As mentioned, these materials include a solvent based polyurethane (PU/PVP organic solvent), an aqueous based polyurethane (PU/PVP aqueous based), and an aqueous based hyaluronic acid coating (HA coating). The coating lubricity test is designed to measure the lubricity of the coating by measuring the force required to deliver a lens through an IOL delivery system. This test is also a measure of the durability and adhesion of the coating to the lens by delivering an Alcon AcrySof® (model SA60AT) 20.0 D lens (6.0 mm diameter) through a 3.0 mm diameter IOL delivery system.

3.1.2 Experimental Design

This test measured the durability and adhesion of the coating to the lens by measuring the force required to deliver an IOL through a 3.0mm diameter IOL delivery system (Alcon Monarch® “C” Delivery System). Briefly, the cartridge was filled with VISCOAT® viscoelastic prior to loading the lens, similar to that performed during cataract surgery. The lens was loaded into the test cartridge with the anterior side facing up with the trailing haptic allowed to extend from the cartridge. The lens optic was biased the down against the floor of the cartridge. The trailing haptic was positioned under the trailing haptic post if available. The loaded cartridge was inserted into the injector. The plunger was advanced forward until the plunger head was at the cartridge ramp. The Instron crosshead was advanced until it was in close proximity to the

handpiece knob. The load was set to zero at this point. The crosshead advanced the lens through the delivery system at the set rate of 270 mm/min (recommended delivery rate suggested to physicians). The Instron was stopped once the lens exited the cartridge. The force versus displacement data was recorded and saved in the computer. Upon completion, the lenses were inspected (16X microscope) for coating delamination or damage.

3.1.3 Results

Lubricity test results indicate that the hyaluronic acid (HA) coating was not significantly different from the uncoated control (t-test: $p > 0.05$) as seen in Figure 3.2. A significant difference was observed between PU based coatings and the uncoated control (t-test: $p < 0.001$) in reducing lens delivery forces. A significant difference was also observed between PU based coatings and the HA coatings ($p < 0.02$). However, no significant difference was observed in lens delivery forces between the PU-based coatings (t-test: $p > 0.19$). Based on this data, the PU coatings were further tested to determine which coating was most effective in reducing lens delivery forces.

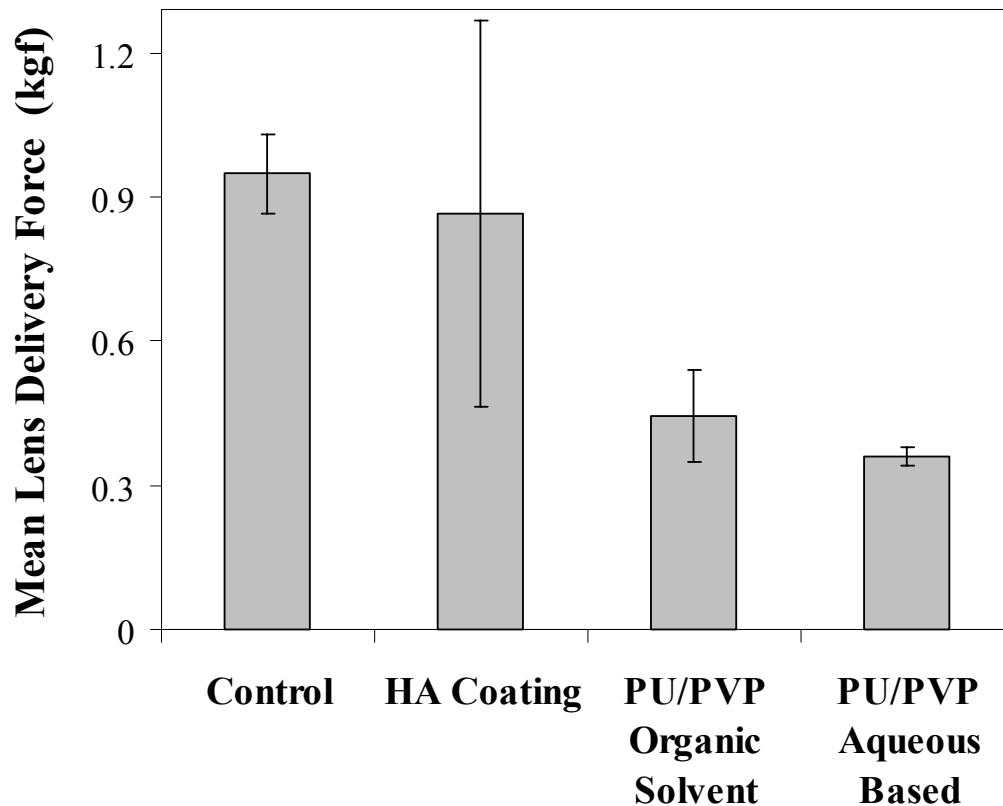


Figure 3.2 Maximum forces for selected lubricious coatings required to deliver an IOL through a lens delivery system. (n=6 in all cases). A significant difference was observed between PU based coatings and uncoated (t-test: $p < 0.001$) and HA coatings (t-test: $p = 0.62$). No significant difference observed between PU coatings (t-test: $p = 0.054$).

Maximum lens delivery forces for additional samples coated with aqueous based and organic solvent polyurethane coatings were evaluated (n=18 each case). A significant difference was observed between the lens delivery force for aqueous based coating and organic based coating (t-test: $p < 0.001$). Further evaluation indicated that the aqueous based PU/PVP coating produced lower lens delivery forces (Figure 3.3) indicating more lubricity than the organic based polyurethane coating.

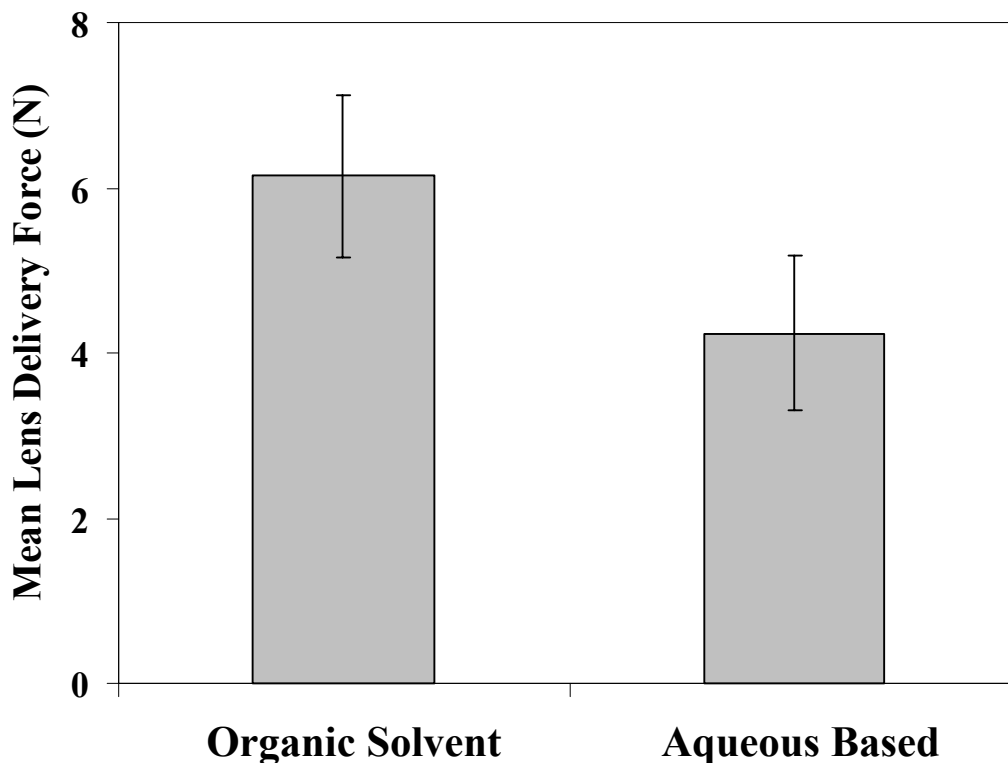


Figure 3.3 Mean lens delivery forces for lubricious polyurethane coatings, aqueous based and organic solvent (n=18). Vertical bars denote standard deviation. A significant difference was observed between lens delivery forces for aqueous based and organic based coatings (Student's t-test: $p < 0.001$).

3.1.4 Conclusion – Select Coating for Drug Delivery Platform

In summary, preliminary lubricity testing indicated the hyaluronic acid coating did not provide sufficient lubricity compared to the polyurethane coatings. As a result, the HA coating was eliminated as a candidate for use as a drug delivery platform. On the other hand, both polyurethane coating utilizing PVP as a lubricious component provided increased lubricity and were subjected to additional lubricity testing. After extensive testing, the aqueous based PU/PVP coating provided significantly more

lubricity and offered additional benefits associated with drug delivery. For example, the polyurethane coating using an organic solvent possessed limitations relating to incorporating drugs. By using an aqueous based coating drugs possessing various properties could be incorporated into the coating, including drugs that are incompatible/insoluble or drugs that could have been degraded upon exposure to organic solvents.

Within the scope of this experiment, the aqueous based PU/PVP coating not only provided superior lubricity but also provided a platform with many advantages for drug delivery. The aqueous-based systems offered flexibility in formulation that produced different coating properties and varying drug delivery properties. Based on this data, the aqueous based PU/PVP coating was selected as the platform for drug delivery and was subjected to additional testing.

3.2 Coating Adhesion Testing

3.2.1 Introduction

The Adhesion Test was designed to measure adhesion strength of the aqueous based PU/PVP coating to the IOL via the Adhesion Tape Test Method in accordance with ASTM D-3359 “Adhesion by Tape Test”, Method B: parallel lines or “cross hatch pattern” method.

3.2.2 Experimental Design

A crosshatch pattern was cut into the coated lens using a calibrated blade. After creating a cross hatch pattern in the coating, tape was applied to the coating. The tape was allowed to dwell 1 minute and then it was removed manually at a steady rate. A

control material, polypropylene sheets, was coated to verify that the method was performing as designed. The grid area was then inspected and rated according to the scale in Figure 3.4.


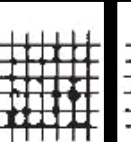

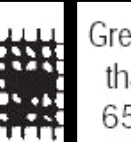
<i>Coating Delamination</i>	0%	1-5%	6-15%	16-35%	36-65%	>65%
Surface of cross-cut area from which flaking has occurred. (Example for 6 parallel cuts)	None					Greater than 65%
Classification	5	4	3	2	1	0

Figure 3.4 Classification chart for rating coating adhesion strength. (Paul N. Gardner Comp., Inc.)

3.2.3 Results

All samples were coated with the aqueous based PU/PVP coating. All coated IOLs (n=20) did not experience any coating delamination or adhesion problems as indicated by ratings of 5 (= 0% delamination) for all test samples (Figure 3.5). The control material experienced adhesion problems and the coating delaminated when the tape was removed as indicated by ratings of 1 to 0.

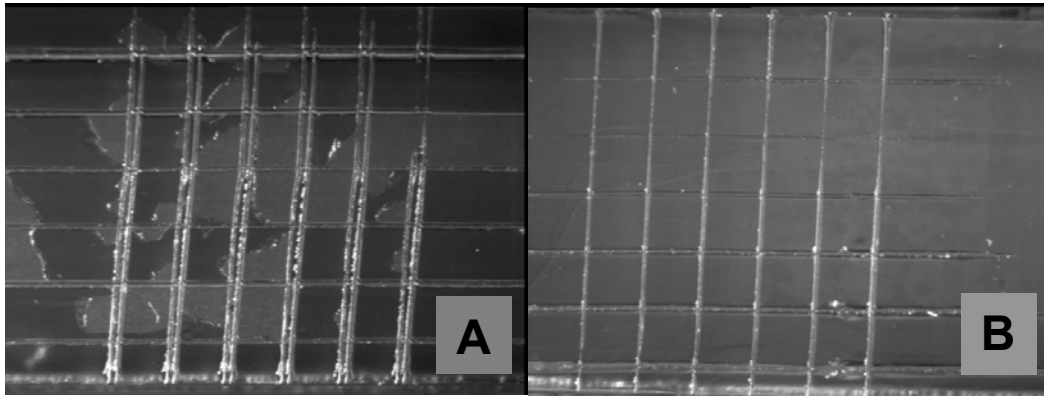


Figure 3.5 Tape test results for aqueous based PU/PVP coated lens. Control samples, untreated polypropylene samples (A), exhibit poor coating adhesion as noted by coating delamination. IOL material (B) exhibited strong adhesion to coating material as indicated by no observation of coating delamination.

3.3 Extractable Test Method – Leachable Impurities from Coating

3.3.1 Introduction

The objective of the study was to determine the allowable limits of leachable or extractable impurities from the aqueous based PU/PVP coating, specifically polyurethane (PU) and polyvinylpyrrolidone (PVP).

3.3.2 Experimental Design

All samples were coated with the aqueous based PU/PVP coating and sterilized. The coated samples were extracted in 5 mL of saline solution (0.9% NaCl) at 37°C for 72 hours (conditions identical to those in toxicity study). After extraction, the amount of leachable polyvinylpyrrolidone (PVP) and polyurethane (PU) was quantified. Extracts were analyzed for leachable PVP and PU separately using gas chromatography (68). The average amounts of extractable or leachable PVP and PU per lens were calculated. These quantities tested were tested in the toxicity studies (i.e., sensitization and ocular

irritation tests) and thus were considered as proof-safe levels or minimum acceptance criteria of extractable for coated lenses upon receipt of favorable results.

3.3.3 Results

The average amount of extractable or leachable PVP and PU from the aqueous based PU/PVP coating was 26.9 and 49.0 μg per sample, respectively. (Table 3.2) These levels were later used for toxicity testing to determine if these levels were safe and did not have a toxic effect.

Table 3.2 Leachable levels (PU & PVP) from aqueous based PU/PVP coating.

Group	PVP ($\mu\text{g}/\text{sample}$)	Polyurethane ($\mu\text{g}/\text{sample}$)
1	26	50
2	28	50
3	26	60
4	29	50
5	26	40
6	27	50
7	29	50
8	26	60
9	25	40
10	27	40
Average	26.9	49.0

3.4 Toxicity Testing – MEM Cytotoxicity Test Method

3.4.1 Introduction

In vitro tests were conducted on coated samples using the aqueous based PU/PVP coating to determine the potential for cytotoxicity. Toxicological studies were

conducted to determine the potential for cytotoxicity based on ISO 10993: Biologic Evaluation of Medical Devices for cytotoxicity guidelines (69).

3.4.2 Experimental Design

Mouse fibroblast cells were exposed to test extract (aqueous based PU/PVP coating extract), reagent control, positive control, and negative control in open wells containing single strength Minimum Essential Medium (MEM) supplemented with 5% serum and 2% antibiotics (1X MEM) in a gaseous environment (5% carbon dioxide) at 37°C for 24 hours.

Following incubation, the cultures were examined microscopically (100X) to evaluate cellular characteristics and percent lyses per well documented procedures. Cellular characteristics were evaluated using the grading scale in Table 3.3.

Table 3.3 Grading scale for evaluating cellular characteristics and percent lyses.

Grade	Reactivity	Observation
0	None	Discrete intracytoplasmic granules; no cell lysis
1	Slight	Not more than 20% of the cells are round, loosely attached; some cell lyses present
2	Mild	Not more than 50% of the cells are round and devoid of intracytoplasmic granules; no extensive cell lyses
3	Moderate	Not more than 70% of the cell monolayer contains rounded cells or are lysed
4	Severe	Nearly complete destruction of the cell monolayer

Each culture was evaluated for percent lysis using the chart in Table 3.4. To validate this test, the reagent control and the negative control must have a reactivity of

none (grade 0) and the positive control must have a grade 3 or 4.

Table 3.4 Grading scale for determining the percent lysis for cell cultures.

Grade	Observation
Slight	< 20% lysis
Mild	20 – 50% lysis
Moderate	50 – 70% lysis
Severe	> 70% lysis

The test sample would meet the requirements of the test if the biological response is less than or equal to grade 2 (mild). These results provided the maximum levels that produce a toxic environment.

3.4.3 Results

Under the conditions of this study, the 1X MEM aqueous based PU/PVP coating extract showed no evidence of causing cell lysis or toxicity (Table 3.5). The 1X MEM aqueous based PU/PVP coating extract met the requirements of the test. The reagent control, negative control, and the positive control performed as anticipated.

Table 3.5 Cytotoxicity results of aqueous based PU/PVP coating extracts. (n=3)

Sample Description	Confluent Monolayer	Percent Rounding	Percent Lysis	Grade	Reactivity
Coating Test (1A)	(+)	0	0	0	None
Coating Test (1B)	(+)	0	0	0	None
Coating Test (1C)	(+)	0	0	0	None
Negative Control (1A)	(+)	0	0	0	None
Negative Control (1B)	(+)	0	0	0	None
Negative Control (1C)	(+)	0	0	0	None
Reagent Control (1A)	(+)	0	0	0	None
Reagent Control (1B)	(+)	0	0	0	None
Reagent Control (1B)	(+)	0	0	0	None
Positive Control (1A)	(-)	90	90	4	Severe
Positive Control (1B)	(-)	90	90	4	Severe
Positive Control (1C)	(-)	90	90	4	Severe

3.5 Accelerated Aging - Coating Stability Test Method

3.5.1 Introduction

Accelerated aging studies are intended to determine the stability of the aqueous based PU/PVP coating for a period of time by subjecting the samples to elevated temperatures and humidity.

3.5.2 Experimental Design

Briefly, samples coated with aqueous based PU/PVP coating were placed in humidity controlled ovens at 43 ± 2.5 °C and a relative humidity (RH) of 40% to 50%. Samples were pulled at accelerated time points of 1.5, 2, and 3 years (70). Samples were allowed sufficient time to equilibrate to ambient conditions before testing. Testing for each time point was completed and compared to initial results, including measuring

the amount of leachable or extractable PVP and PU as well as lens delivery testing. Aging times were determined based on the well documented equations from ISO 11979-6 (39). Lenses were inspected before and after delivery to determine the effects of aging on coating cosmetic appearance and coating adhesion.

3.5.3 Results

The average (n=5) amount of extractable PVP and PU from the aqueous based PU/PVP coating was initially (t=0) 247 µg and 206 µg per sample, respectively. The average (n=5) amount of extractable PVP and PU per sample after 3 years accelerated aging was 245 µg and 210 µg, respectively. Results indicate that there is no significant difference in extractable levels of PVP and PU between the coating that was subjected to accelerated aging and initial coating results (Student's t-test: $p>0.3$). There was also no significant difference in lens delivery testing including coating integrity following delivery between initial and aged coating (Student's t-test: $p>0.05$).

3.6 Biocompatibility Testing – Acute Intracutaneous Reactivity Test Method

3.6.1 Introduction

In vivo biocompatibility tests in rabbits were conducted on aqueous based PU/PVP coated samples to determine the potential to produce irritation and sensitization at levels observed in extractable testing.

3.6.2 Experimental Design

The aqueous based PU/PVP coating was extracted in sodium chloride and cotton seed oil at 37°C for 72 hours. Coating extracts and negative controls were injected intracutaneously into five separate sites on one side of three rabbits. Similarly,

the corresponding reagent control was injected on the opposite side of each rabbit. Sites were observed immediately after injection, 24 hours, 48 hours, and 72 hours post injection for erythema and edema based on standard ISO test methods as directed by FDA guidance documents (38, 39).

3.6.3 Results

All injection sites appeared normal immediately following injection. The Primary Irritation Index Characterization for each extract is summarized in Table 3.5. Under the conditions of this study, there was no evidence of significant irritation or toxicity immediately after injection, 24 hours, 48 hours, and 72 hours post injection from the aqueous based PU/PVP coating extracts injected intracutaneously into rabbits. The Primary Irritation Index Characterization for the extracts was negligible.

Table 3.6 Biocompatibility results for aqueous based PU/PVP coating extracts. (in sodium chloride and cotton seed oil, n=3)

Extraction Solvent	Animal #	Test Score Average	Control Score Average	Primary Irritation Score	Primary Irritation Score Total	Primary Irritation Index Characterization
Saline control	1	0.0	0.0	0.0	0.0	Negligible
	2	0.0	0.0	0.0		
	3	0.0	0.0	0.0		
Cotton Seed Oil	4	.04	0.3	0.1	0.1	Negligible
	5	0.1	0.1	0.0		
	6	0.5	0.3	0.2		

3.7 Overall Discussion – Physical Properties of Lubricious Coating

The aqueous based PU/PVP coating (LubriLAST coating Patent No. 6,238,799 & 6,866,936, AST Products, Inc.) overcomes many of the physical and processing limitations of current hydrophilic coatings. The technology uses a simple, aqueous-based process that produces a superior interpenetrating network-type lubricious coating that is slippery only when it is wet. The coating consists of a chemically cross-linked supporting PU network with long-chain hydrophilic PVP molecules intertwined within its polymer matrix. Crosslinking the supporting PU matrix enhances coating integrity and improves cohesive properties. Lens delivery and adhesion data demonstrated the superior adhesion of the coating to the lens. These properties allow the coating to be stable and not erode from the surface under relatively mild conditions as readily as polymers deposited by simple evaporation. Accelerated aging demonstrated that the coating is in fact stable at elevated temperatures in the presence of moisture. In summary, the coating provided lubricity and superior adhesion but also provided a very flexible and durable coating.

Unlike coatings that use organic solvents there is no need to capture and dispose of hazardous materials. The use of a coating with an organic solvent posed issues related to manufacturing as well as limitations relating to incorporating drugs or other bioactive agents. Eliminating organic solvents also allows the ability to incorporate bioactive ingredients that are incompatible or that could be degraded upon exposure to organic solvents. Leachable data indicated that only low levels of polyurethane and

PVP are extracted from the coating. In addition, cytotoxicity and biocompatibility testing verified that these levels of leachables are safe.

The aqueous based PU/PVP coating not only provides superior lubricity and adhesion but also provides a platform for drug delivery. Aqueous-based systems offer flexibility in formulation. By varying the chemistries and formulations, different coating properties can be enhanced to provide a very flexible and resilient coating while also enhancing surface lubricity and releasing bioactive agents. By modifying the supporting polymer network, different specifications may be achieved (37). This PU/PVP coating was later modified for drug delivery and is described in the following chapters.

CHAPTER 4

AIM 2: DETERMINE MOST EFFECTIVE PHARMACOLOGIC AGENTS

The specific aim is to investigate the effects of pharmacologic agents on LEC proliferation and migration, and inflammatory cell activation through in vitro testing. This series of experiments determined the concentration level required to effectively reduce inflammation by inhibiting inflammatory cells and reduce capsular fibrosis by inhibiting LECs migration and proliferation (Figure 4.1). Human lens epithelial cell lines (cell line CRL-11421, ATCC) and isolated human peripheral blood monocytes (human volunteers) were used for this investigation. The optimal drug concentrations were determined based on a series of in vitro tests, including LECs growth inhibition assay (4.1), LECs migration assay (4.2), and inflammatory cell activity assay (4.3).

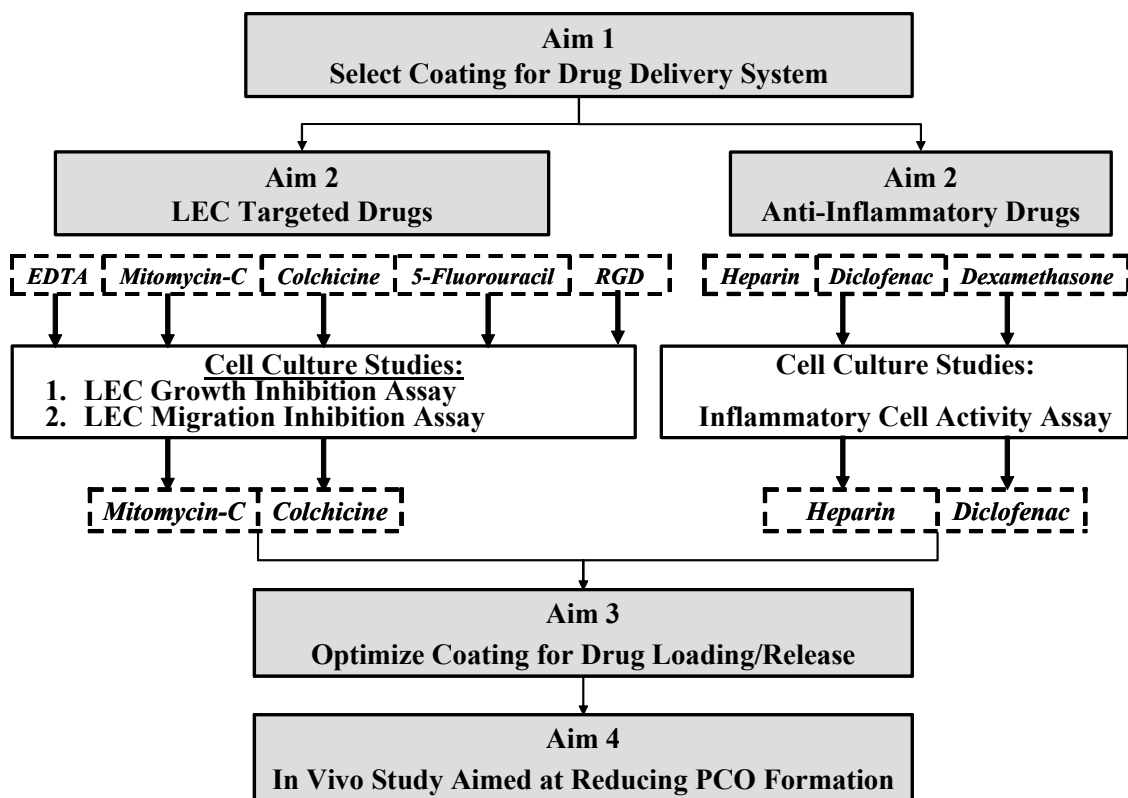


Figure 4.1 Experimental design for Aim 2.

4.1 LEC Growth Inhibition Assay

4.1.1 Introduction

The purpose of this test is to determine minimum effective concentrations of selected drugs to inhibit human lens epithelial cell (cell line CRL-11421, ATCC) proliferation according to the ISO method (9363-1:1994(E)).

4.1.2 Experimental Design

One (1.0) mL of the test article extracts or controls were added, in triplicate, to each well of a 24-well tissue culture plate. Separate plates are created for the Time 0 controls. 200 μ L of a LEC suspension (2×10^5 cells/mL) were added to each well, and the plates placed in a $37 \pm 1^\circ\text{C} / 5 \pm 1\%$ CO₂ humidified incubator. After approximately one hour, the Time 0 plates were removed, and the wells washed three times in Phosphate Buffered Saline (PBS, without calcium or magnesium). After the final wash, 1.0 mL of PBS were added to the wells and the plates stored at $2 - 8^\circ\text{C}$. After 72 hours, the remaining plates were removed from incubation and the wells washed three times in PBS. The PBS was removed from the Time 0 plates at this time. Negative (non-toxic) controls consisting of DMSO and EMEM were included. A moderately positive (moderately toxic) control consisting of black rubber as well as a highly positive (toxic) control consisting of CdCl₂ was included.

For the protein determination, 2.0 mL of Lowry E were added to each well and BSA control. The samples were placed into incubation in the dark, for approximately 1 hour at room temperature. Next, 0.2 mL of Lowry F were added to each sample, mixed well and the samples returned to the dark and incubated at room temperature for

approximately 30 minutes at which time the resultant solutions were read on a spectrophotometer at 660 nm.

The percentage of Growth Inhibition (%GI) was determined using the following method:

$$\%GI = 100 - [100 \times \{(T - C_o) / (C_E - C_o)\}]$$

T = mean absorbance @ 660nm of test article at various time points

C_o = mean absorbance @ 660nm of negative control at t=0 of the assay

C_E = mean absorbance @ 660nm of negative control at end of assay

The %GI is the ratio of the difference in protein level of the test article and initial levels compared to the difference in protein level of the negative control and initial levels. Therefore, if the drug has no effect, the protein levels for the test article will be the same as the negative control at any time point. As a result, the difference between test article and initial reading compared to negative control and initial readings is the same resulting in 0% GI.

Final evaluations of the validity of the assay were based upon the criteria listed below. The following criteria must be met for a test to be considered valid. The high positive control, CdCl₂, should induce a %GI greater than or equal to 100%. The moderately positive control, black rubber, should induce a %GI of at least 50%. The negative control replicates should induce a relative %GI less than 10%. A %GI between 50-100% was indicative of severe inhibition. A %GI of 100% means that no cellular growth was noted. Treatments that induced inhibition rates (%GI) over 50% were considered to have induced a positive response.

4.1.3 Results

The growth inhibition assay evaluated the potential of the drug to induce inhibition of LEC growth as indicated by the amount of protein release. The negative controls harvested at 72 hours induced inhibition rates between 0 and 7.4%. The positive controls both induced growth inhibition rates of 100% as indicated by the absence of protein. With these results, the assay was determined to be valid.

Mitomycin-C inhibited cell growth effectively. LEC growth inhibition (GI) was present at all concentrations for MMC (Figure 4.2) as indicated by 100%GI. The lowest concentration to generate an inhibitory response was 0.0005 mg/mL.

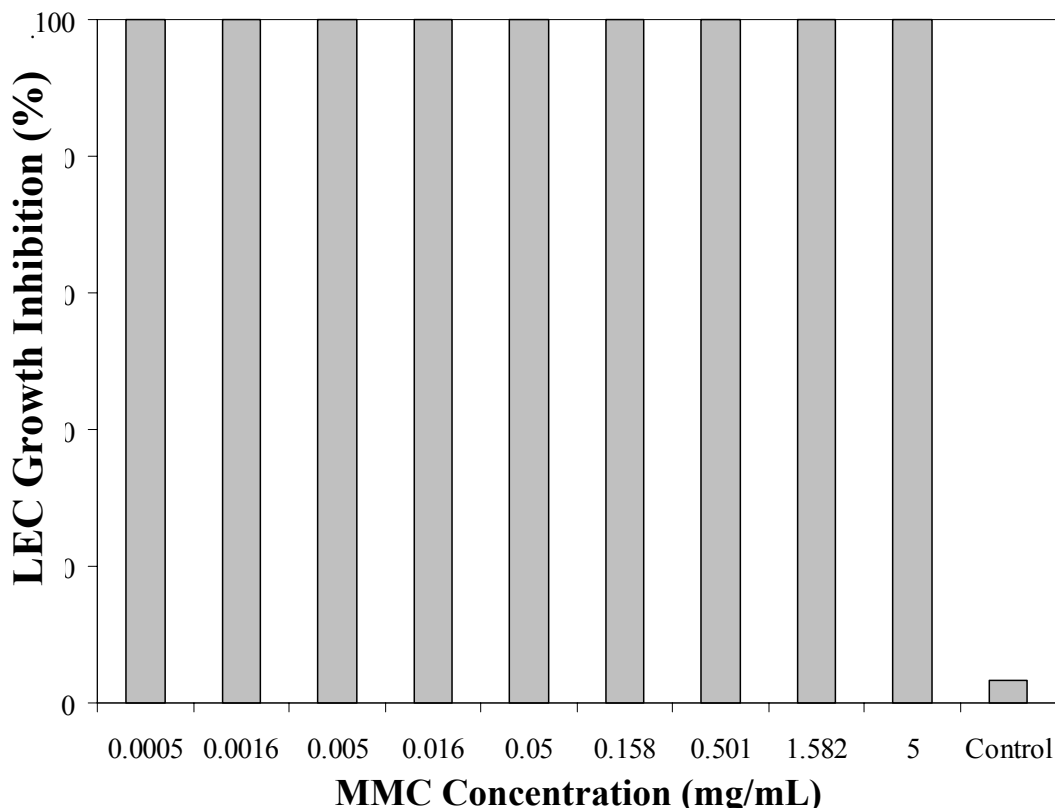


Figure 4.2 Percentages of LEC growth inhibition for various concentrations of MMC versus the saline control.

Colchicine also effectively inhibited cell growth. LEC growth inhibition (GI) was present at all concentrations for colchicine (Figure 4.3) as indicated by 100%GI. The lowest concentration to generate an inhibitory response was 0.0005 mg/mL.

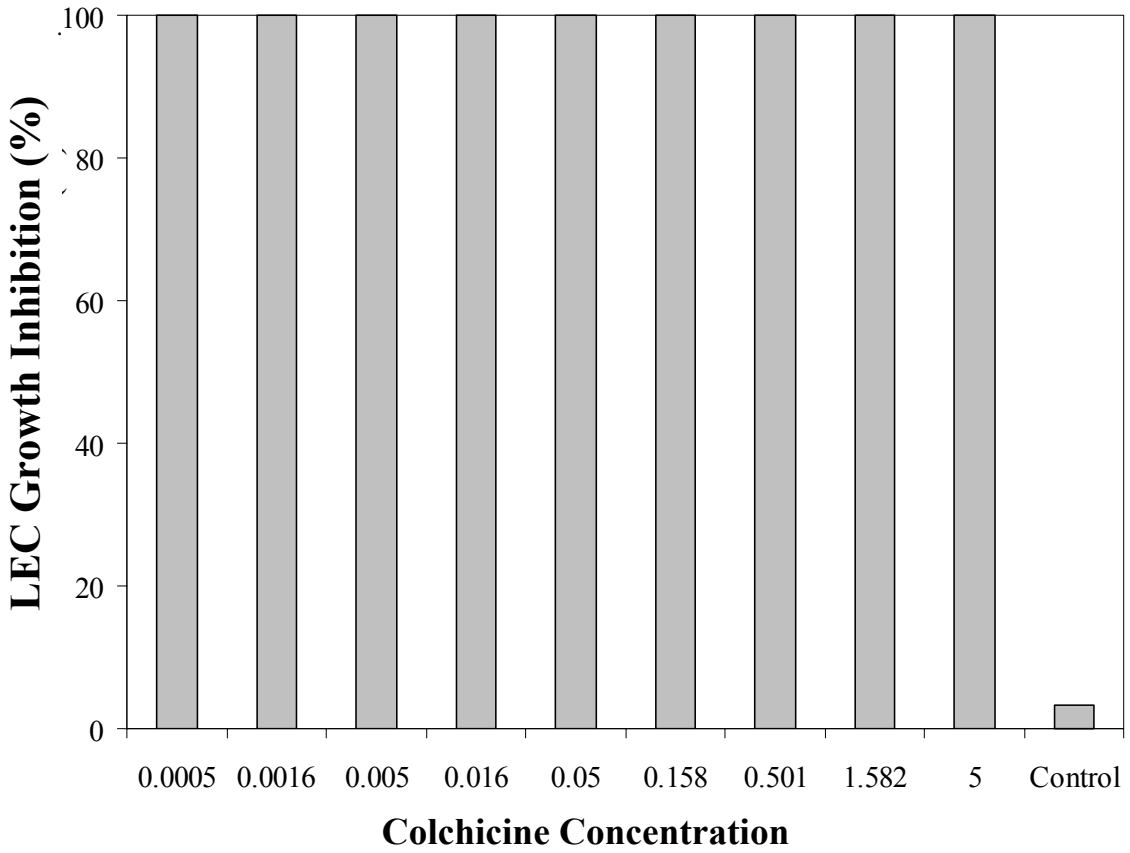


Figure 4.3 Percentages of LEC growth inhibition for various concentrations of colchicine versus the saline control.

5-Fluorouracil produced a dose dependent response for inhibiting cell growth. Significant cell growth reduction (>50% GI) was observed in the presence of 5-fluorouracil concentrations of 1.582 mg/mL. Growth inhibition was greatly enhanced to >75% with 5-fluorouracil concentrations of 5 mg/mL (Figure 4.4).

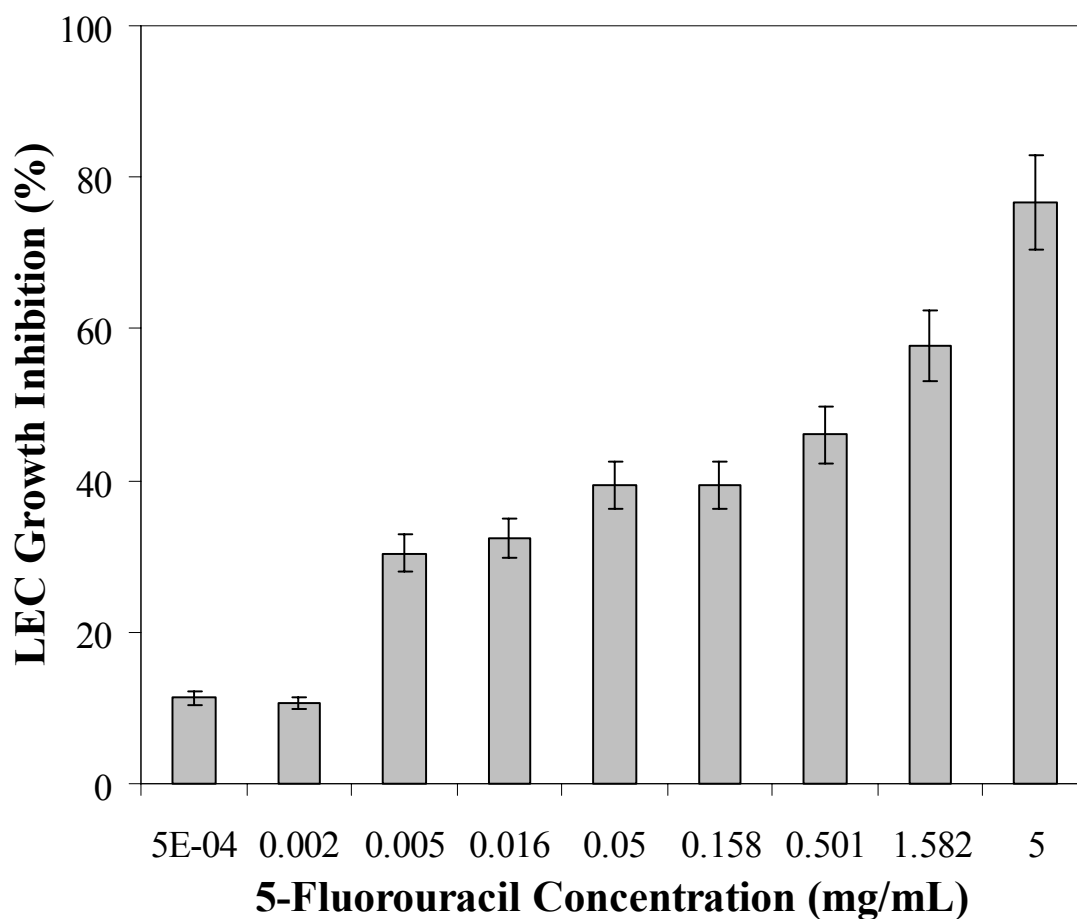


Figure 4.4 Percentages of LEC growth inhibition for various concentrations of 5-fluorouracil.

EDTA exerted dose-dependent growth inhibition. The cell proliferation inhibition effect of EDTA was not stable when EDTA concentrations <0.01 mg/ml. Significant growth inhibition (>50% GI) was observed when EDTA concentrations reached 0.32 mg/ml. At 1.0 mg/ml or higher, LEC growth inhibition reached >90% (Figure 4.5).

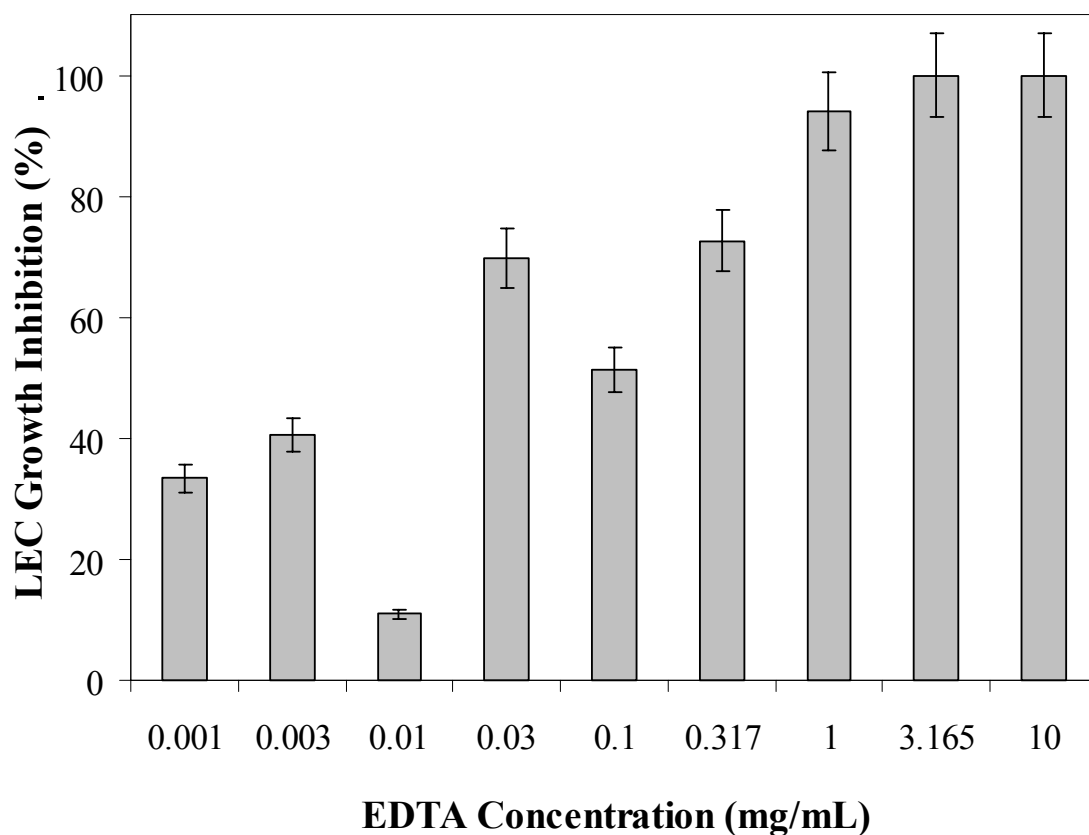


Figure 4.5 Percentages of LEC growth inhibition for various concentrations of EDTA.

RGD peptide also produced a dose dependent response for inhibiting LEC growth (Figure 4.6). RGD-peptide was in effective in completely inhibiting LEC growth at low concentrations. Significant growth inhibition (>50% GI) was only observed when RGD-peptide concentrations reached 5.0 mg/ml. Since RGD required high concentrations to inhibit LEC growth, RGD was removed from future study.

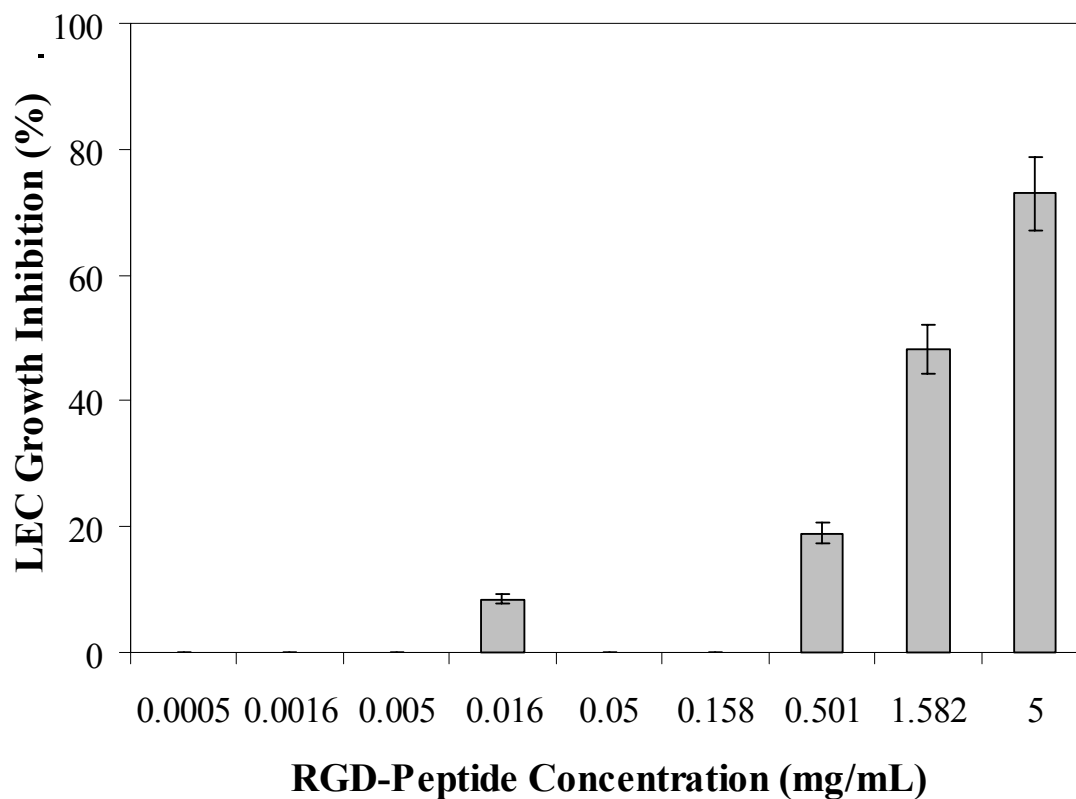


Figure 4.6 Percentages of LEC growth inhibition for various concentrations of RGD-peptide.

Dexamethasone was not effective in inhibiting LEC growth. No concentrations inhibited LEC growth as indicated by >50% GI (Figure 4.7). Since dexamethasone has minimal effect on LEC growth, we thus removed dexamethasone from future study.

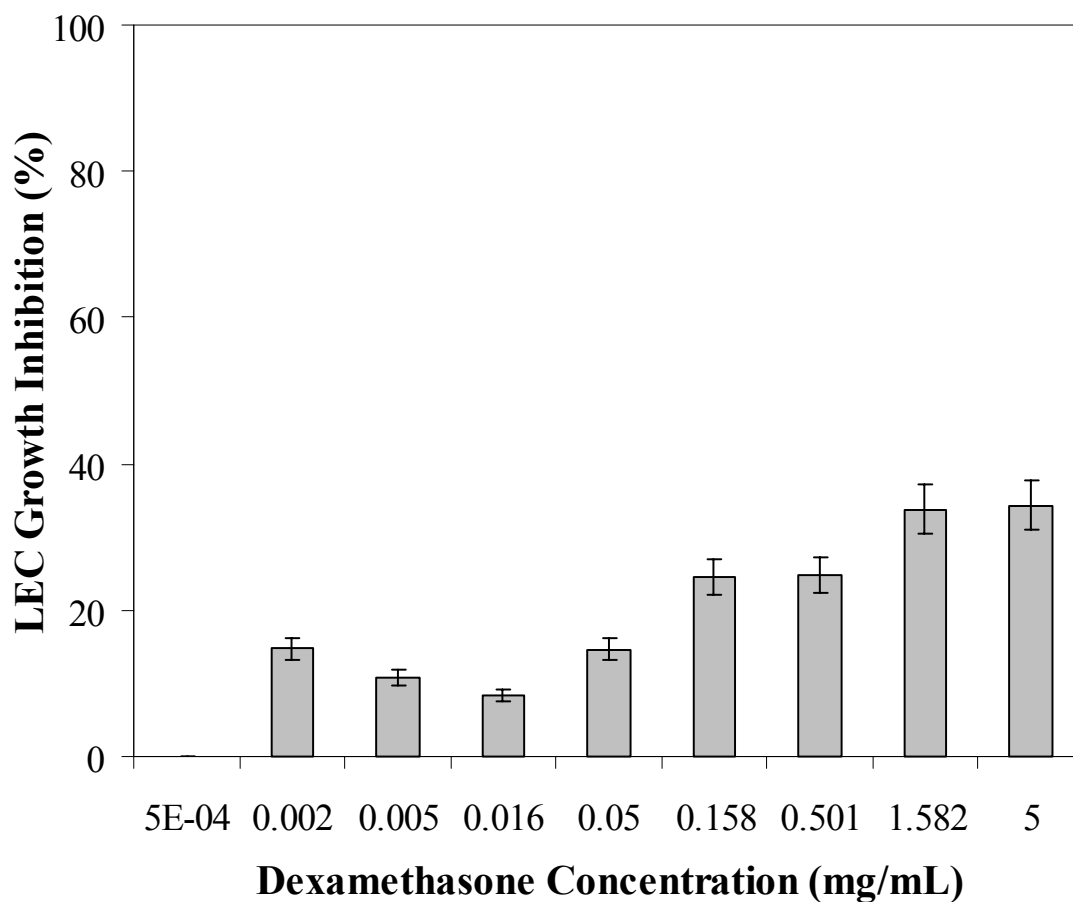


Figure 4.7 Percentages of LEC growth inhibition for various concentrations of dexamethasone.

Diclofenac also produced a dose dependent response in inhibiting LEC growth. Diclofenac demonstrated that it was a potent LEC growth inhibitor. Diclofenac concentrations of >0.158 mg/mL inhibited LEC growth (>50% GI) as observed in Figure 4.8. At concentrations of 0.5 mg/ml or higher, LEC growth inhibition reached >90%.

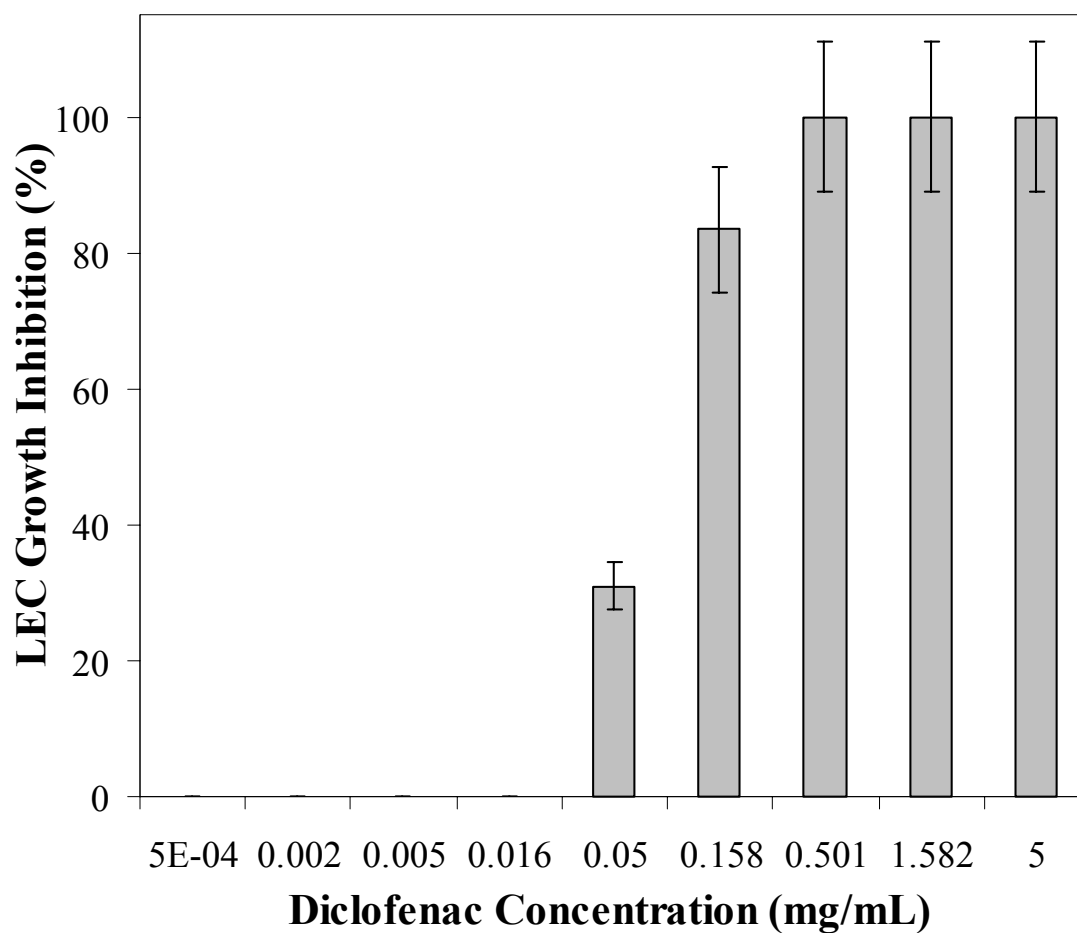


Figure 4.8 Percentages of LEC growth inhibition for various concentrations of diclofenac.

Heparin, rather unexpectedly, had minimal impact on LEC growth. It must be noted that low molecular weight (4500 Da) heparin was utilized for this study. Low MW heparin was not effective in inhibiting LEC growth as indicated by > 50% GI (Figure 4.9). Growth inhibition ranged from 29.2% at 0.003 mg/mL to 0% at 2.5 and 0.792 mg/mL.

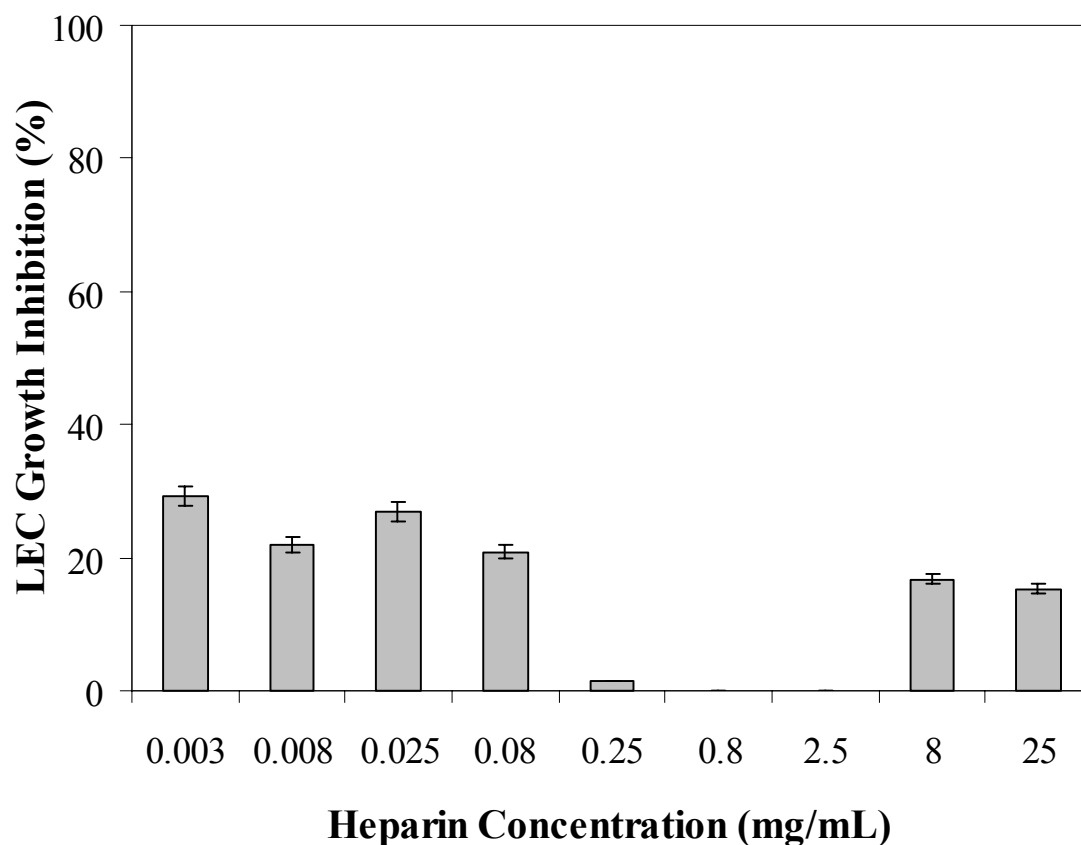


Figure 4.9 Percentages of LEC growth inhibition for various concentrations of heparin.

4.2 LEC Migration Assay

4.2.1 Introduction

The purpose of this test is to evaluate the inhibitory effects of drugs on the migration of human lens epithelial cell (cell line CRL-11421, ATCC).

4.2.2 Experimental Design

The test article and controls were prepared under aseptic conditions just prior to use. The vehicle, E-MEM + 10% FBS, was used to dilute the test article. The following dilutions were used: 5.0, 1.58, 0.5, 0.16, 0.05, 0.02, 0.005, 0.002 and 0.0005 mg/mL final concentration in culture.

Once the test article or control dilutions were prepared, cells were added at a concentration of 10,000 cells/mL. Labeled 60 mm plates were set up with a sterile tissue culture ring in the center of the plate. A volume of approximately 0.2 mL of diluted cell suspension was seeded into each ring. If necessary, additional test or control article were added to flood the plate. The plates were incubated for approximately 3 hours at $37 \pm 1^\circ\text{C}$ in a humidified atmosphere of $5 \pm 1\%$ CO_2 in air. After 3 hours, the location of the rings was marked. Once marked, the rings were removed and the plates photographed. The plates were then returned to incubation. The plates were observed and photographed by a phase-contrast microscope at 1, 3, 5 and 7 days. Untreated culture medium served as the negative control. Positive controls were prepared by mixing 0.1 mL of 10 mM CdCl_2 in 9.9 mL of culture medium.

Final evaluation of the validity of the assay and test article results was based upon the following criteria and scientific judgments. The negative control plates should

show evidence of new growth throughout the area beyond the original ring location. The positive control should not show evidence of growth beyond the original ring location. The assay was not valid if any of the above criteria was not met.

The distance from the initial culture ring to the leading edge of growth were photographed, measured, and recorded. The percent cell confluence was determined and compared to controls at each time point. If cells were not present beyond the original ring location, the drug effectively inhibited cell migration. Likewise, if confluent layer of cells was present past the original ring location, then the drug was ineffective in inhibiting cell migration. The percent cell confluence was then calculated for each individual drug concentration at various time points up to 14 days.

4.2.3 Results

The negative cultures, LEC monolayers exposed to media only, exhibited healthy growth throughout the experiment past the original ring location. The cells appeared to be healthy as indicated by the cell morphology, i.e. elongated or flattened. It must be noted that when healthy cells attach to the surface of the cell culture plate, the cells spread out and appear elongated or flattened. The positive cultures, LEC monolayers exposed to CdCl₂, exhibited a toxic response as indicated by complete cell death or rounded cells. As a result, the positive cultures did not contain cell growth past the original ring location and showed no signs of cellular activity. Therefore, the system was responding normally and met the criteria for a valid assay. Cell migration assay results for each individual drug over a range of concentrations are discussed in the following section.

The effect of EDTA on cell migration was dose dependent. When exposed to concentrations lower than 0.16 mg/ml, EDTA had little effect on LEC migration (Figure 4.10). Figure 4.13A illustrates the non-inhibitory effect (>90% LEC confluency) of EDTA at concentrations of 0.16 mg/mL or lower. At concentrations of 0.50 mg/mL (Figure 4.10) EDTA blocked adhesion molecule integrins and inhibited >80% of LEC migration while concentrations of 1.58 mg/mL (Figure 4.10) inhibited 100% of LEC migration.

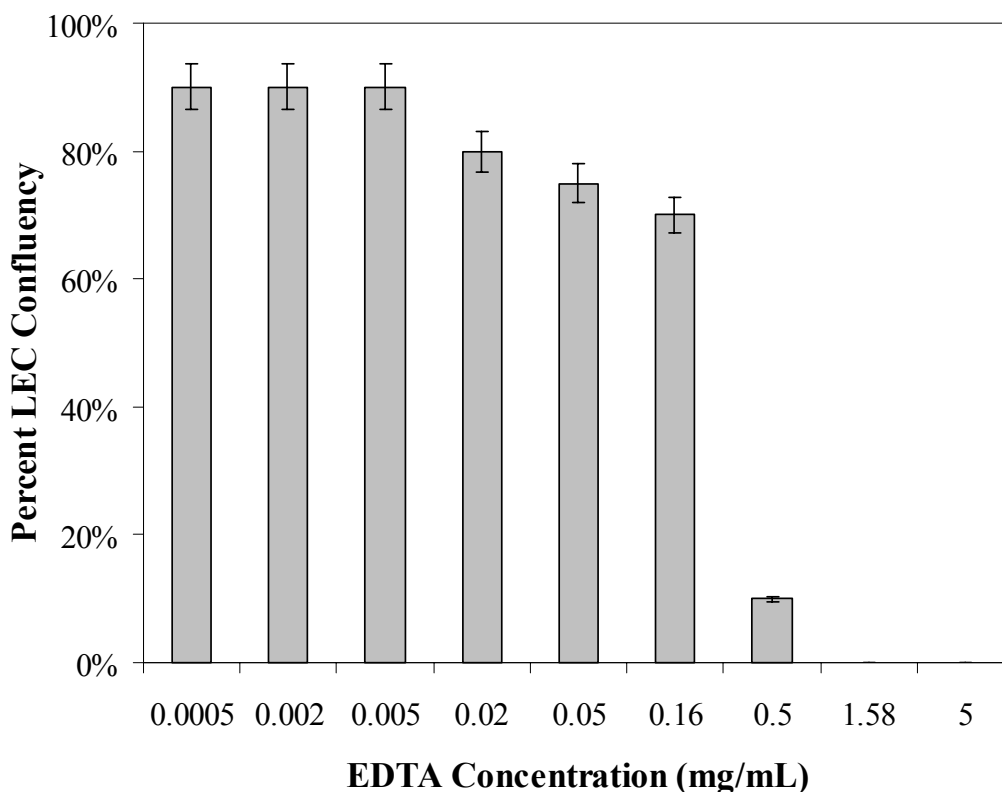


Figure 4.10 The percentage of LEC confluency following the treatment of various concentration of EDTA after 14 days. The LEC monolayer confluency was reduced for concentrations of EDTA above 0.32 mg/mL. Concentrations above this level possessed less than 10% confluency indicating the EDTA effectively inhibited cell migration.

The effect of RGD-peptide on cell migration was dose dependent RGD-peptide has also been shown to reduce LEC colonization by blocking adhesion molecules. Below 0.02 mg/ml, RGD-peptides had no influence on LEC survival as indicated by >80% LEC confluency. With concentrations above 0.05 mg/ml, less LEC migration was observed (Figure 4.11). Concentrations as low as 0.16 mg/mL effectively inhibited cell migration as indicated by <30% confluency past the original ring location. When the concentration reached 1.58 mg/ml or higher, RGD-peptide caused almost 100% of LECs detachment and thus inhibited LEC migration.

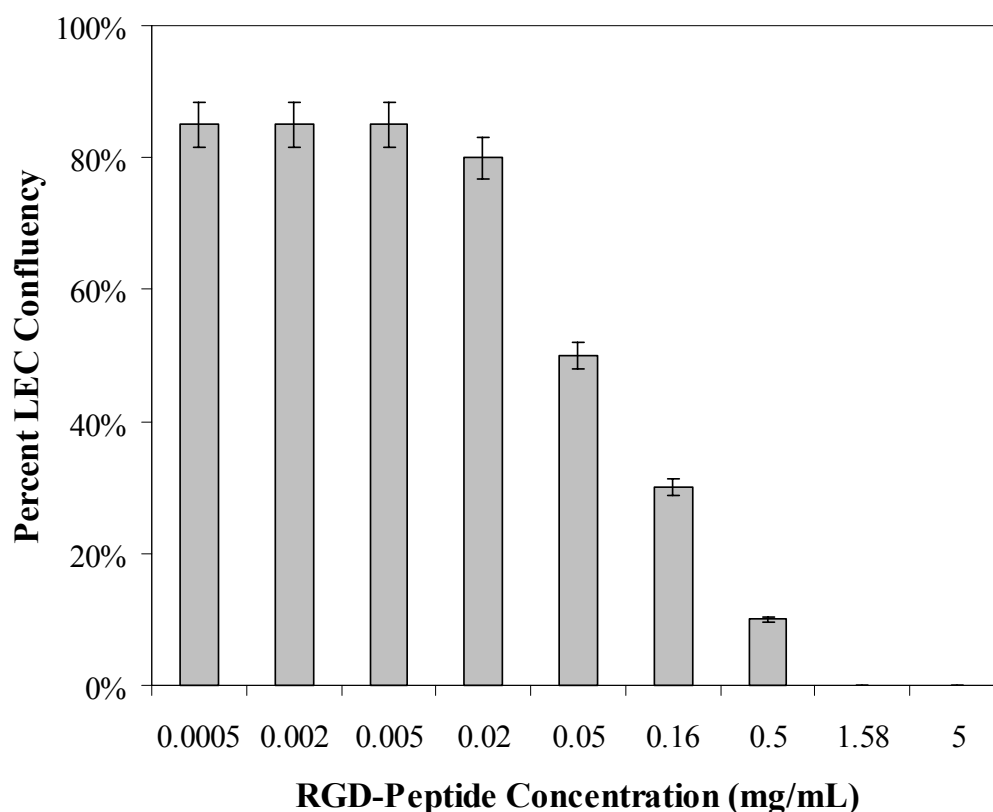


Figure 4.11 The percentage of LEC confluency following the treatment of various concentration of RGD-peptide after 14 days.

The reduction of LEC migration by low MW heparin treatment was dose-dependent. With concentration less than 0.005 mg/ml, heparin had no influence on LEC activity. The LEC confluency started to decrease when heparin concentrations were higher than 0.02 mg/ml (Figure 4.12). To achieve >70% cell inhibition, it was critical that the heparin release was 0.5 mg/ml or higher.

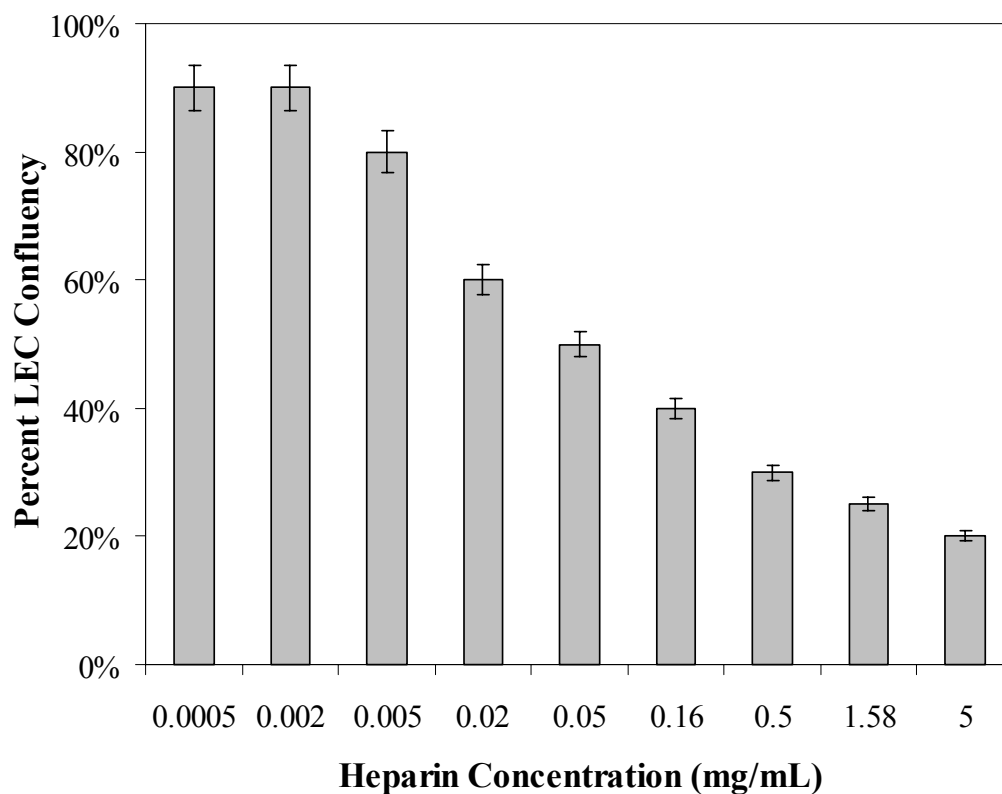


Figure 4.12 The percentage of LEC confluency following the treatment of varying concentrations of heparin after 14 days.

5-Fluorouracil (5-FU) has shown to have a potent effect on reducing LEC migration/proliferation. With only 0.0005 mg/ml of 5-FU, LEC migration was partially inhibited migration as indicated by 40% LEC confluency. Concentrations as low as 0.002 mg/mL effectively inhibited cell migration after 14 days as indicated by <30% confluency past the original ring location (Figure 4.13). When the concentration reached 0.050 mg/ml, 5-FU caused all LECs to detach from test surfaces and thereby completely inhibit LEC migration.

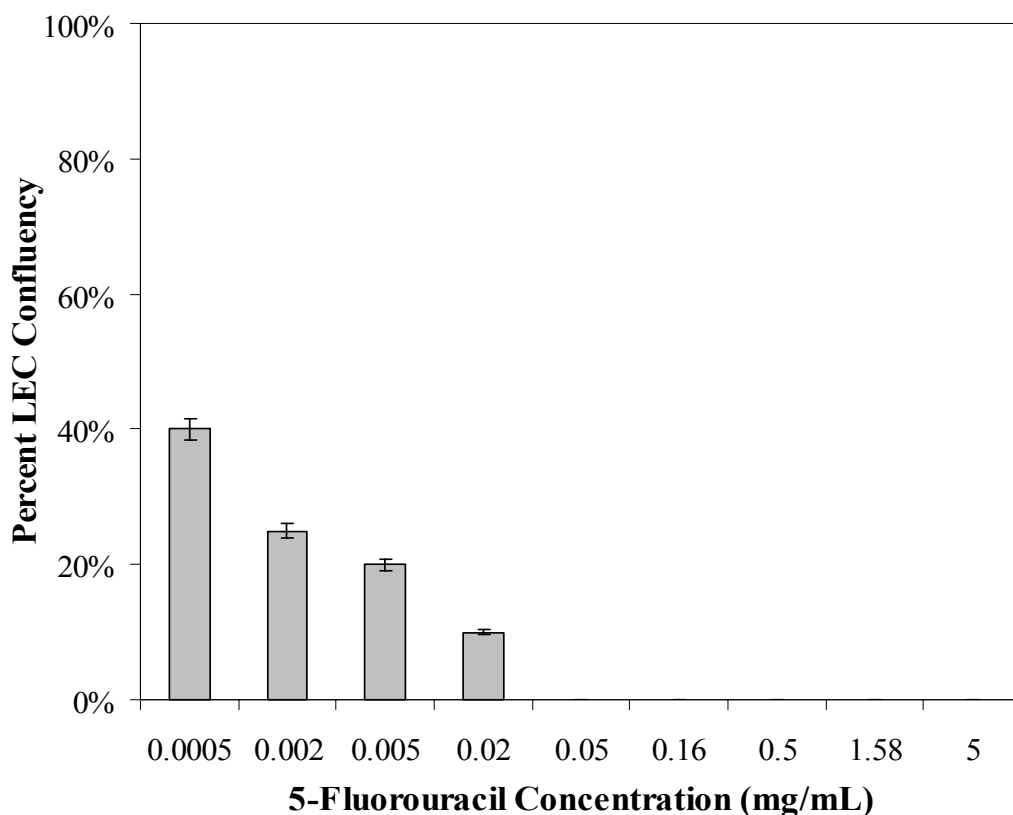


Figure 4.13 The percentage of LEC confluency following the treatment of various concentration of 5-FU after 14days. LEC migration as measured by percent confluency past original ring location after exposure to varying concentrations of 5-fluorouracil for 14 days. Concentrations of 0.002 mg/mL and higher are sufficed to inhibit cell migration as indicated by <30% confluency.

All colchicine concentrations (0.0005 to 5.0mg/mL) inhibited LEC migration up to 14 days after exposure as indicated by 0% LEC confluency past the original ring location. The addition of colchicine caused cell morphology changes from elongated, healthy cells to rounded cells indicating loss of cell function.

All MMC concentrations (0.0005 to 5.0mg/mL) inhibited LEC migration up to 14 days after exposure as indicated by 0% LEC confluency past the original ring location. After the addition of MMC, cell morphology changed from elongated, healthy cells to rounded cells indicating loss of cell function.

4.3 Inflammatory Activity Assay

4.3.1 Introduction

The purpose of this test is to evaluate the inhibitory effects of drugs on the inflammatory response using cultured human peripheral blood mononuclear cells (PBMC). PBMCs are involved in the inflammatory response system in humans. Use in an in vitro system allows sufficient modeling to capture potential responses to systemic insults.

4.3.2 Experimental Design

PBMCs or monocytes were isolated from whole blood obtained from human volunteers (with human subject protocol in submission) using Ficoll gradient separation according to published procedures. Monocytes were further isolated from PBMC by cell attachment onto a tissue culture dish overnight. Three dilutions (0.10, 1.0, 10.0 mg/mL) of the test material and controls were prepared in DMEM supplemented with 10% fetal bovine serum, 2 mM glutamine, 100 U/mL penicillin, 100 µg/mL streptomycin at 37°C

in 5% CO₂. The anti-inflammatory actions of the drugs were tested at the cytokine level. Specifically, cell culture supernatants were harvested and analyzed for released cytokines (TGF-beta, IL-6, IL-1 β , and IFN- γ ; IL-10) by enzyme-linked immunosorbent assay (ELISA) according manufacturer's recommendations.

The cell density was adjusted to 2.5×10^4 cells/mL with culture media. The cell suspension (1.0mL) was seeded into each well of a 24 well plate. The test article dilution or control was added at 100 μ L/culture. Untreated culture medium served as the negative control. The spent culture medium was removed and 1.0mL of medium added. The negative control or test article dilution (0.1mL) was added to the appropriate well. The plates were returned to incubation for approximately 24 hours.

Quantifications of TGF- β 1, IFN- γ , IL-10, IL-1 β , or IL-6 production were made using R&D Systems ELISA kits (Minneapolis, MN). TGF- β 1 were evaluated by kit DB100B, IFN- γ by kit DIF50, IL-10 by kit D1000, IL-1 β by kit DLB50, and IL-6 by kit DY206. The manufacturer's instruction for use of the kits was followed. Final evaluation of the validity of the assay and test article results was based upon the criteria listed below and scientific judgments. The negative control plates should show no significant evidence of TGF- β 1, IFN- γ , IL-10, IL-1 β , or IL-6. The positive controls for each ELISA type (TGF- β 1, IFN- γ , IL-10, IL-1 β , or IL-6) should demonstrate a positive response. The assay was not valid if any of the above criteria was not met.

4.3.3 Results

No cytokines were detected for all concentrations of dexamethasone (DEX), diclofenac (DI), heparin (HEP), or colchicine (COL). Under the conditions of this study,

all concentrations effectively reduced the inflammatory response by inhibiting PBMC cell growth. The negative control and the positive control performed as anticipated. As a result, dexamethasone, diclofenac, heparin, and colchicine demonstrated that each effectively reduces inflammatory responses in vitro by inhibiting PBMC cell growth at concentrations as low 0.1 mg/mL as indicated by absence of chemical mediators (Figure 4.14).

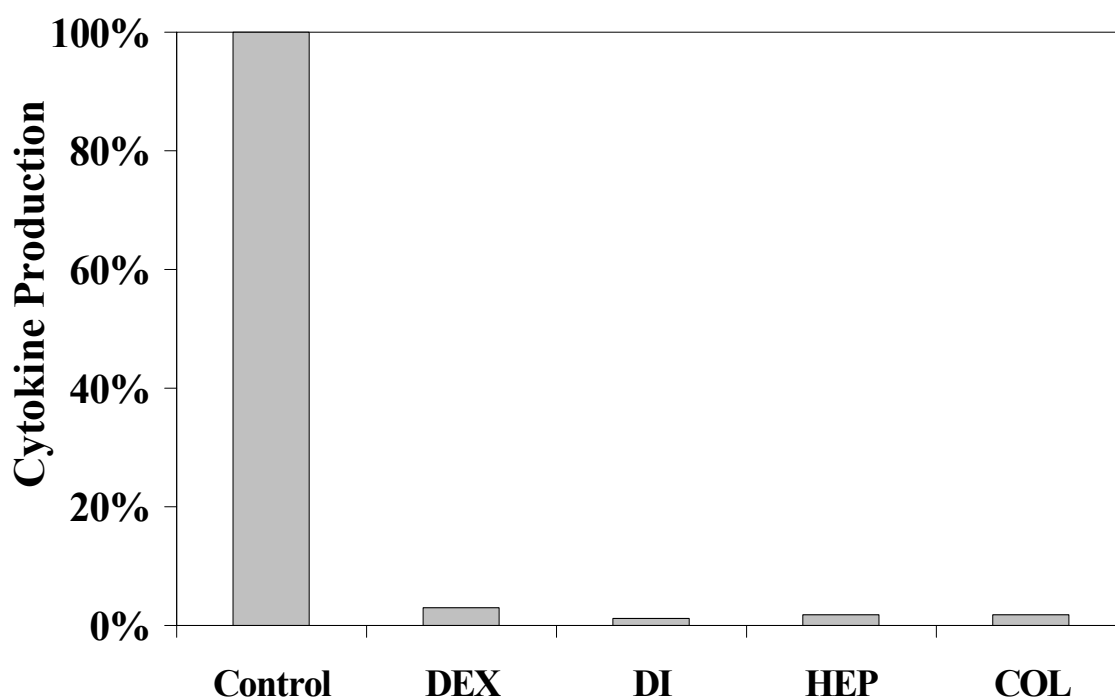


Figure 4.14 Inflammatory cell responses to pharmacologic agents. All concentrations effectively inhibited inflammatory cell activation as indicated by cytokine production, including TGF- β 1, IFN- γ , IL-10, IL-1 β , or IL-6.

4.4 Overall Discussion

Our overall goal is to design a drug release system which is capable of releasing a variety of pharmacological agents at effective concentration to reduce PCO formation. To achieve the goal, in vitro studies were carried out to determine the effective doses of various drugs in diminishing proliferation and migration of LEC and inflammatory cells. Specifically, we find:

1. MMC effectively inhibited LEC migration and LEC growth at concentrations as low as 0.0005 mg/mL. MMC appears to preferentially attack the rapidly dividing LECs, inhibited DNA synthesis, and produced cell death by apoptosis and necrosis.
2. Colchicine effectively inhibited LEC migration and LEC growth at concentrations as low as 0.0005 mg/mL. Colchicine also inhibited inflammatory cell activation at concentrations of 0.010 mg/mL. Results indicated that colchicine was effectively bonded with directly to microtubules disrupting polymerization and dynamics leading to inhibition of cell growth and migration.
3. Low MW heparin was ineffective in inhibiting LEC growth. Data indicates that low MW heparin does not effectively antagonize the function of selectins (cell-surface adhesion molecules) and therefore did not affect LEC growth. Unfractionated, high MW heparin may produce drastically different in vitro results due to increased in potency associated with the molecular weight of these molecules. However, low MW heparin has reduced non-specific binding

compared to high MW heparin which results in higher bioavailability that may affect in vivo performance. In vitro testing demonstrated that low MW heparin effectively inhibited inflammatory cell activation at low concentrations.

4. 5-FU inhibited LEC migration at relatively low concentrations (0.002 mg/mL) but had little effect on LEC growth. The inconsistent results may be associated with drug concentrations used in the study. 5-FU is transformed inside the cell into different cytotoxic metabolites which are then incorporated into DNA and RNA, that induce cell death. The LEC migration study contained significantly more drug per cell. It should be mentioned that this differential LEC growth and migration inhibition effect was not observed with other drugs.
5. RGD-peptide is the recognition motif for cell adhesion receptors and has been used to block cell adhesion and migration. However, our results have shown that substantial amounts of RGD-peptide are required to occupy all cell-surface adhesion receptors and effectively inhibit LEC migration and proliferation.
6. EDTA has been shown to inhibit LEC attachment/migration by redistributing or removing calcium and magnesium ions that are required for cell adhesion. Our results indicate that a minimum concentration of 0.5 mg/mL is required to inhibit cell migration.
7. Diclofenac, a non-steroidal anti-inflammatory drug (NSAID), inhibits the activation of inflammatory cells by inhibiting the release and/or production of chemical mediators. Our results have pointed out that diclofenac effectively inhibits inflammatory cell activation at concentration as low as 0.1 mg/ml.

Diclofenac inhibits LEC growth at concentration as low as 0.05 mg/mL. Diclofenac also inhibits the release and/or production of inflammatory cytokines.

8. Dexamethasone effectively inhibits inflammatory cell activation at concentration as low as 0.1 mg/ml. The minimal concentration of dexamethasone to inhibit LEC growth is 0.158 mg/ml.

In summary, LEC in vitro studies indicated that MMC and colchicine required minimum concentrations (0.0005 mg/mL) to effectively inhibit LEC migration and proliferations. Diclofenac, heparin, colchicine, and dexamethasone all required minimum concentrations (0.10 mg/mL) to effectively inhibit inflammatory cell activation as indicated the inflammatory cell studies. However, dexamethasone is a steroid which presents adverse effects including elevation of intraocular pressure, inhibition of wound healing, and facilitation of infections. As a result, diclofenac and heparin were further evaluated along with MMC and colchicine for drug loading and release properties associated with the aqueous based PU/PVP coating.

Table 4.1 Summary of minimum concentrations to effectively inhibit LEC growth, LEC migration, and inflammatory cell activation as determined by in vitro testing.

Pharmacologic Agent	Minimum Concentration (mg/mL) to Inhibit		
	LEC Growth*	LEC Migration**	Inflammatory Cell Activation
Mitomycin-C	0.0005	0.0005	N/A
Colchicine	0.0005	0.0005	N/A
5-Fluorouracil	1.582	0.002	N/A
EDTA	0.32	0.50	N/A
RGD Peptide	5.0	0.16	N/A
Heparin	>5.0	0.50	0.10
Diclofenac	>5.0	N/A	0.10
Dexamethasone	0.158	N/A	0.10

* LEC growth inhibition >50%

** LEC migration inhibition as indicated by <30% cell confluence

CHAPTER 5

AIM 3: OPTIMIZE COATING FOR DRUG LOADING & RELEASE

This series of experiments varied the coating formulation and process conditions in order to determine maximal drug loading and drug release kinetics. This included evaluation of two different drug loading methods, mix drug into coating solution and absorb drug into coating (Figure 5.1), in order to provide maximum drug loading capacities for the aqueous base PU/PVP coating. Specifically,

- I. Mix drug into coating solution: Interest drugs were mixed with lubricious coating solutions. Drug-loaded coating solution was then used to create hydrophilic coatings on IOLs.
- II. Adsorb drug into coating: IOLs were covered with lubricious coating. The coating is then swelled thereby absorbing the drug and impregnating it into the polymer matrix of the coating upon drying. Coating crosslink densities were varied using a designed experiment to optimize drug loading.

To examine the drug loading and release properties of these two coating methods, congo red dye was used as model drug in the early stage of this investigation. Based on the information obtained from the model drug- congo red, coatings were then further engineered to release four PCO-reducing drugs, including mitomycin-C, cholchicine, heparin, and diclofenac. Using in vitro model, the drug loading and release

profiles were determined (Figure 5.2). Specifically, we will first establish spectrophotometry methods to determine drug concentration in vitro (section 5.1.). To prolong the drug release duration, we then study coating preparation to maximize drug loading properties (section 5.2). Finally, the drug release properties (drug release amount and duration) were further improved in vitro (section 5.3).

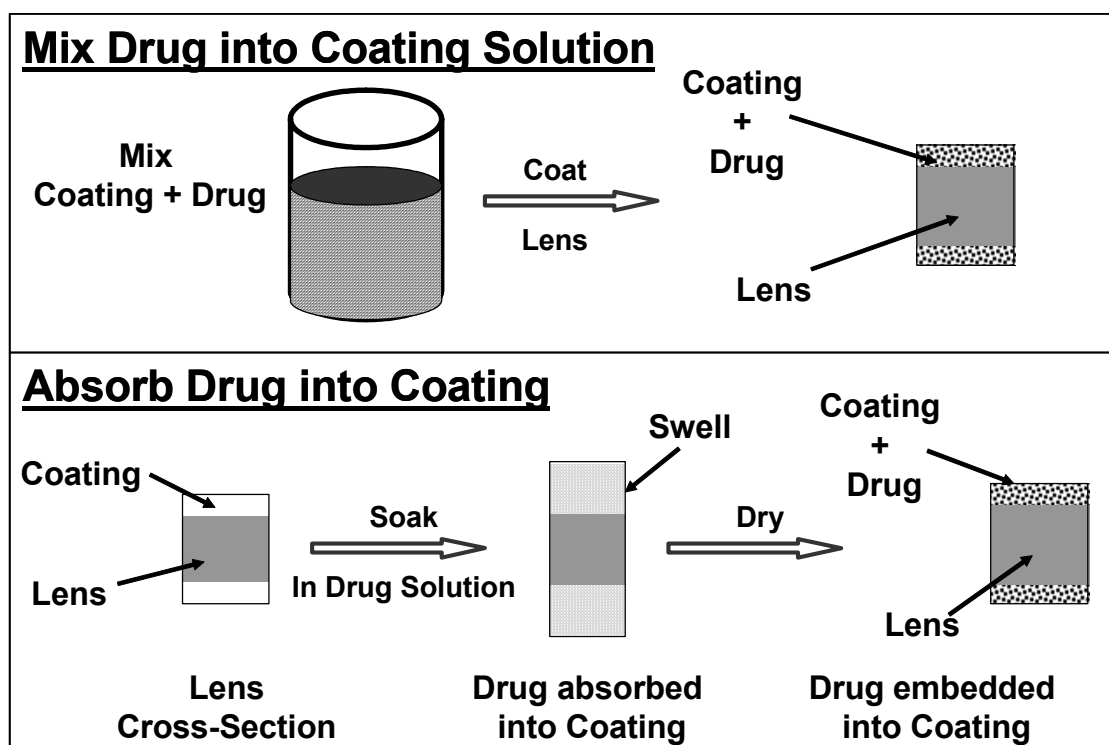


Figure 5.1 Drug loading methods to incorporate drugs into the lens hydrogel coating.

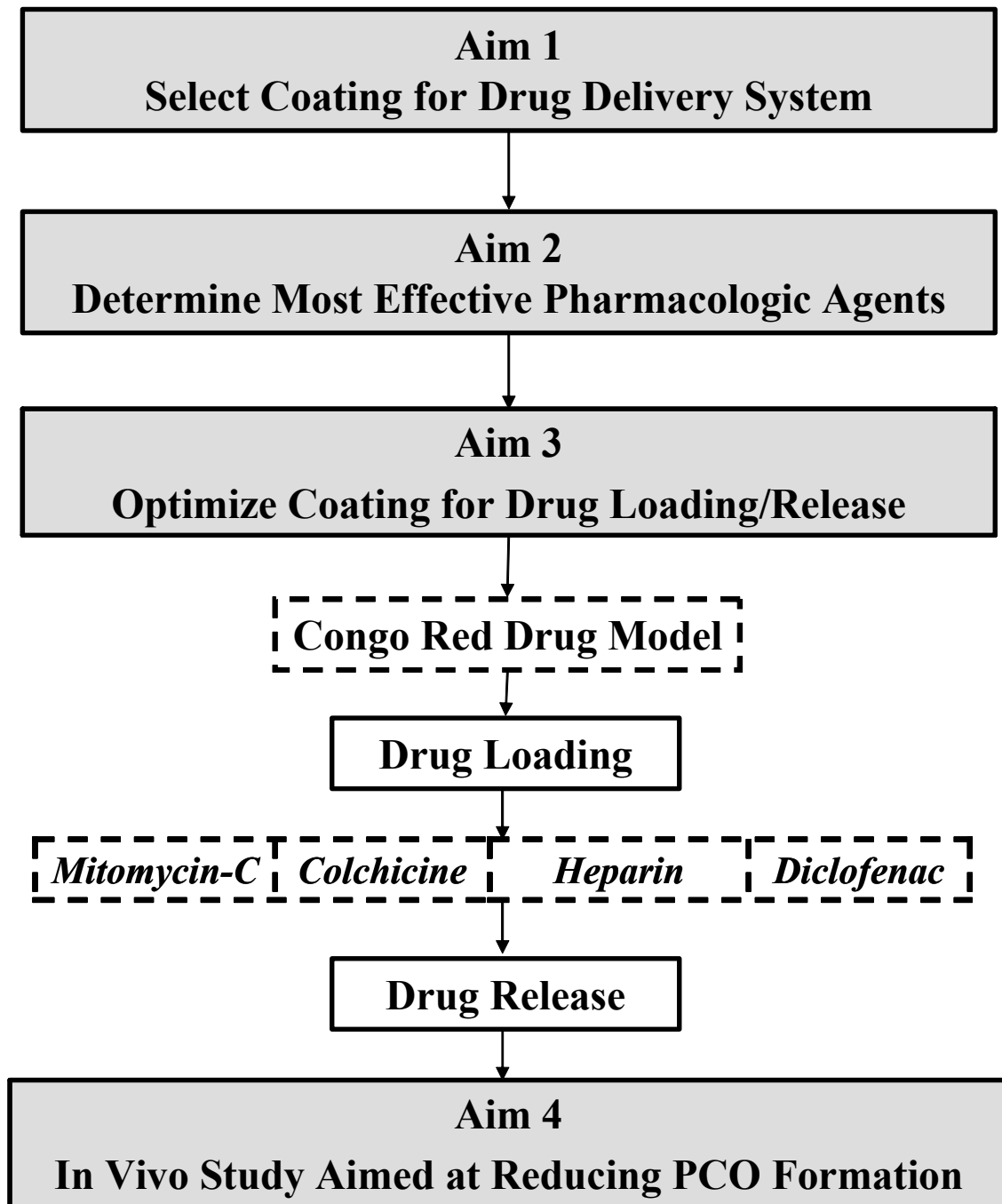


Figure 5.2 Flow chart of experimental design sequence for Aim 3.

5.1 To establish spectrophotometric measurements of drug concentrations in vitro

5.1.1 Introduction

A standard curve was produced by measuring the absorbance of known concentrations for each drug at specific wavelengths. A standard curve was then used to calculate the concentration level of unknown drug solutions.

5.1.2 Experimental Design

The absorbance of known drug concentrations was measured with a UV-visible spectrophotometer (Lambda 35 UV/Vis Spectrophotometer, Perkin Elmer, Wellesly, MA) at a specific wavelength. The wavelength for each drug, including congo red (model drug), diclofenac, colchicine, mitomycin-C, and heparin, was determined by choosing the most responsive and broadest peak over a full wavelength scan. Known concentrations of the drug or drug model were prepared in balanced salt solution (BSS) and measured at the specified wavelength with the spectrophotometer. The range of concentrations varied for each drug depending on the solubility of the drug and the target concentrations under this study. The resultant values produced a standard curve for each drug of absorbance versus drug concentration. This curve was then used to calculate concentration levels for unknown drug solutions (70).

5.1.3 Results

Conge red (Figure 5.3) was utilized as a drug model for screening experiments to optimize drug loading and release. Congo red has similar size and possesses similar properties as the selected drugs. As a result, it was expected to have similar drug release kinetics as the selected drugs. It has a known maximum absorbance at 497nm (Merck

Index). Congo red (MW=696.66) was visible even at low concentrations which allow gross evaluations of uptake and release. The standard curve for congo red illustrated a linear relationship (R-squared: 0.985) between drug concentration and absorbance with a minimum detection level of 47.2 $\mu\text{g/mL}$.

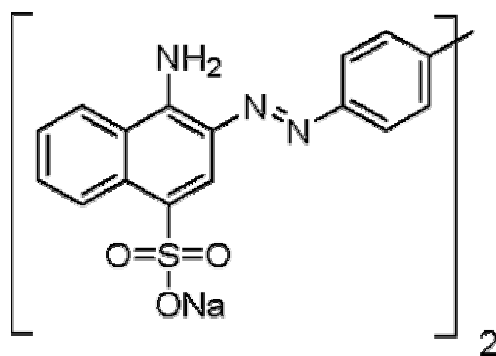


Figure 5.3 Molecular structure of the congo red drug model.

Diclofenac ($\text{C}_{14}\text{H}_{11}\text{NCl}_2\text{O}_2$, or 2-[2-(2,6-dichlorophenyl) aminophenyl] ethanoic acid) is soluble in water (50 mg/mL) and is a relatively small molecule with a molecular weight of 296.148 g/mol (Figure 5.4) (Merck Index).

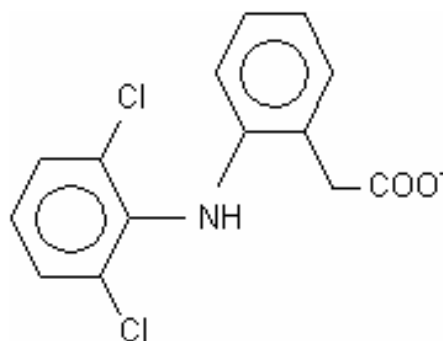


Figure 5.4 Chemical structure of diclofenac.

Diclofenac has a maximum absorbance at 340 nm as indicated by the most responsive and broadest peak over a full wavelength scan. The standard curve of various concentrations of diclofenac was then established (Figure 5.5). The diclofenac standard curve resulted in a linear relationship ($R^2 = 0.999$) between drug concentration and Absorbance (@340 nm). An R-squared term near 1.0 indicates that the curve is a good predictor of concentration with a known absorbance within the range of values analyzed. The limit of detection for diclofenac using this analytical technique was 0.39 mg/mL.

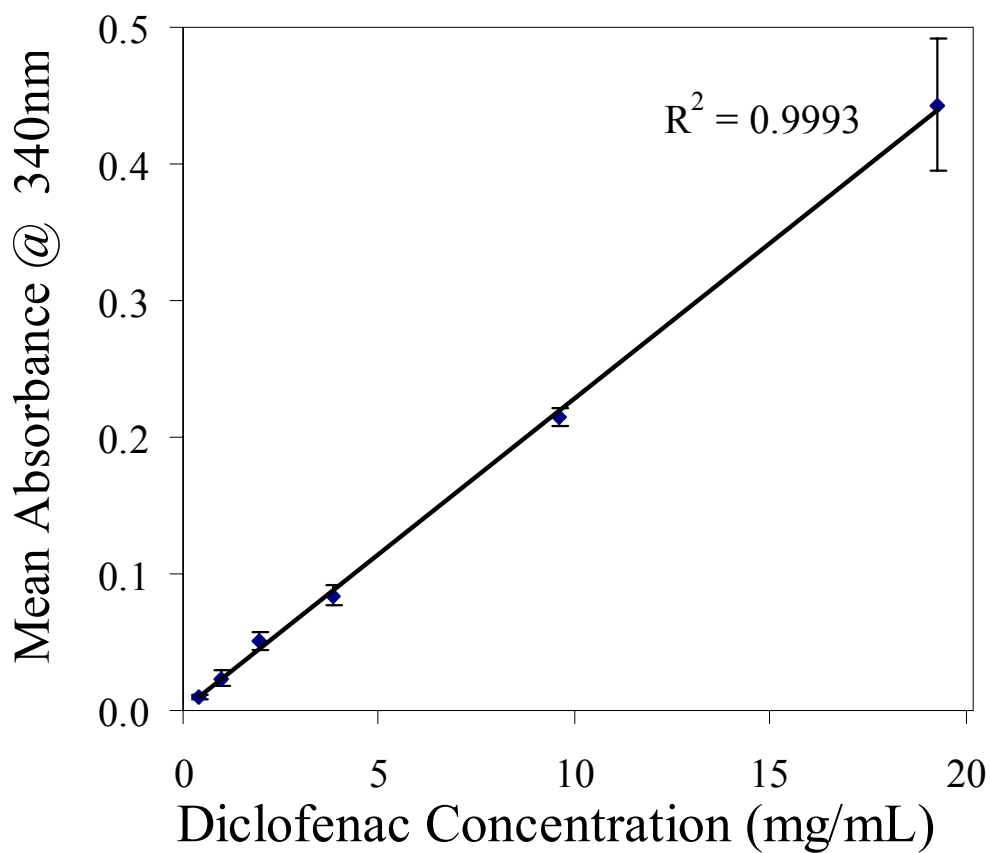


Figure 5.5 Standard curve for diclofenac. (n=5 for each point)

Colchicine ($C_{22}H_{25}NO_6$) is soluble in water (10 mg/mL) and is a relatively small molecule with a molecular weight of 399.44 g/mol (Figure 5.6) (Merck Index).

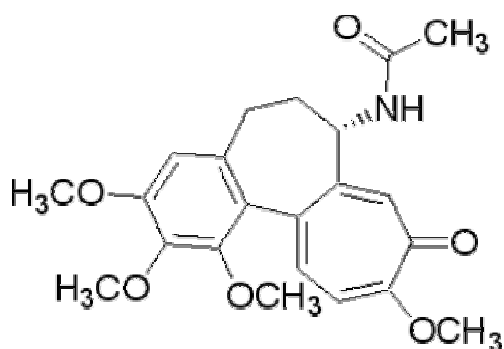


Figure 5.6 Molecular structure of colchicine.

Colchicine has a maximum absorbance at 410 nm as indicated by the most responsive and broadest peak over a full wavelength scan. The standard curve between colchicine concentrations and absorbance (@410 nm) has also been established ($R^2 = 0.986$) (Figure 5.7) with a minimum detectable concentration of 8.3 $\mu\text{g/mL}$.

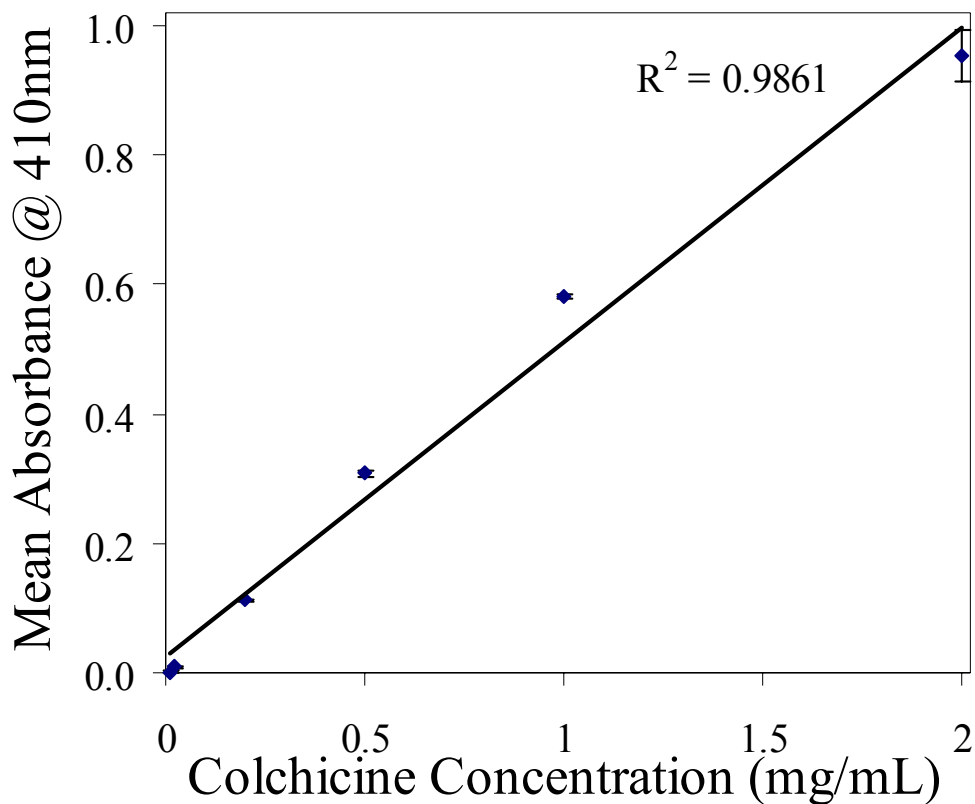


Figure 5.7 Standard curve for colchicine. (n=5 for each point)

Mitomycin-C ($C_{15}H_{18}N_4O_5$) is soluble in water (0.5 mg/mL) and is a relatively small molecule with a molecular weight of 334.33 g/mol (Figure 5.8) (Merck Index).

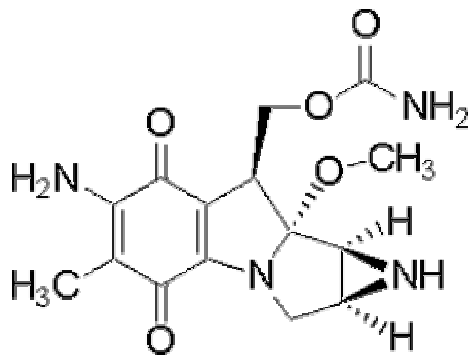


Figure 5.8 Chemical structure of MMC.

MMC absorbance was measured and its concentration standard curve was established at 600 nm (Figure 5.9) as indicated by the most responsive and broadest peak over a full wavelength scan. The minimum detectable concentration for MMC using this analytical technique was 10 µg/mL.

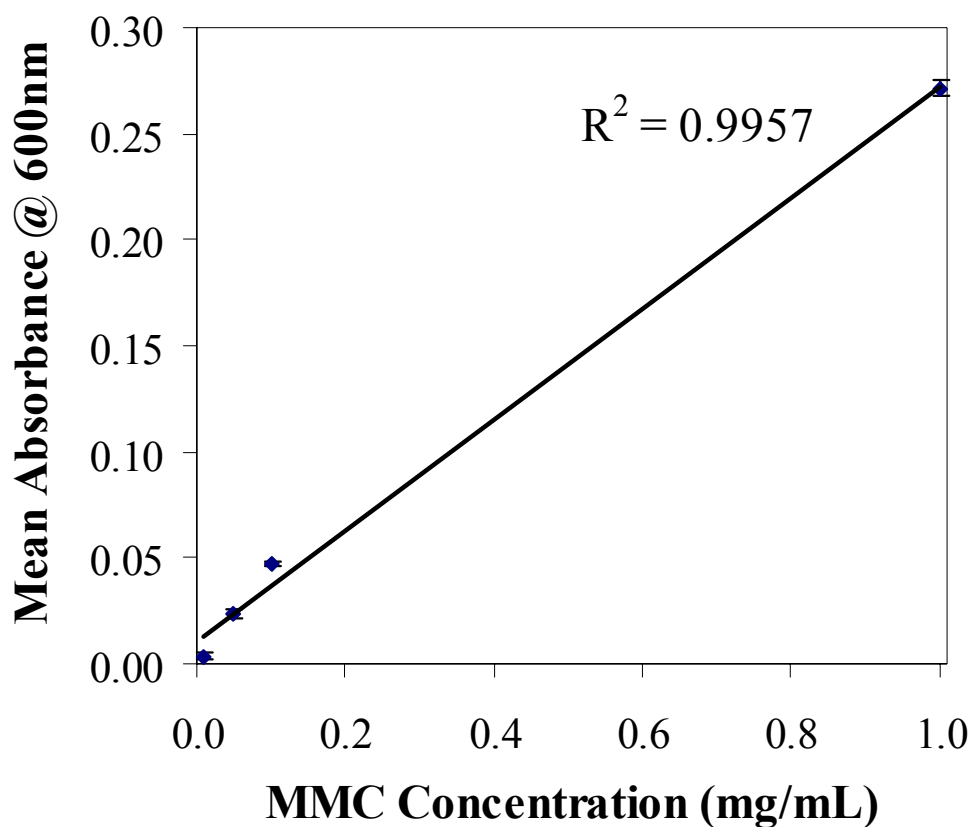


Figure 5.9 Standard curve for mitomycin-C. (n=5 for each point)

Low molecular weight heparin (Figure 5.10) (4.0 to 4.5kDa) with a solubility limit of 1mg/mL in water (Merck Index). Low MW heparin is depolymerized which destroy approximately 30% of the active sequences on unfractionated heparin. As a

result, low MW heparin has a lower affinity for proteins with reduced non-specific binding. As a result of reduced non-specific binding, low MW heparin has higher bioavailability.

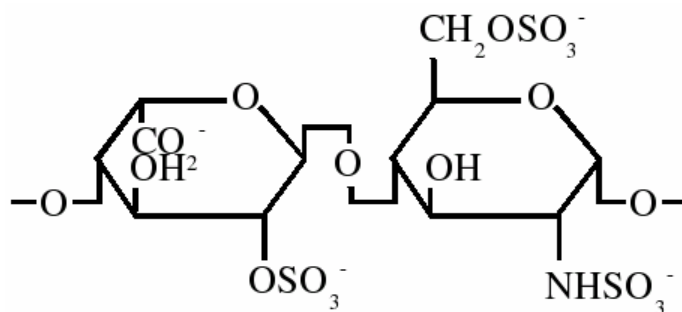


Figure 5.10 Molecular structure of heparin.

Heparin has maximal absorption at 280 nm as indicated by the most responsive and broadest peak over a full wavelength scan. The heparin standard curve (Figure 5.11) resulted in a linear relationship ($R^2 = 0.999$) between drug concentration and absorbance at 280nm. The minimum detectable concentration for heparin using this analytical technique was 10 mg/mL.

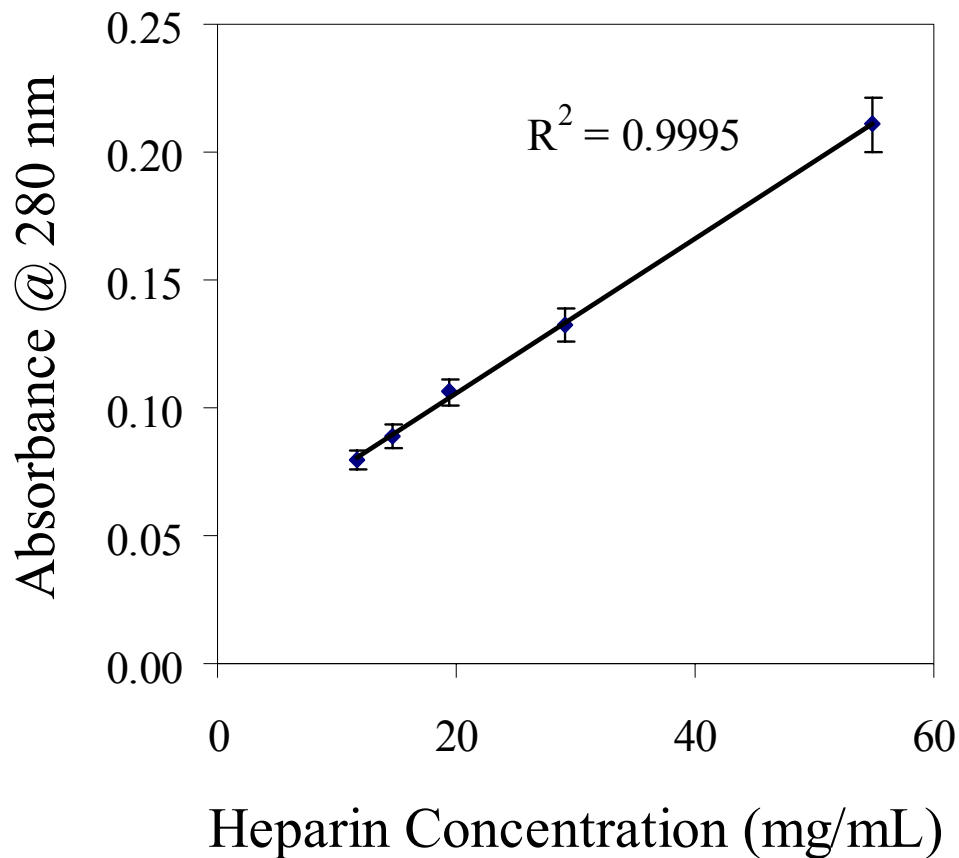


Figure 5.11 Standard curve for heparin (n=5 for each point).

5.2 Maximize Drug Loading

5.2.1 Introduction

The drug loading and release studies first investigated different methods to load drug into the PU/PVP coating. Congo red was utilized for screening experiments in determining optimal methods for maximum drug loading and controlled release.

Designed experiments were utilized to determine the optimal formulation and process conditions to obtain desired loading rates for the drug delivery system. Factors

included in this experiment included amounts of crosslinker, drug loading methods, drug concentration level, surface treatment, PVP content, and dry time. Two drug loading techniques were evaluated using the congo red drug model including (1) drug absorption into the coating (by swelling the coating) and (2) mixing the drug with the coating solution directly prior to applying to the lens. Each factor was evaluated based on its influence on effecting drug loading.

5.2.2 Experimental Design

In order to determine the method with maximum drug loading capabilities, a fractional factorial designed experiment was carried out to assess the following factors: 1) the drug loading method, 2) the amount of crosslinker, and 3) the drying process. A fractional design was utilized to explore the factors at two conditions (Table 5.1). Fractional factorials are efficient designs used to screen many factors to find the main factors that affect the measured response, i.e. drug loading and release.

Table 5.1 Key factors and testing conditions included in drug loading designed experiment.

Controlled Factors	Process Conditions	
	#1	#2
Drug Loading Method	Absorb drug into coating	Dissolve drug into coating solution
Crosslinker Content (Weight %)	0.73	1.50
Coating Dry Time (hours)	4	22

The amount of drug loaded into the coating was determined by the amount of total drug released. IOLs were coated with a single layer of coating, approximately 10 microns thick. The coating with low crosslinker concentration contained 0.254 mg/mL of congo red while the high crosslinker concentration contained 0.241 mg/mL of congo red. After coating, IOLs were dried in a 65°C oven for either 4 or 22 hours. Coated lenses were placed in 0.5 mL of balanced salt solution (BSS) at 37°C for drug release studies and measured at 24 hours. After 24 hours, lenses were removed and placed in new vials containing fresh BSS. The absorbance of the solution was measured using UV-Vis spectrophotometer at the appropriate wavelength to determine the concentration of the drug released during that 24 hours time period. The concentration of the test samples was obtained from the standard curve produced from known drug concentrations (70). All experiments were run in triplicate. Each experiment was completed using the same lot of materials and the same operator to eliminate any other sources of variation. All experiments were performed on the same day.

Data was analyzed using Design Expert 6.0 statistical software (Stat-Ease Inc.). Analysis included analysis of variance (ANOVA), lack of fit test, curvature test, and power calculations to obtain a model that provided a best fit curve for the data. Upon data analysis, a chart was produced to predict drug loading/release rates within the scope of the experiment.

5.2.3 Results

Drug loading properties were markedly different between two drug loading methods - (I) absorbed drug, and (II) drug premixed with coating solution. Spontaneous

drug adsorption method yields poor drug release profile after 24 and 48 hours. After 24 hours, the amount of drug released was 0.1 mg/mL for absorbed drugs while the drug premix coating produced higher drug release concentrations with 0.34 mg/mL. Rather disappointedly, these studies also uncovered that the majority of the drug was released within 48 hours. After 24 hours, drug loading method was the key factor to significantly (ANOVA, $p < 0.05$) affect drug loading (Appendix A) as indicated by the steepness of the curve in Figure 5.12. The steeper the slope of the line indicates that the factor has a more significant effect on the response, in this case 24 hour drug release.

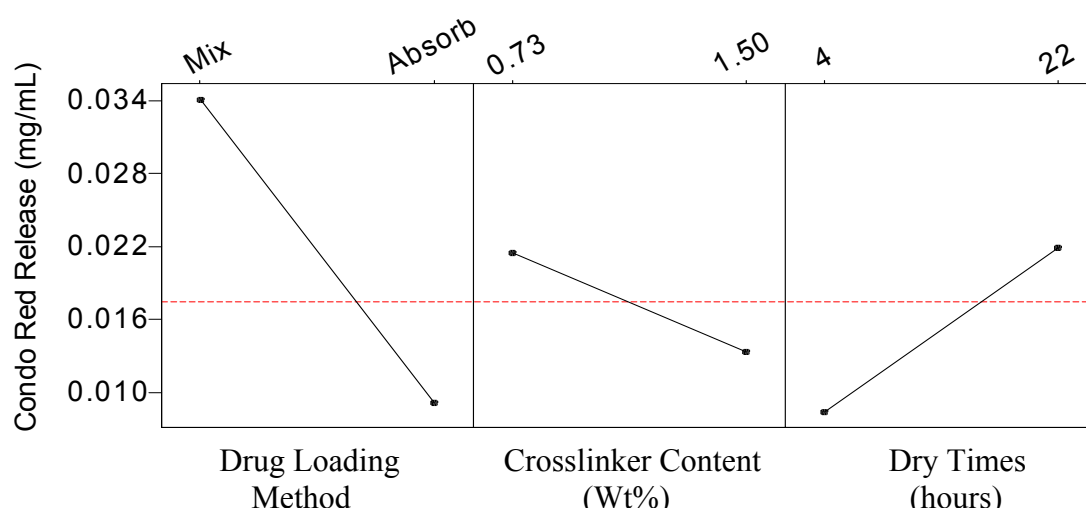


Figure 5.12 Main factors effecting drug loading after 24 hours. The drug loading method affected the amount of drug loaded into the coating as indicated by drug release after 24 hours (Left panel, ANOVA, $p < 0.05$). However, crosslinker content (middle panel) and dry time (right panel) have minimal effect on drug loading capability.

After 48 hours, the drug loading method was the only factor to significantly (ANOVA: $p < 0.05$) affect the amount of drug release (Appendix B). Factors that

significantly effected drug release are indicated by lines with high slope values as seen in Figure 5.13. Mixing the drug with the coating directly proved to provide the maximum drug concentration (Figure 5.13). Further experiments must be completed regarding other factors including amount of crosslinker to optimize the drug release properties.

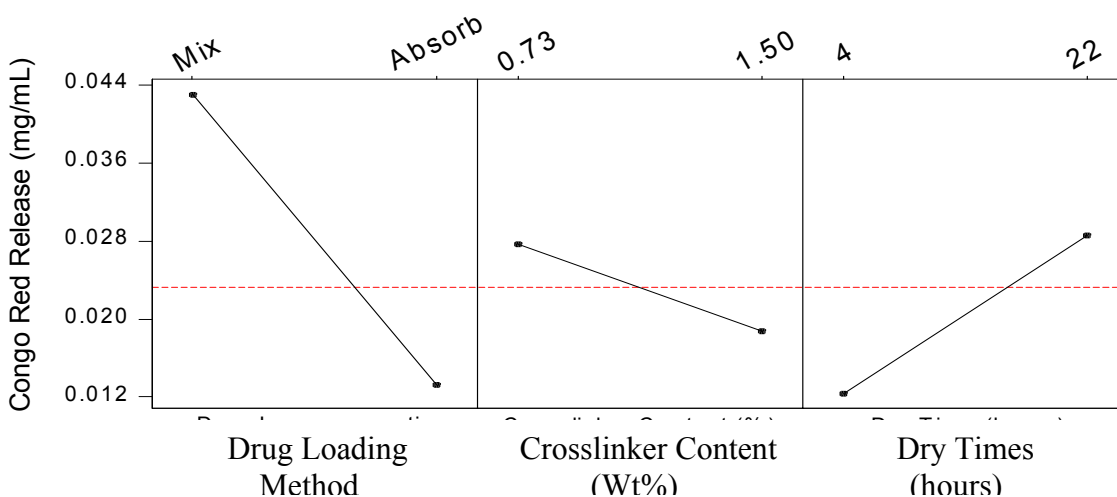


Figure 5.13 Factorial analyses on determining the critical factors effecting drug loading after 48 hours. Mixing the drugs with coating materials substantially enhance drug loading capability (left panel) (ANOVA, $p < 0.05$). However, crosslinker content (middle panel) and coating dry time (right panel) has insignificant influence on drug loading properties.

After 72 hours, almost all congo red was released from the coating. No congo red was detected in the test solution after 96 hours indicating that the congo red is completely released after 72 hours. These results represented a major setback to our proposed work, since the minimal drug release duration to achieve significant in vivo outcome is approximately 10 days. In order to reduce the release rate, other factors

including hydrophilicity of the coating (PVP content) and drug concentration must be evaluated.

5.3 Optimize Coating to Improve Drug Loading & Release Properties

5.3.1 Introduction

The results from previous studies have shown that the premixing the drug with the coating solution produced significantly increased levels of drug loading and extended drug release profiles compared to the spontaneous adsorption method. Thus, in subsequent experiments, all drug loading procedures were performed with drug mixed directly with the coating. The drug loading study also revealed that the drug release duration was only 24-72 hours and not adequate for combating PCO formation. In order to extend the drug release duration, the existing coating preparation and formulation was modified. This series of studies evaluated the effects of PVP content, crosslinker content, coating thickness, surface treatments, and curing times on drug release properties.

5.3.2 Experimental Design

To extend the drug release duration without affecting the chemical properties of the coating, we completed a series of experiments. Study #1 investigated the effect of varying drug concentration. Study #2 investigated the effect of PVP concentration to reduce the amount of drug released as well as extending drug release duration. Study #3 investigated the ability of an outer layer to slow the release of the drug and extend drug release duration. With data obtained from these studies, drug release properties were optimized in Study #4 using a designed experiment by varying PVP content, crosslinker

content, and surface treatment. Finally, using established coating condition, study #5 was aimed to document the drug release profile of all PCO-reducing drugs.

Study #1 varied the PVP content of the coating. Initial coating studies utilized 20% PVP content which resulted in short drug release times on the order of 3-5 days. Since hydrophilicity of the coating affect solution exchange and subsequent drug release, it is likely that the concentration of PVP in coating has impact on drug release. To test this hypothesis, we produce different coatings with PVP contents ranging from 20%, 14%, 5%, to 2%. Diclofenac concentration was held constant at 31 mg/mL. Lenses were coated with a single layer of coating and dried in a 65°C oven for 4 hours. Lenses were tested in the same manner as described previously.

Study #2 optimized drug release using a designed experiment. This study utilized information gathered from Study #1 in determining the range of conditions for this study. This designed experiment evaluated the effects of plasma treatment, crosslinker content, and PVP content (hydrophilicity of coating) on drug release properties (Table 5.2). Lenses were tested in the same manner as described previously.

Table 5.2 Key factors included in the fractional factorial designed experiment.

Controlled Factor	Process Parameter	
	#1	#2
Surface Plasma Treatment	Low ¹	High ²
Crosslinker Content (Weight %)	0.73	1.50
PVP Content	0	2

¹ Low plasma treatment (100% Argon, 100 Watts, 250mTorr, 2 minutes)

² High plasma treatment (100% Argon, 400 Watts, 250mTorr, 5 minutes).

Study #3 optimized PVP content of the coating. Additional studies were completed to extend release rates further by eliminating PVP in coating preparation. PVP content for this experiment included 2% and none. Diclofenac concentration was held constant at 31 mg/mL. Lenses were coated with a single layer of coating and dried in a 65°C oven for 4 hours. Lenses were tested in the same manner as described previously and measured using the spectrophotometer.

Coated lenses were placed in 0.5 mL of balanced salt solution (BSS) at 37°C for drug release studies and measured at 24 hours. After 24 hours, lenses were removed and placed in new vials containing fresh BSS. The absorbance of the solution was measured using UV-Vis spectrophotometer at the appropriate wavelength to determine the concentration of the drug released during that 24 hours time period. The concentration of the test samples was obtained from the standard curve produced from known drug concentrations (70).

Study #4 determined drug release properties for each drug. This series of experiments used data obtained from the previous experiment to determine drug properties for each drug targeted for in vivo testing. As a result, all drugs were mixed with the coating for maximal loading and all coatings were prepared with no PVP and 1.5% crosslinker for optimal release characteristics. Various concentrations were tested in order to meet effective dosing levels for each of the drugs as determined by in vitro cell studies. All drug release profiles were determined using the same manner as described previously.

5.3.3 Results

5.3.3.1 Study #1: Varying PVP Content of Coating

To slow down the drug release rate, PVP content was varied from 20% to 2% for coating loaded with 31 mg/mL of diclofenac. As expected, the drug release rates decreased as the PVP content decreased as seen in Figure 5.14. With 20% PVP content, 98.2% of the drug was released after 5 days on average (n=3). However, with 2% PVP only 71.9% of the total drug was released after 5 days on average (n=3) (Figure 5.15).

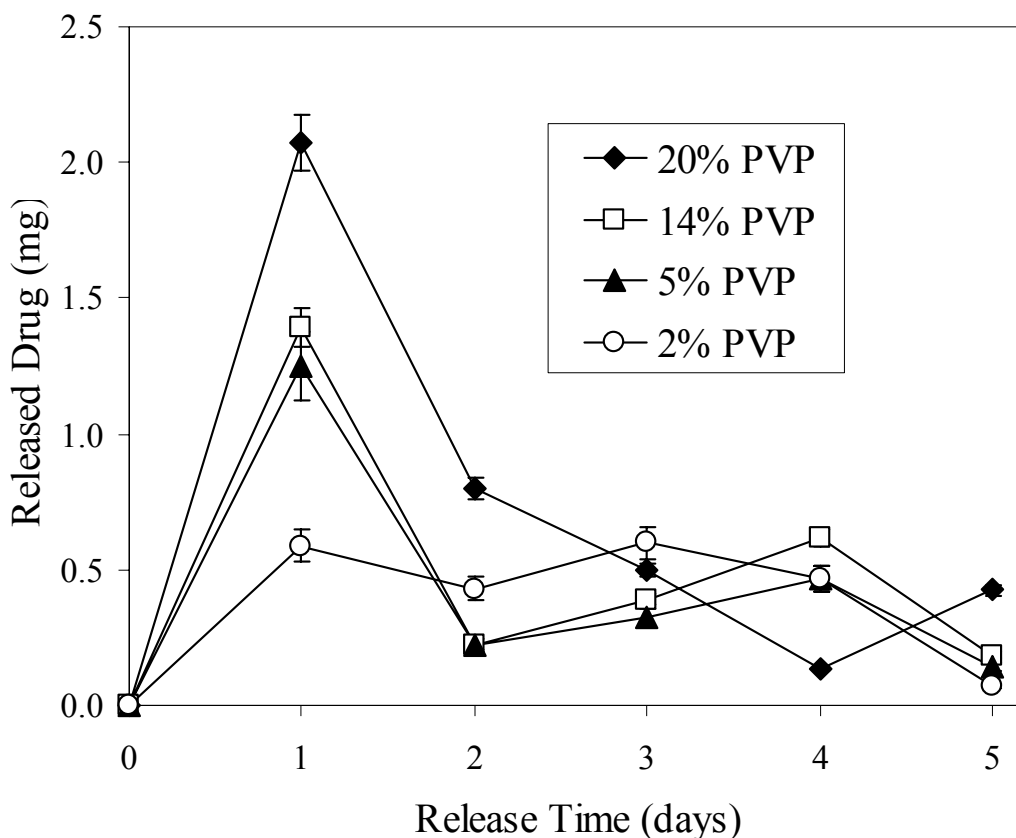


Figure 5.14 Effect of PVP content on daily release of diclofenac. The amount of diclofenac released on a daily basis was significantly affected by the PVP content. Coating with 2% of PVP released diclofenac at a steady rate for 4 days while other concentrations decreased significantly after 1 day release.

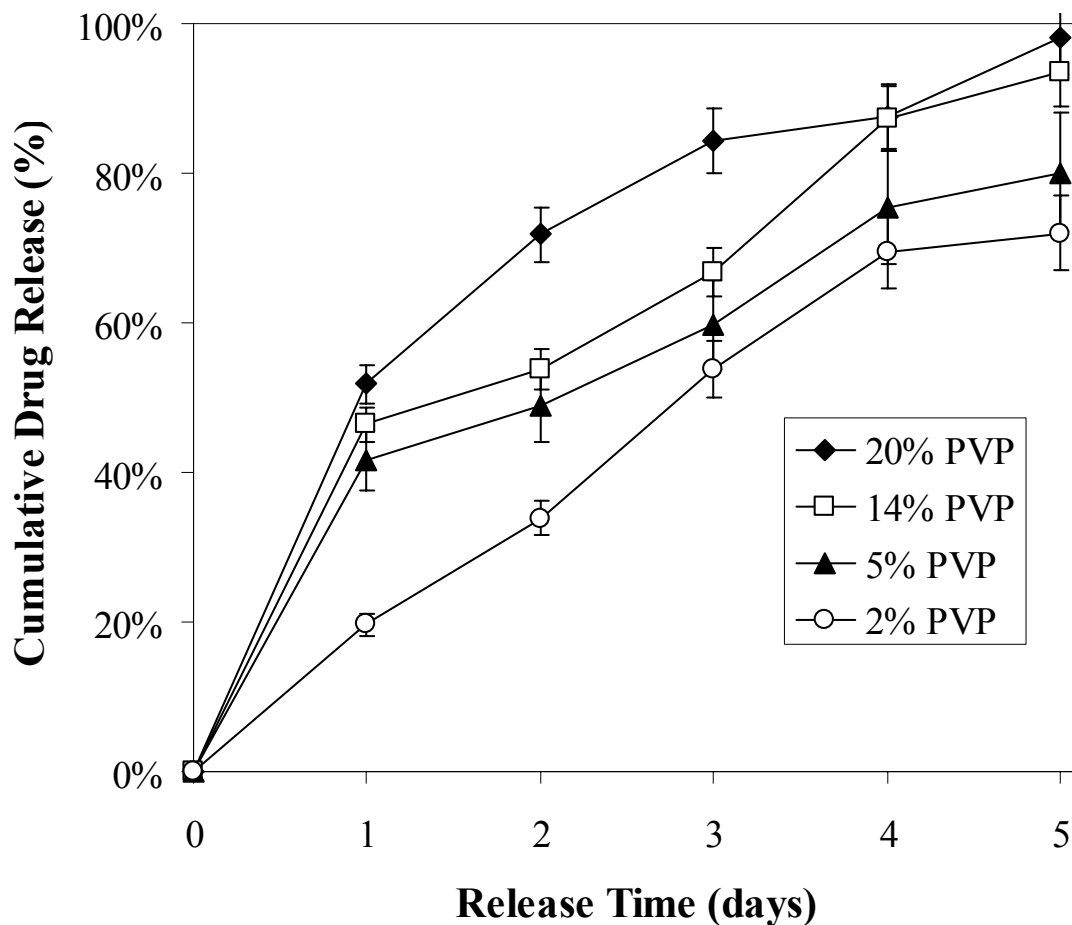


Figure 5.15 Effect of coating PVP content on drug release duration. Reduction of PVP content in the coating formulation significantly prolongs the duration of drug released over 5 days.

5.3.3.2 Study #2: Drug Release Optimization

An experiment was designed (DOE) to optimize drug release properties using congo red. This study varied PVP content (0 to 2%), plasma surface treatment (with and without treatment), and crosslinker content (0.73 to 1.50%) in order to reduce release

rates and extend release times. Data was obtained on 8 different groups and analyzed (Appendix C) using Design Expert 6.0 statistical software. PVP content and crosslinker content significantly (ANOVA: $p < 0.05$) effected the amount of drug release (Figure 5.16). In reducing the amount of PVP in the coating, release rates are decreased significantly (reflected by deep slope of design analysis). In increasing the crosslinker content of the coating, release rates are decreased and duration extended significantly (reflected by deep slope of design analysis). On the other hand, crosslinking the surface of the coating (plasma surface treatment) did not significantly affect drug release rates.

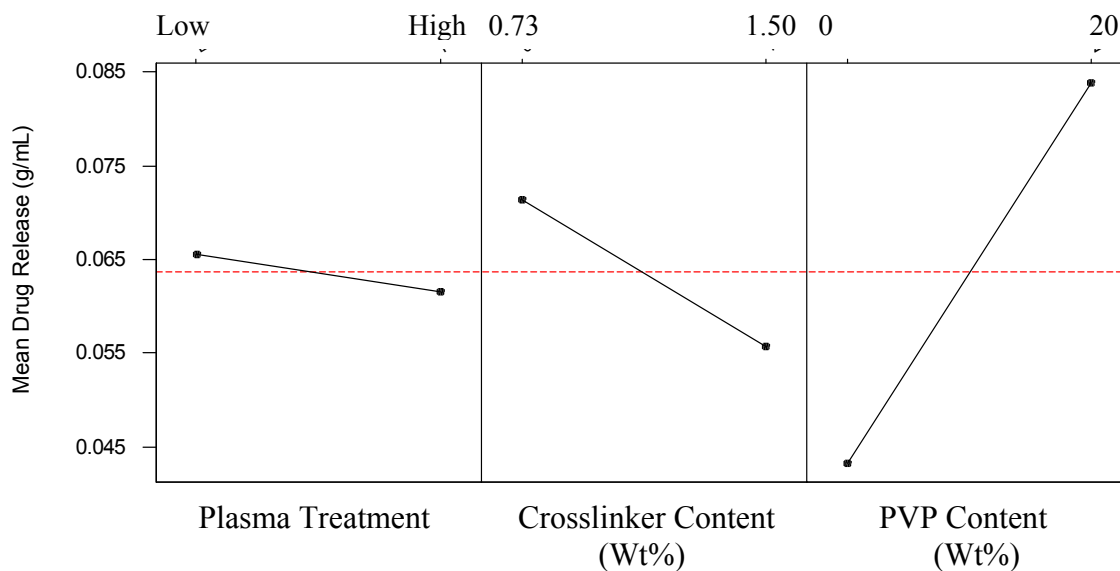


Figure 5.16 Main factors effecting drug release properties. The PVP content (right panel) and amount of crosslinker in the coating (middle panel) significantly influenced drug release properties ($p < 0.05$). As the crosslinker content increased, the crosslink density of the coating also increased thereby decreasing the release rate. Plasma treating the surface (left panel) did not significantly alter drug release properties ($p > 0.05$).

5.3.3.3 Study #3: Optimization of PVP Content in Coating

Based on previous results, PVP content reduced even further in an attempt to further reduce release rates and extend release time. PVP content was varied from 2% to none. Results indicated that drug release rates were further decreased by eliminating PVP from the coating (Figure 5.17).

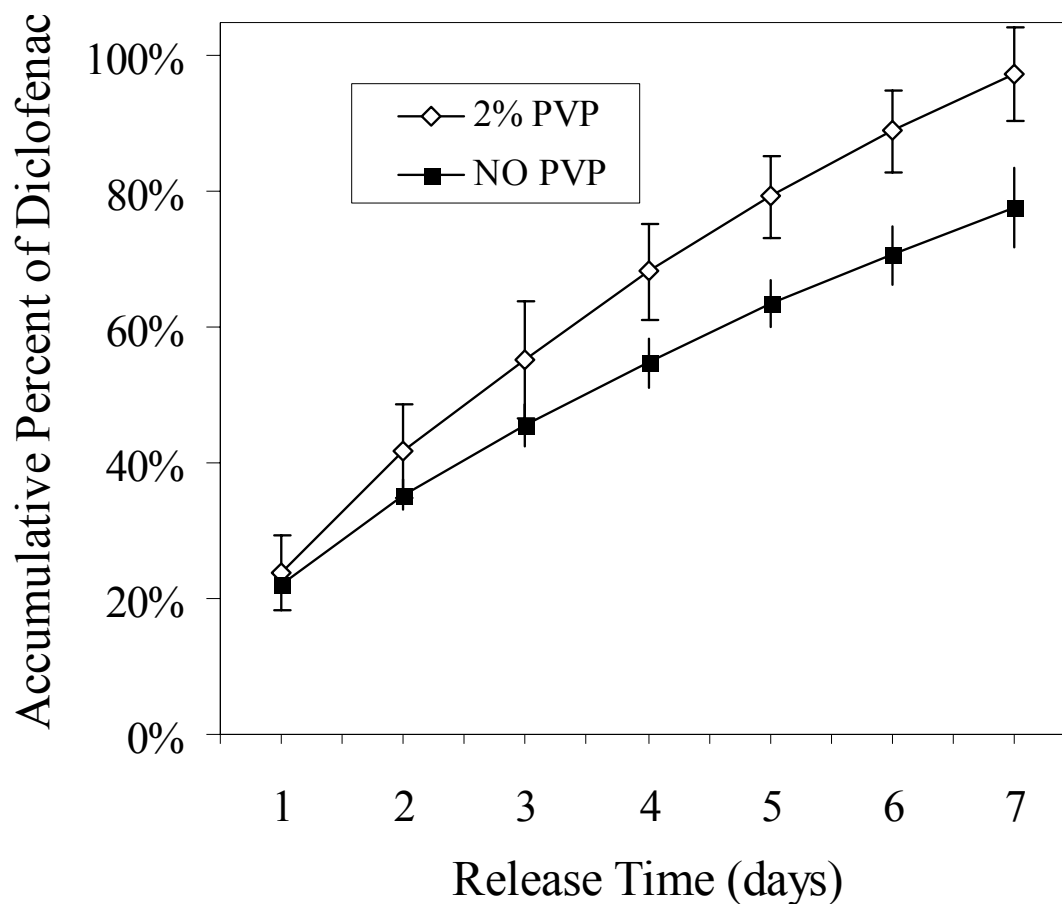


Figure 5.17 Effect of eliminating PVP from coating on release rates. Eliminating PVP from the coating decreased release rates further.

Upon identifying optimal conditions for the coating formulation and process conditions, the release kinetics for each of the selected drugs was completed using the following procedure: 1) crosslinker content of coating 1.50%, 2) no PVP in coating formulation, 3) 4 hours dry time, and 4) no plasma treatment.

5.3.3.4 Study #4: Determine Drug Release Properties for Each Drug

The concentration of each of the drugs will be varied to determine the optimal concentration individually.

DICLOFENAC: Diclofenac coating solutions were varied in order to determine the release rates for various drug concentrations incorporated into the coating. The range of concentrations included 5.2, 14.9, 42.8, and 80.1 mg/mL of diclofenac to coating solution. The calculated total drug loading for each concentration is 0.5453, 1.636, 4.699 and 8.795 mg, respectively. Diclofenac is soluble in water up to 50 mg/mL. One concentration was chosen outside this range in order to determine the effects of concentrations of stability of the coating and effects on release rates. The others dissolved easily into the coating solution while the high concentrations did not as indicated by the presence of undissolved crystals in the coating solution. Lenses were coated with 7 layers of each coating. Coating thicknesses were not significantly different as indicated by dry weight measurements of the coated lens.

The release rates for each of the coatings for the first 3 days were significantly different. From day 4 to day 10 drug release rates leveled off and remained nearly consistent throughout this time period (Figure 5.18). The lens coated with 5.2 mg/mL did not record any levels above the limit of detection (0.20 mg for diclofenac). All data

points for lenses with 5.2 mg/mL diclofenac coating are estimated diclofenac levels. Drug levels near the end of the 10 day period for the other concentrations also fell below the limit of detection of the proposed test method. In order to determine if additional coating was present in the coating, lenses were soaked in BSS for an additional 18 days at physiologic conditions. After this time, the solution was measured.

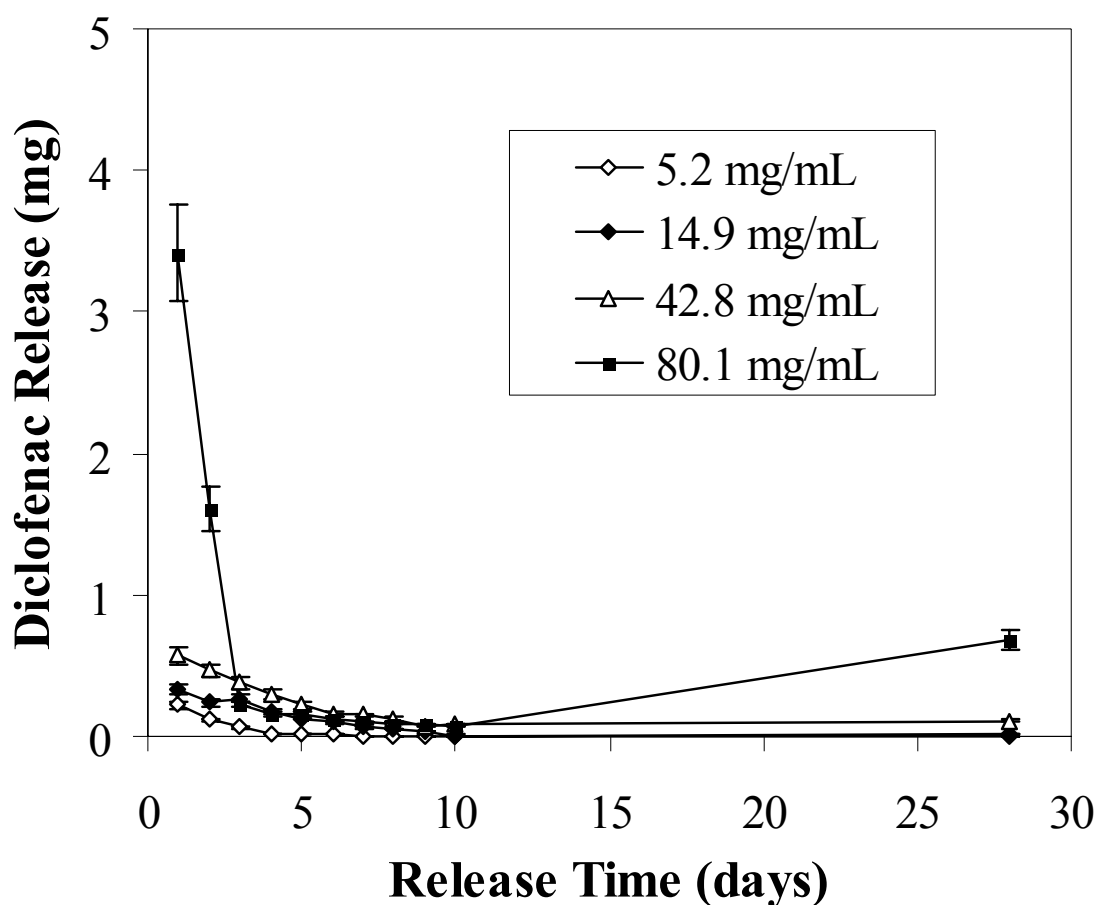


Figure 5.18 Diclofenac release rates (mg/day) under physiologic conditions. (in BSS @ 37°C) Diclofenac release was detected after 10 (n=3) for coatings loaded with varying drug concentration levels as denoted in the legend. (Brett: Please adjust the maximal Y-axial value to 4).

After an additional 18 days (28 days total), diclofenac levels for 5.2 mg/mL and 14.9 mg/mL fell below the limit of detection. The other concentrations obtained measurable levels of diclofenac indicating that extended release was achieved (Figure 5.19). The presence of diclofenac at this point indicates that the drug is released over the course of a minimum of 2 weeks and possibly up to 4 weeks.

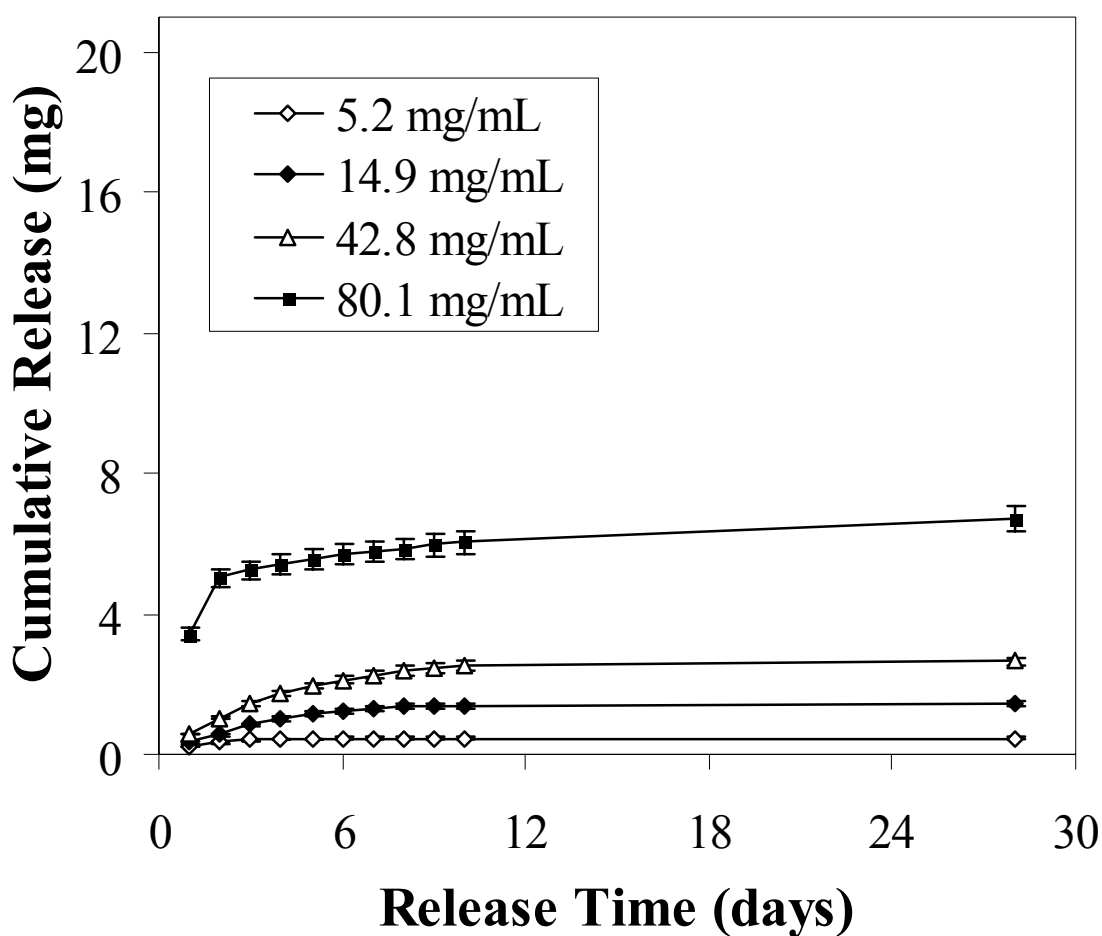


Figure 5.19 Diclofenac cumulative release rates (total mg) under physiologic conditions. (in BSS @ 37°C) Diclofenac release was detected after 28 days (n=3) for coatings loaded with 42.8 and 80.1 mg/mL. The lower concentration levels were below the limit of detection and an estimate is provided in the graph.

The cumulative percentages of diclofenac released for each coating concentration was calculated and is illustrated in Figure 5.20. With loading concentrations of 5.2, 14.9, and 42.8 mg/mL, nearly 100% of the drug was released by day 18. We have also observed that high drug loading concentration (such as 80.1 mg/mL) affects the coating integrity and prompt small particulate release. Such coating instability has later found to worsen foreign body reactions (please see chapter 6).

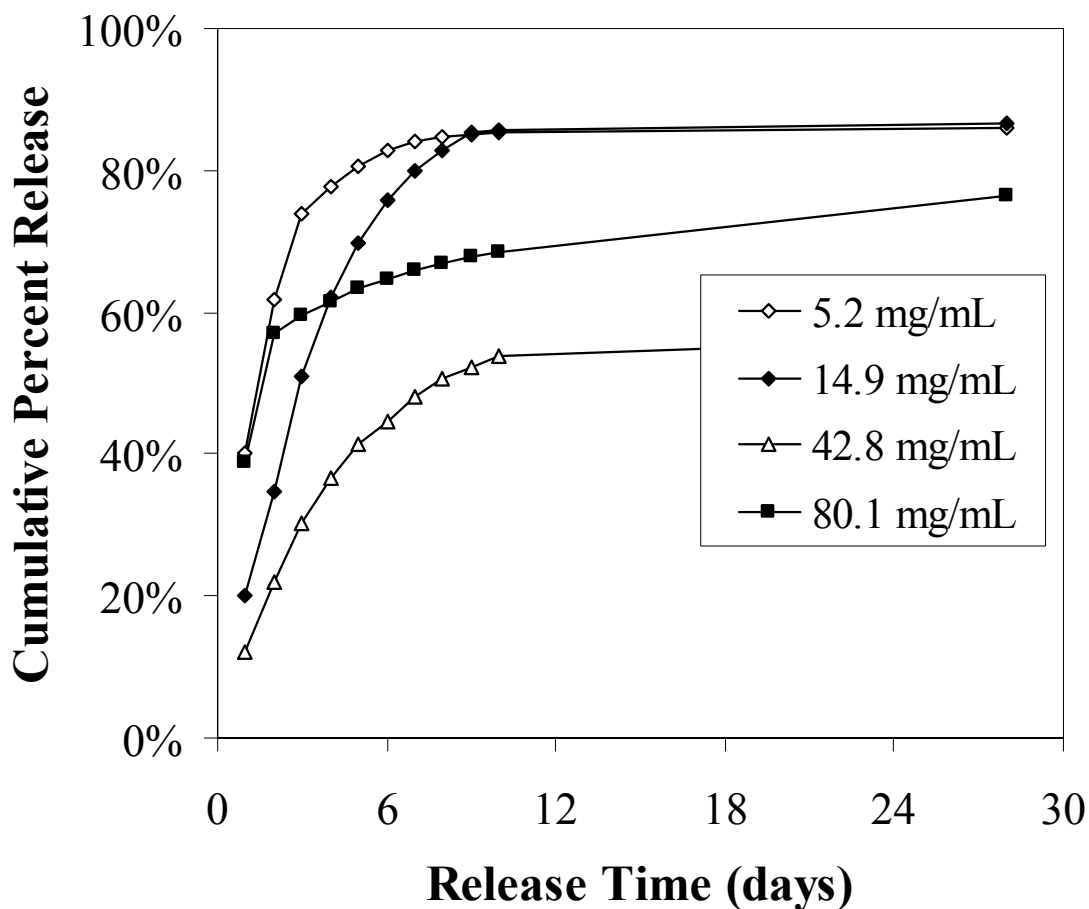


Figure 5.20 Diclofenac cumulative percent release under physiologic condition. (in BSS @ 37°C) Diclofenac was almost completely released after 28 days (n=3) for all coatings. The lower concentration levels were below the limit of detection and an estimate is provided in the graph.

COLCHICINE: Release rates for colchicine were obtained for coatings with a range of concentrations, including 2.6, 10.5, 30.3, and 61.2 mg/mL. The quantity of drug contained within the coating for each lens was calculated based on the weight gain of the lens after coating and known shrinkage and weight changes of coating after drying. Lenses coated with 2 mg/mL drug-coating solution contained approximately 0.0316 mg of colchicine. Lenses coated with 10 mg/mL drug-coating solution contained approximately 0.116 mg of colchicine. Lenses coated with 30 mg/mL drug-coating solution contained approximately 0.336 mg of colchicine. Lenses coated with 30 mg/mL drug-coating solution contained approximately 0.694 mg of colchicine. Based on in vitro studies, the target concentration for colchicine is 0.0005 mg/mL based on results that showed LEC migration and proliferation was inhibited at concentrations as low as 0.0005 mg/mL. The limit of detection for colchicine using this analytical technique was 0.0083 mg/mL. Drug concentrations were obtained on each sample for 8 days. However, after 8 days all concentrations fell below the limit of detection. At this time, the test solution was replaced and lenses were allowed to soak for an additional 18 days (28 total days) in order to obtain measurable drug concentrations. In vitro drug release data indicates that lenses coated with 2.6 mg/mL coating solution released these quantities for 8 days and then falls below the limit of detection (Figure 5.21 & 5.22). However, based on calculated drug loading for these lenses, only 80% of the drug is released after 8 days (Figure 5.23). Lenses coated with 10.5 mg/mL coating solution, as well as the higher concentration coating solutions, released quantities above 0.0083

mg/mL for at least 8 days. Based on calculated drug loading, lenses coated with 10.5 mg/mL contain approximately 30% of the total drug after 28 days.

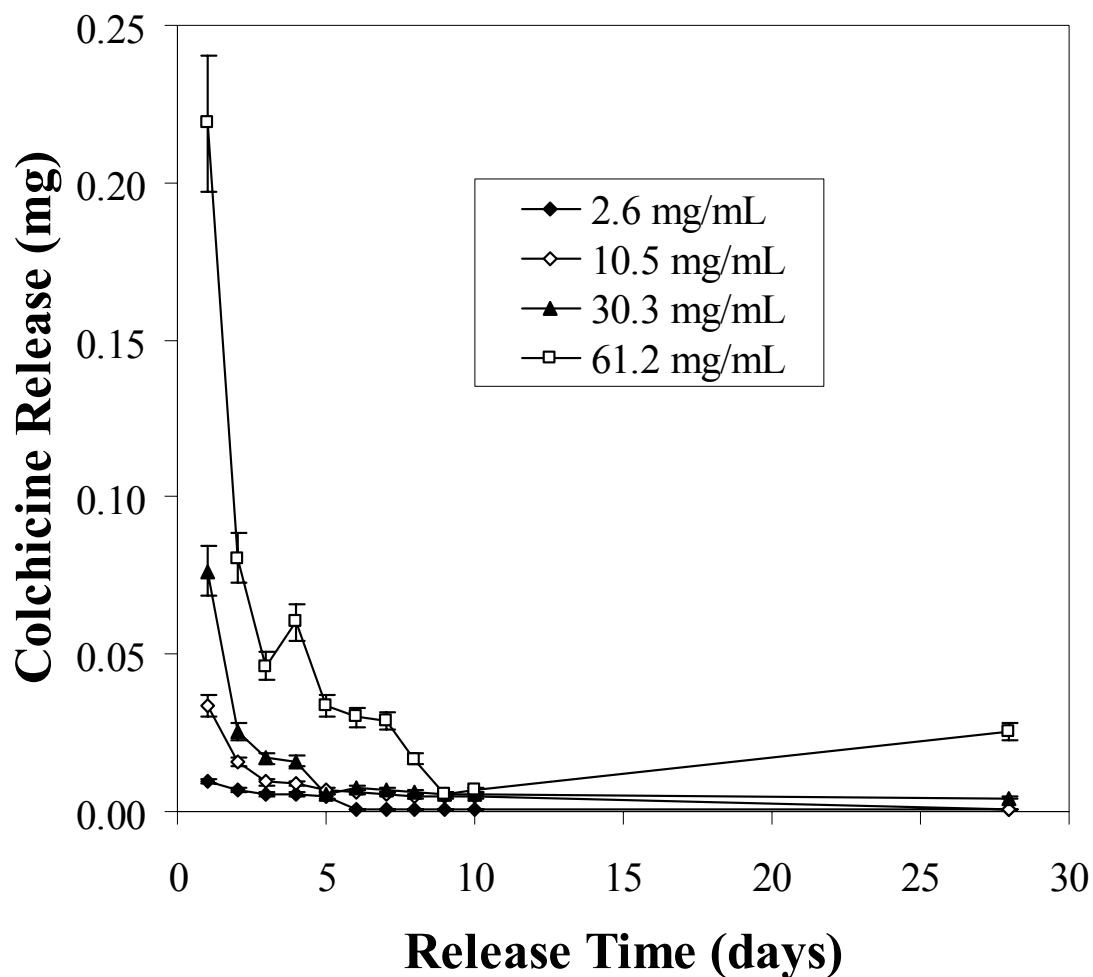


Figure 5.21 Colchicine release under physiologic conditions. Colchicine release was detected even after 10 days in BSS at 37°C (n=3) for coatings loaded with varying drug concentration levels as denoted in the legend.

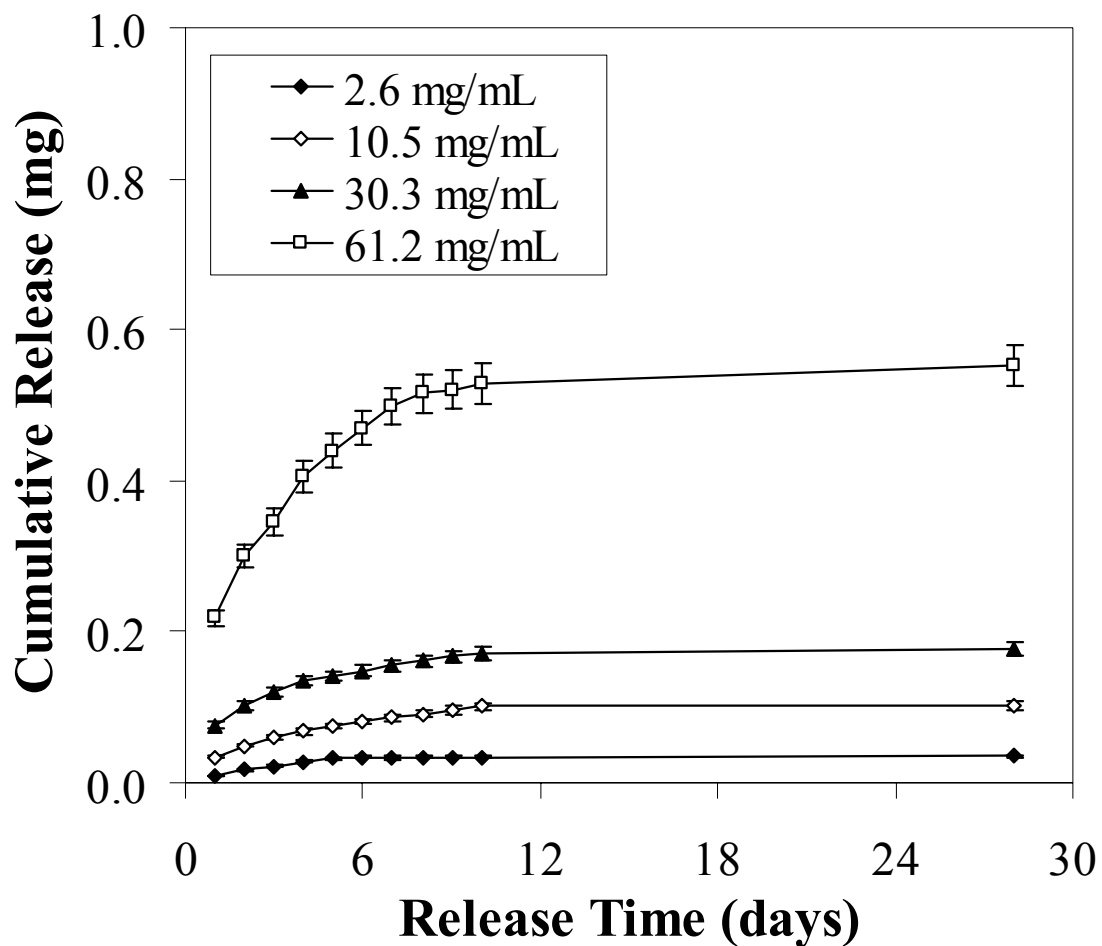


Figure 5.22 Colchicine cumulative release under physiologic conditions. Colchicine release was detected after 28 days in BSS at 37°C (n=3) for coatings loaded with varying drug concentration levels as denoted in the legend.

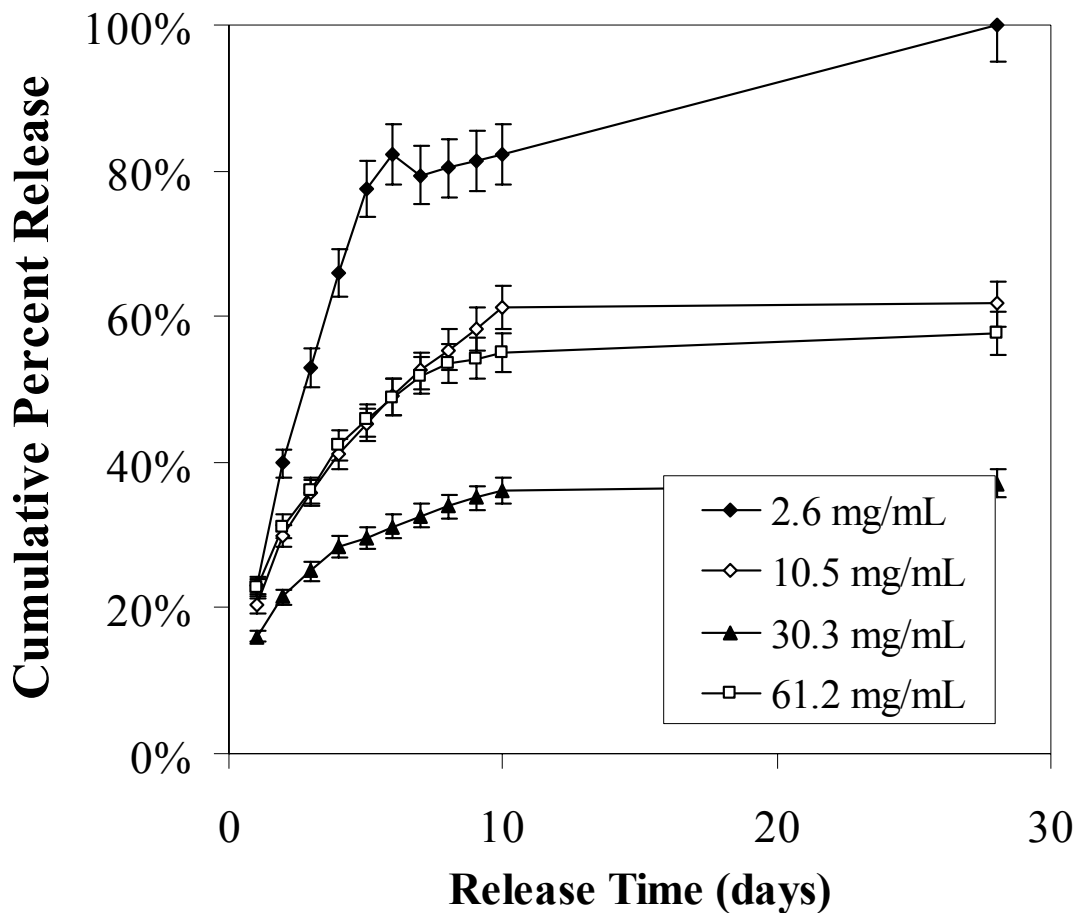


Figure 5.23 Colchicine cumulative percent release under physiologic conditions. Colchicine release nearly 100% by day 5 for the 2.6 mg/mL coating. Only a small quantity was detected for this concentration after an additional 18 days (28 days total). The other concentrations detected colchicine after 28 days in BSS at 37°C (n=3) for coatings loaded with varying drug concentration levels.

MITOMYCIN-C: The quantity of drug contained within the coating for each lens was calculated per previously described methods. Lenses coated with 2mg/mL drug-coating solution contained approximately 0.138 mg of MMC. Based on in vitro studies, the target concentration for MMC is 0.0005 mg/mL based on results that showed LEC migration and proliferation was inhibited at concentrations as low as

0.0005 mg/mL. The limit of detection for MMC using this analytical technique was 0.010 mg/mL. After 11 days, MMC continued to be released from the coating at levels above the limit of detection (Figure 5.24). After the initial 2 days of drug release, drug release rates do not vary significantly. Approximately 20% of the total MMC loaded into the lens remains after 11 days of soaking in BSS at 37°C as seen in Figure 5.25.

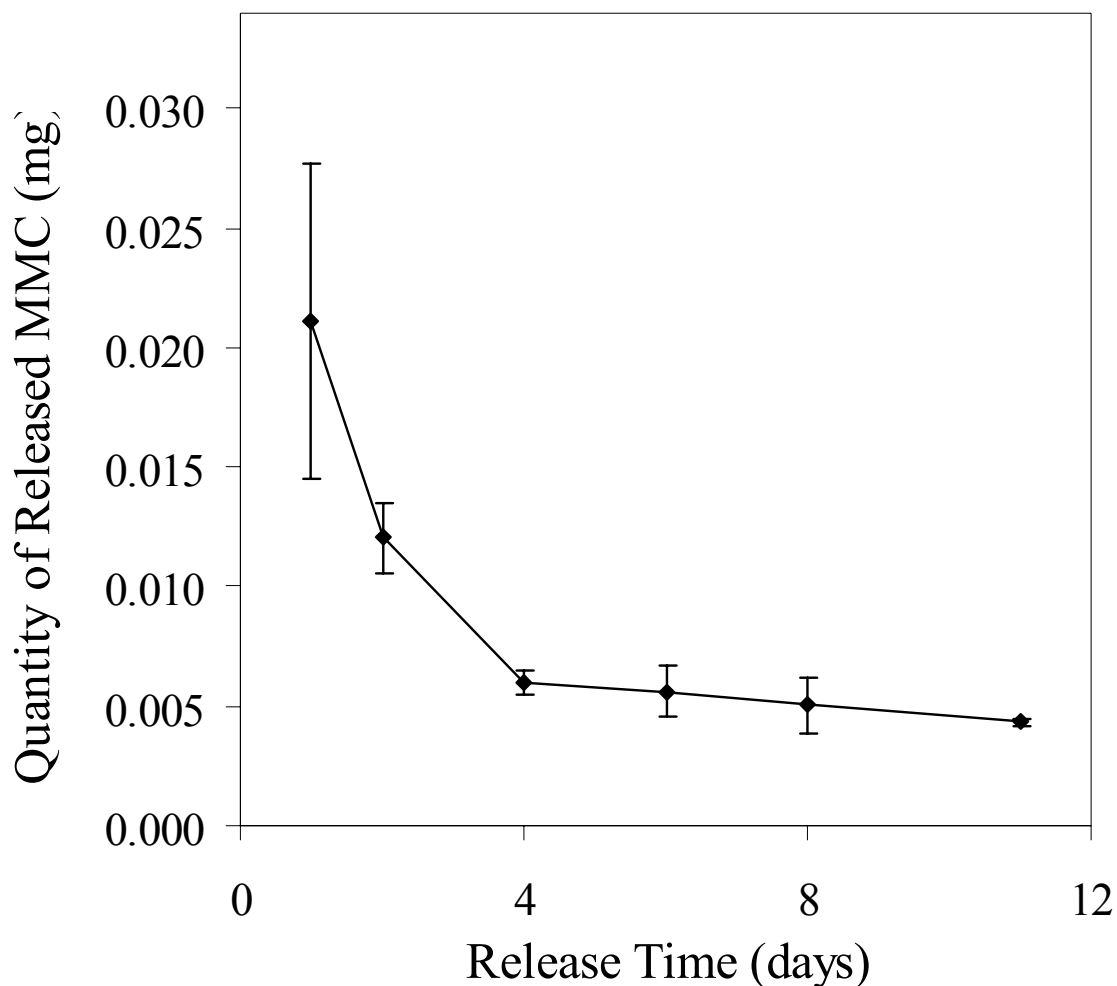


Figure 5.24 MMC daily release rates under physiologic conditions. MMC was released up to 11 days after hydrating in BSS at 37°C. (n=3) Levels after 11 days are above the detection limit for MMC for this method.

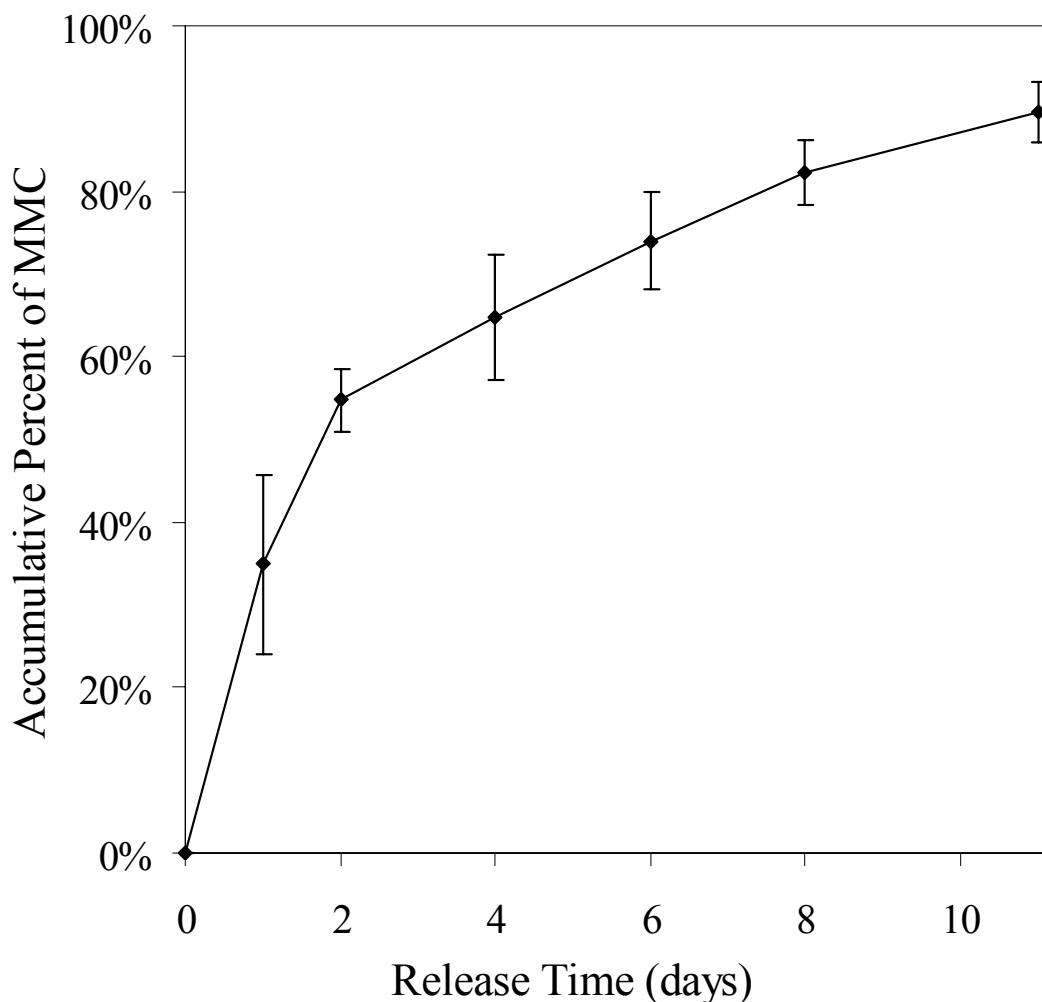


Figure 5.25 MMC cumulative percent release under physiologic conditions. After 11 days in BSS at 37°C, approximately 20% of the total MMC loaded into the coating remains.

5.4 Overall Discussion on Drug Loading and Release

Release of a drug entrapped within a polymer matrix is dependent upon several factors: 1) the hydrophilicity of the polymer matrix, 2) the hydrolytic degradation of the polymer matrix, 3) porosity of crosslink density of polymer matrix, 4) polymer-drug interactions, 5) molecular weight (MW) of drug, and 6) drug solubility in the medium.

The coating utilized in this study is not designed to release drug through coating degradation. The drug is entrapped in the coating, not bound. The aqueous based PU coating, in this case, is slightly charged and will have electrostatic interactions if the drug is oppositely charged. If the drug is not charged, release of the drug is dependent on diffusion through the polymer matrix.

Diffusion systems entail the drug diffusing out of the polymer matrix. Release rates are dependent upon chemical structure of polymer matrix, pore size or crosslink density of the polymer matrix, dissolution rate of drug, and MW of the drug. Following implantation, the coated is hydrated by the surrounding medium (aqueous humor). Hydration will swell the polymer matrix and allow drug to diffuse through the polymer.

Ion exchange phenomenon is driven by electrostatic interactions between the polymer matrix and oppositely charged drugs. The interaction is strongly governed by the pH of the medium or by the presence of competing ions. As mentioned, the aqueous based PU coating is slightly charged and may be exploited to control drug release if the drug is oppositely charged. The coating contains functional groups attached to the backbone of the polymer and therefore can exchange ions with ions in solution. These exchangeable ions are not limited to small, inorganic ions and cations present in the surrounding medium, but can be organic ions of significant molecular weight, i.e. drugs. A drug ion and an inorganic ion are exchanged. The reaction is an equilibrium, the position of which will depend on many factors including salt concentration in the aqueous phase. This property allows drugs to be loaded onto a polymer matrix and then released *in vivo* by the salts present in aqueous humor or surrounding medium.

Initial studies observed complete release (100%) of congo red (model drug) from the coating within 24 hours. Congo red and the coating contain oppositely charged ions and its release is governed by the ion exchange phenomenon. Congo red was released quickly because of the hydrophilic nature of the coating and high solubility of the drug in BSS. A maximum drug release was observed within the first hour. This is a common phenomenon in drug delivery system, known as burst effect, which is caused by the presence of a high concentration of drug near the surface. A maximum release within the first hour raises some concerns of toxicity. In order to decrease the release rate, the hydrophilicity of the coating must be decreased. The crosslink density of the polymer matrix may also be modified to decrease the diffusion rate of the drug.

Subsequent studies investigated the effect of PVP content (hydrophilicity) of the coating in order to reduce the drug release rates. Data indicated that by removing PVP, drug release was decreased but maintained at levels above those determined from cell culture testing. Results also have shown that increasing crosslinker content to 1.50% had a significant effect on decreasing release rates and prolonging drug release from the coating. By increasing the crosslinker content the crosslink density of the coating was increased. This made it more difficult for the drug to diffuse out of the coating and decreased release rates.

Based on *in vitro* cell studies, effective concentrations for each of the selected drugs was, 0.10 mg/mL for diclofenac, 0.0005 mg/mL for colchicine, and 0.0005 mg/mL for MMC. Drug release kinetic measurements for each of the selected drugs

demonstrated that the effective concentration of each drug was achieved up to 10 days. After 10 days, additional drug was not released and present in the matrix of the coating. Drug was detected after 30 days, however, these values were below the detection limit of the test method. Alternate test methods, i.e. fluorescence, may provide detection at lower concentrations than the current method. We are also aware that many drugs in high concentrations may yield cell toxicity.

CHAPTER 6

AIM 4: IN VIVO TESTING OF DRUG DELIVERY SYSTEM

The objective of Aim 4 is to determine the effect of a drug-eluting IOL coating on reducing PCO formation in vivo. Based on the results obtained from previous in vitro studies, we have demonstrated that the drug delivery system can deliver drugs up to and exceeding 10 days at effective concentrations. The effectiveness of multi-drug and single drug eluting coating system to combat PCO was then tested in vivo using a rabbit implantation model (Figure 6.1).

In the Phase I study, animals were implanted with lenses loaded with combination of anti-inflammatory and anti-proliferative drugs. In Phase II and III studies, animals were implanted with lenses loaded with either an anti-inflammatory or anti-proliferative drug in order to observe the different response in the presence of a single drug. To the best of our knowledge, drug eluting lens coating system has not been done before and can not be found in published literature. Therefore, this research was aimed to develop the first generation of drug delivery lens coating. For the reason of economy and to broad our investigation to cover multiple drug delivery strategy, only one animal was used for each group of samples.

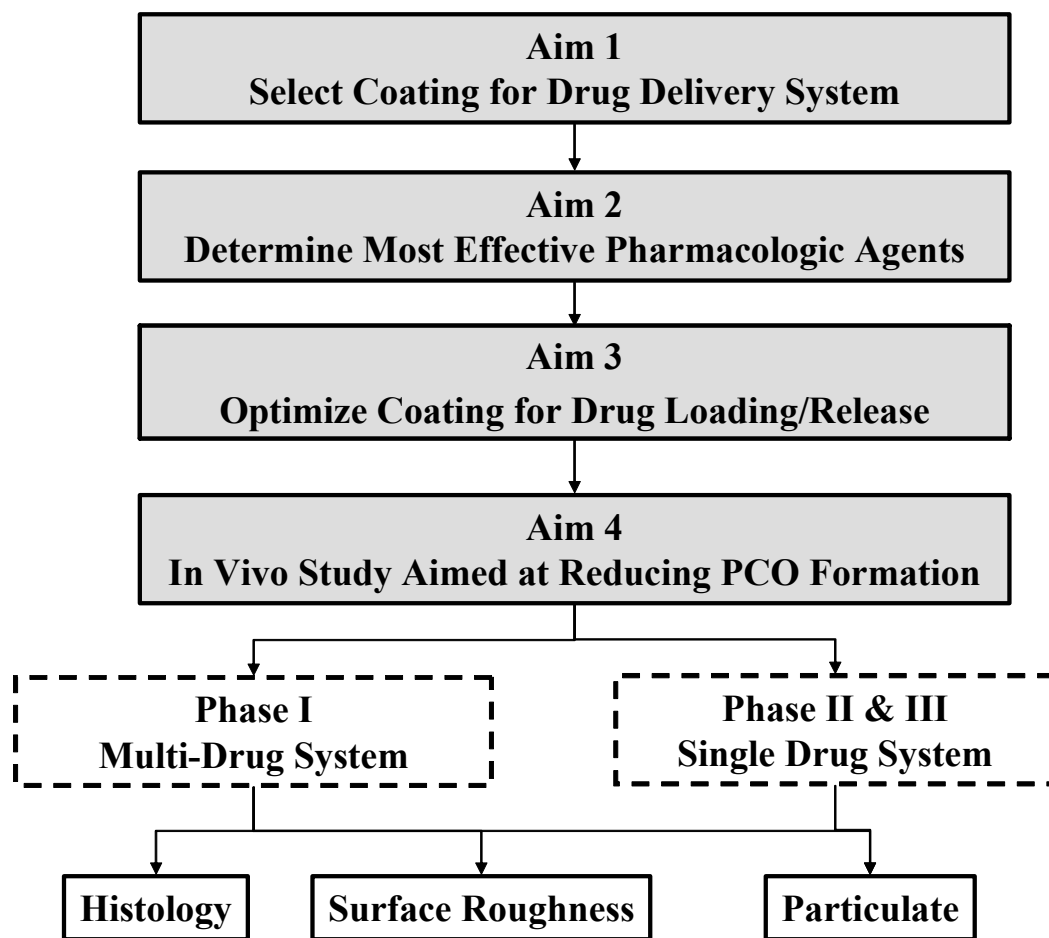


Figure 6.1 Overall experimental design for Aim 4.

6.1 Phase I – Animal Implantation of Multiple Drug System

6.1.1 Introduction

To maximize the anti-PCO activities, IOL coatings were simultaneously loaded with anti-inflammatory and anti-proliferative drugs. Six AcrySof MA60BM intraocular lenses were produced for this investigation. The test objects included 1) an uncoated lens, 2) a coated lens without drugs, 3) a coated lens loaded with diclofenac and colchicine, 4) a coated lens loaded with colchicine, 5) a coated lens loaded with diclofenac and MMC, and 6) a coated lens loaded with heparin and colchicine. All lenses were implanted for 2 weeks in rabbits before performing physiological and histological analyses.

6.1.2 Experimental Design

6.1.2.1 Test Implants

Alcon AcrySof® MA60BM intraocular lenses (21.0D) were used in the following studies. An uncoated IOL and a drug-free coated IOL served as controls. The Alcon AcrySof® lens is composed of an acrylic based copolymer. The coated IOL control is composed of a polyester urethane (no PVP). Each test lenses contained either a combination of drugs or a single drug. Coatings were prepared for each drug or drug combination. The coating solution for diclofenac and colchicine (DI+COL) contained 30 mg/mL of diclofenac and 10 mg/mL of colchicine. The diclofenac and MMC coating (DI+MMC) contained 30 mg/mL of diclofenac and 0.5 mg/mL of MMC. The colchicine only coating (COL) contained 80 mg/mL of colchicine. The heparin and colchicine coating solution (HEP+COL) contained 30 mg/mL for heparin and 10

mg/mL of colchicine. All lenses contained a total of 10 layers of coating and were EtO sterilized prior to implantation. Coating thicknesses were 50 microns on average.

6.1.2.2 Surgical Procedure

Female New Zealand white rabbits (4 lb) were used in this study. All rabbits were treated in accordance with guidelines set by the Association for Research in Vision and Ophthalmology and the Division of Laboratory Animal Resources. The animal protocol was reviewed and approved by the Institutional Animal Care and Use Committee at UTA. The same surgeon performed all operations; the surgeon was masked to IOL selection at the beginning of each procedure in all rabbits. Phacoemulsification and posterior chamber IOL implantation were performed in all cases. A 3.2 mm clear corneal incision was made for the non-coated lens and 6-8 mm for all other coated lenses. The lens substance and cortical material were completely removed. To maintain pupil dilation during surgery and diminish inflammation, epinephrine and heparin were added to the irrigation solution. The capsular bag was then filled with viscoelastic material (VISCOAT[®], Alcon Labs), and the IOLs were implanted into the capsular bag with forceps. VISCOAT[®], which is composed of sodium chondroitin sulfate and sodium hyaluronate, maintains a deep chamber during cataract surgery and protects the corneal endothelium and other ocular tissues.

At the completion of the surgical procedure, each rabbit received subconjunctival dexamethasone 0.25 cc and gentamicin 0.25 cc. Postoperatively, atropine sulfate 1% ophthalmic solution and dexamethasone ophthalmic ointment were

administered twice daily for 3 weeks. Each IOL procedure was documented in an implantation record.

6.1.2.3 Histology

At the end of the study, all eyes with implants were removed. Eyes not containing implants were also removed to compare tissue histologically. A small incision was made at the peripheral cornea and equatorial sclera of the enucleated eye so that neutral buffered formalin 10% was then infused into the globe for a minimum of 48 hours to fix the intraocular tissue. The IOLs and capsule bag were recovered. IOLs underwent hematoxylin and eosin (H&E) staining. Capsule bags were fixed, dehydrated, embedded in wax and then sectioned (76). The tissue sections were placed on glass slides. Following dewaxing, the tissue sections were then H&E stained. After preparation, sections were analyzed using a Leica fluorescence microscope (Leica Microsystems, Wetzlar, GmbH) equipped with a Nikon E500 Camera (8.4V, 0.9A, Nikon Corp., Japan). Microscopy and Image analysis was used to assess the extent of PCO formation by measuring the numbers of IOL-associated cells. The morphological structure of lenses capsule was also used to assess the degree of foreign body reactions and potential of subsequent PCO formation.

6.1.2.4 Surface Analysis

We have carried out two types of surface analyses to assess the surface roughness and coating integrity.

Surface roughness was measured after coating lenses and after hydration in BSS. Surface roughness was measured by Scanning Electron Microscope (SEM)

(Quanta 200 Scanning Electron Microscope, FEI Company, Hillsboro, OR) for dried samples. Environmental Scanning Electron Microscope (ESEM) (Quanta 200 Scanning Electron Microscope in environmental mode, FEI Company, Hillsboro, OR) provided analysis under aqueous environments. Both SEM and ESEM analyses were carried out at Alcon Laboratory research facility.

To determine the stability of the coating after loading with different levels of drugs, particle size analysis was performed on each lens. Lenses were soaked in balanced salt solution (BSS) at 37°C. After 14 days, lenses were removed and the BSS was analyzed for particulate. The size distribution of the particles was analyzed in water by dynamic light scattering using Nanotrak (Microtrac, Inc., Montgomeryville, PA) which is based on dynamic light scattering. The Microtrac Flex software (Microtrac, Inc., Montgomeryville, PA) analyzes the signals to calculate the Doppler shifts corresponding to particle size.

6.1.3 Results – Animal Study Phase I

Histological Evaluation: The overall evaluation of the drug eluting IOL has been mixed. Although cell adhesion and proliferation on the IOL was substantially reduced, we have also uncovered that increased inflammatory responses were found around capsule tissue. Specifically,

(A) IOL implants: The coated IOL required a larger incision (~6 mm) due to limited folding compared to the uncoated control lens (3mm). As a result, all coated lenses experienced heightened inflammation due to the larger incision size. In two cases lens implantation was difficult and required additional cutting to enlarge to

incision. Coated lenses turned opaque upon hydration and thus limited monitoring the condition of the IOL during the 2-week period.

All control groups IOL groups (uncoated IOL and drug-free coated IOL) revealed minimal intraocular inflammatory reaction and IOL surface deposits during the 2-week study. Inflammation was observed visually in rabbit eyes and also histologically after explantation in drug loaded eyes. DI+MMC and DI+COL drug loaded groups revealed minimal intraocular inflammatory reaction and IOL surface deposits while COL and HEP+COL revealed elevated intraocular inflammatory reaction and IOL surface deposits during the 2-week study.

Lenses from each rabbit were extracted, fixated, and stained after 2 weeks implantation. The number of adhered cells on the surface of the IOL were counted (Nikon optical microscope, 20X) after staining. Based on cell morphology, we have observed the presence of both inflammatory cells and LECs. Since both types of cells are essential to PCO fibrotic cell formation, we thus call the adherent inflammatory cells and LECs as “fibrotic cells”. The HEP+COL lens contained the highest number of adhered fibrotic cells to the surface of the IOL (Figure 6.2 & 6.3). Other drug combination lenses effectively reduced LEC growth and inhibition as indicated by the number of adhered cells on the posterior surface of the IOL. Regions with the highest density of fibrotic cell growth and proliferation were captured on digital micrographs (20X) using an optical microscope (Figure 6.4). Digital micrographs of control lenses indicate that the cells are healthy as indicated by cellular characteristics, i.e. elongated.

Drug combination lenses that effectively reduced fibrotic cell growth and proliferation contained cells that were rounded and showed no signs of cellular activity.

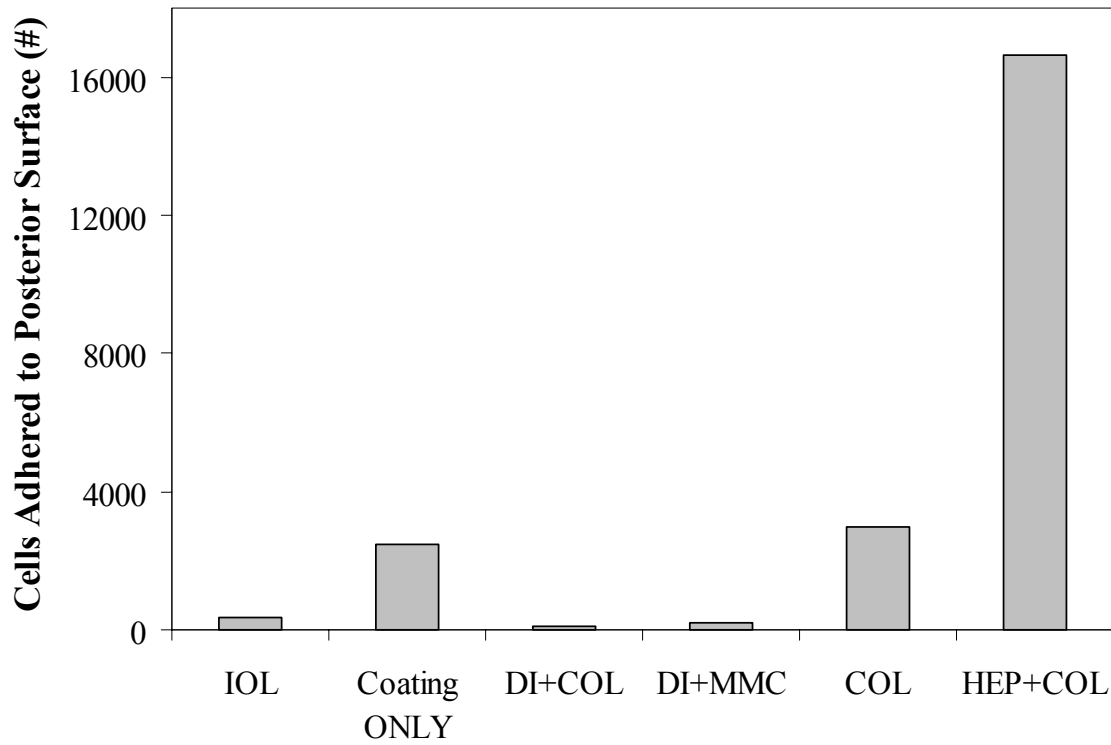


Figure 6.2 Effect of drug eluting coatings on fibrotic cell adhesion to posterior surface of lens. The number of fibrotic cells adhered to the posterior surface of the IOL after 2-week implantation was reduced with multi-drug system (n=1).

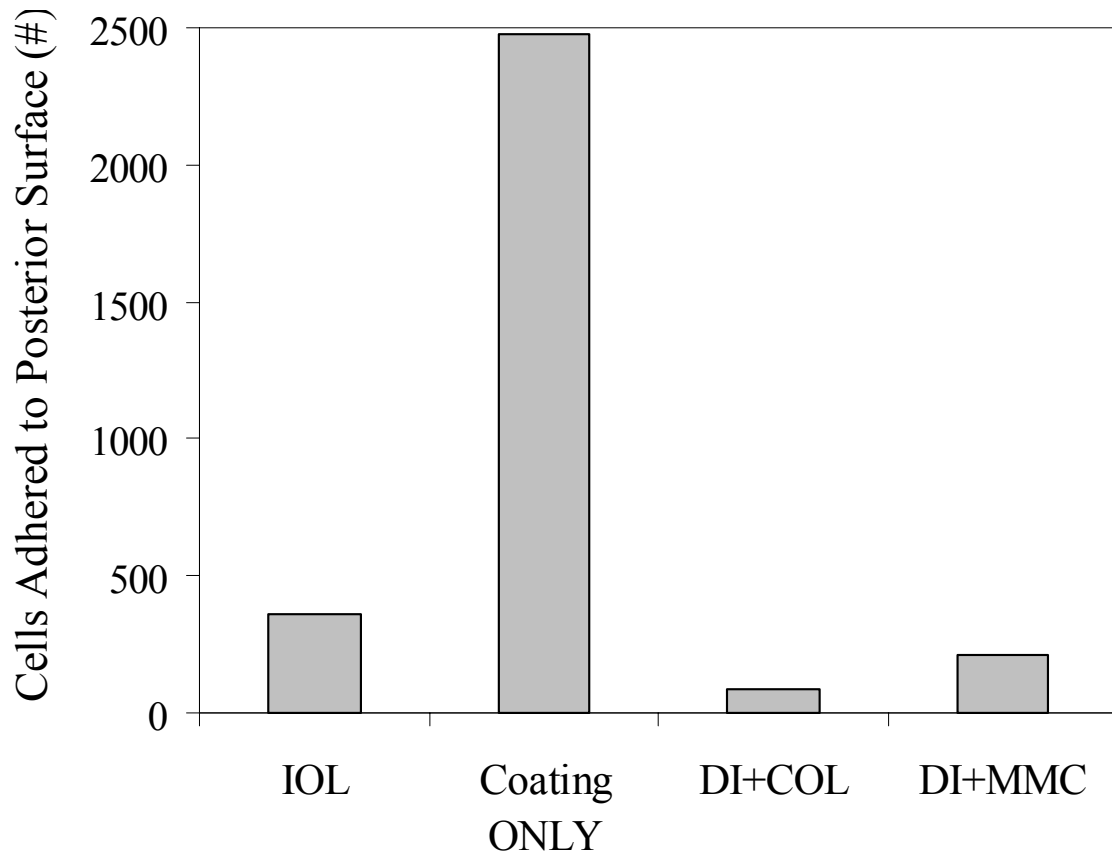


Figure 6.3 Effect of multi-drug regimen on fibrotic cell adhesion to posterior side on lens. Drug combinations of DI+COL and DI+MMC reduced the number of fibrotic cells present of the IOL surface compared to a standard IOL (uncoated) and coating only controls. Fibrotic cells present on the surface of the control IOLs were elongated and healthy. Cells present of the surface of drug loaded lenses shown here were rounded and did not show any signs of cellular activity. (n=1)

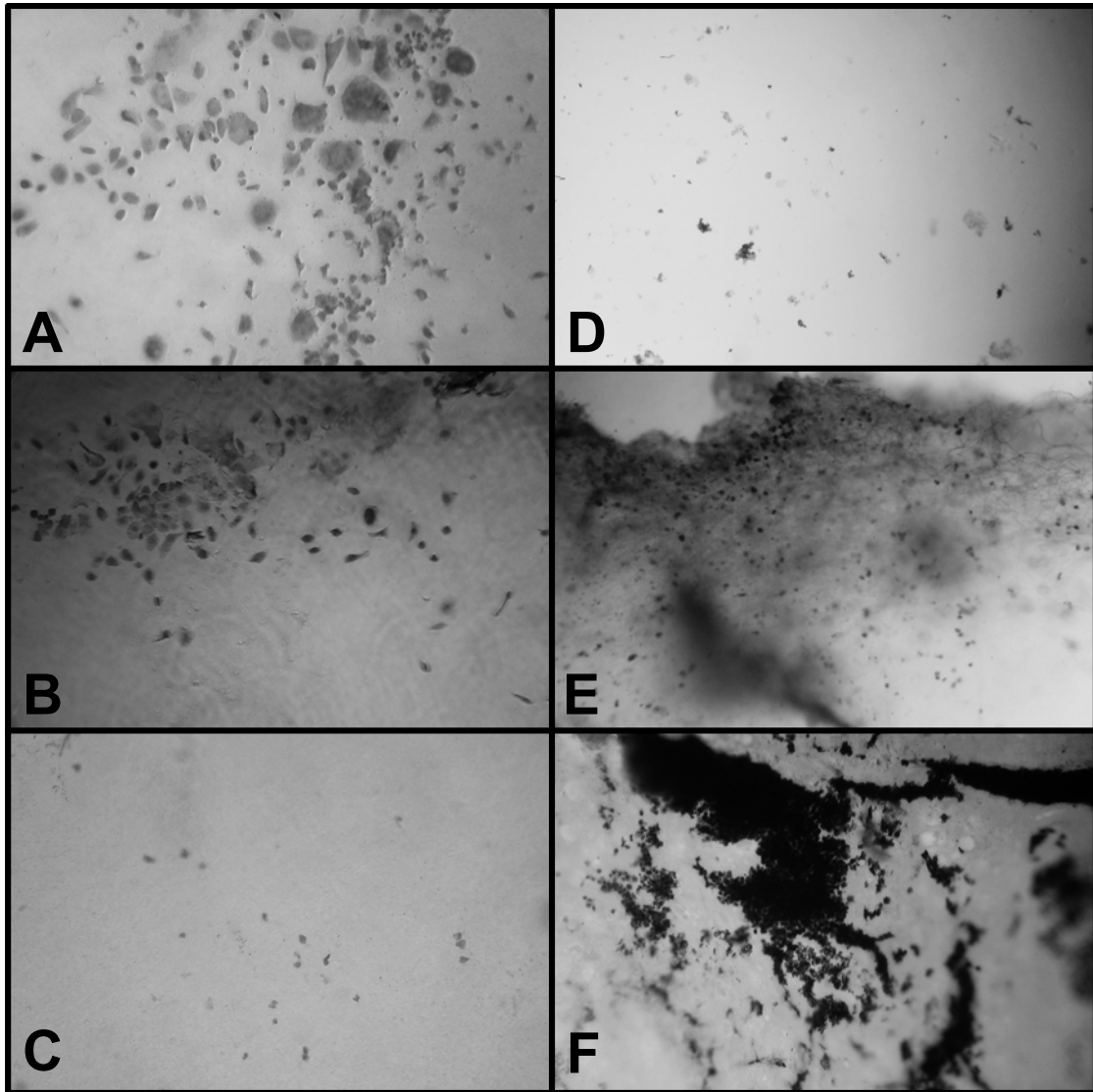


Figure 6.4 Fibrotic cell colonization on lens surfaces following 14 days of implantation in New Zealand White rabbits. These pictures show regions on the posterior surface of the lens with the highest density of fibrotic cell growth and proliferation. Both control lenses had cell growth and migration on the posterior capsule. (A) Alcon AcrySof MA60BM IOL only, (B) Alcon MA60BM IOL + coating only. Drug delivery systems containing the drug cocktails of DI+COL (C) and DI+MMC (D) inhibited cell growth and migration as evident by a significantly reduced cell number compared to controls. COL alone (E) resulted in a significantly increased number of fibrotic cells on the lens surface as well as fibrosis formation. HEP+COL (F) also resulted in increased cell growth and migration.

(B) Inflammation surrounding capsule tissue. Histologic evaluation of the lens capsule was completed following lens extraction after 2-weeks implantation. All globes were prepared for serial paraffin sections and were evaluated with hematoxylin and eosin stains. Control lenses possessed thin posterior capsules and no apparent fibrotic cells accumulation were found on control lens capsule (Figure 6.5).

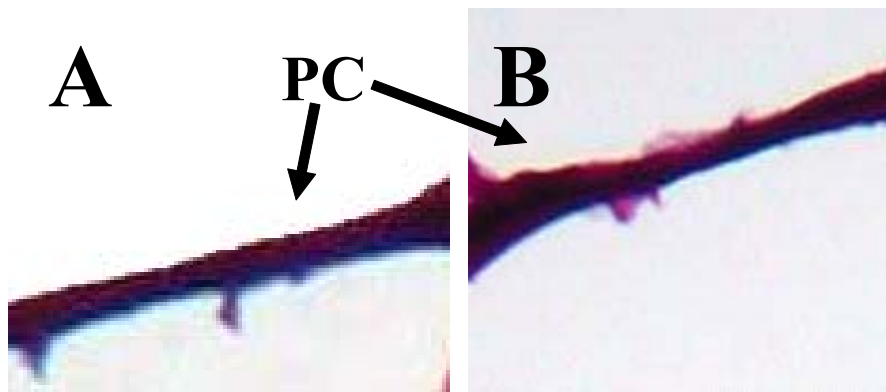


Figure 6.5 Cross section of posterior capsule of control lenses. The uncoated IOL (A) and the drug-free coated IOL (B) possessed thin posterior capsules (PC). No apparent inflammatory responses were found in or around lens capsule and no fibrin deposition was observed with the capsule. (16X)

Although there is very little or no cell activity on drug-eluting IOL, drug-eluting IOLs were often accompanied with inflammatory responses in capsule surrounding tissues. Inflammation was observed visually in rabbit eyes and also during histologic analysis. Rather interestingly, we also observed the accumulation of large amount of fibrin fiber, hallmark of inflammatory responses, outside the posterior lens capsule (Figure 6.6). This unexpected complication forces us to re-examine our current coating preparation.

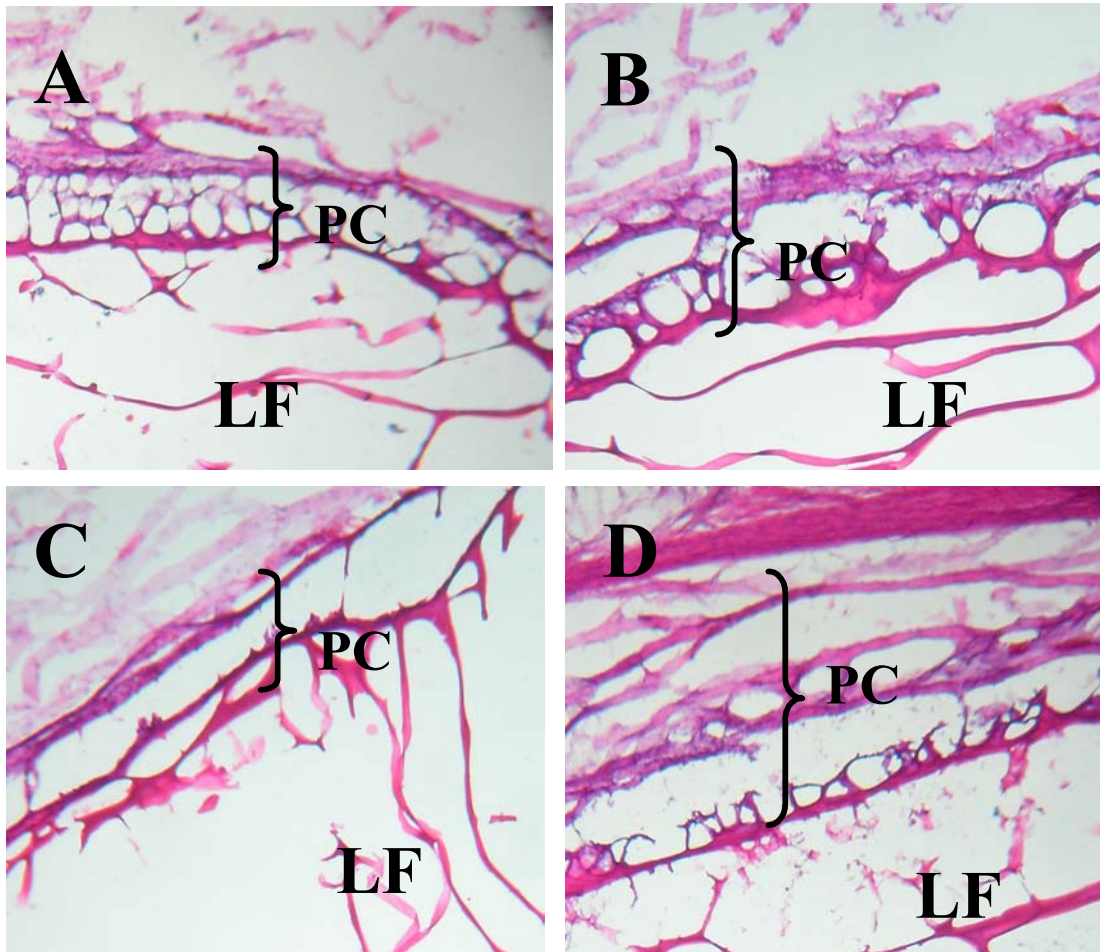


Figure 6.6 Cross section of posterior capsule for drug eluting lenses. All drug-eluting lenses prompted a thickening of the posterior capsule (PC) and fibrin (LF) deposition. (A) DI+COL, (B) DI+MMC, (C) COL, and (D) HEP+COL. (16X)

Surface Roughness Evaluation: The culprit for unwanted side effects. By examining the drug-eluting IOL surfaces using SEM, we observed varying surface roughness for each of the coatings due to drug loading. The colchicine only lens surface (loaded at 80 mg/mL) was rough and contained undissolved crystals within the coating (Figure 6.7A). The HEP+COL coating was also rough and contained pitting on the

surface of the lens (Figure 6.7B). Pitting was the result of elevated levels of heparin, levels above the solubility limit, mixed into the coating resulting in breakdown of the structure of the coating matrix. Shortly following incubation with BSS, the roughness of IOL surface was substantially increased. On the other hand, the drug-free coating control remained smooth along with the DI+COL and DI+MMC lenses.

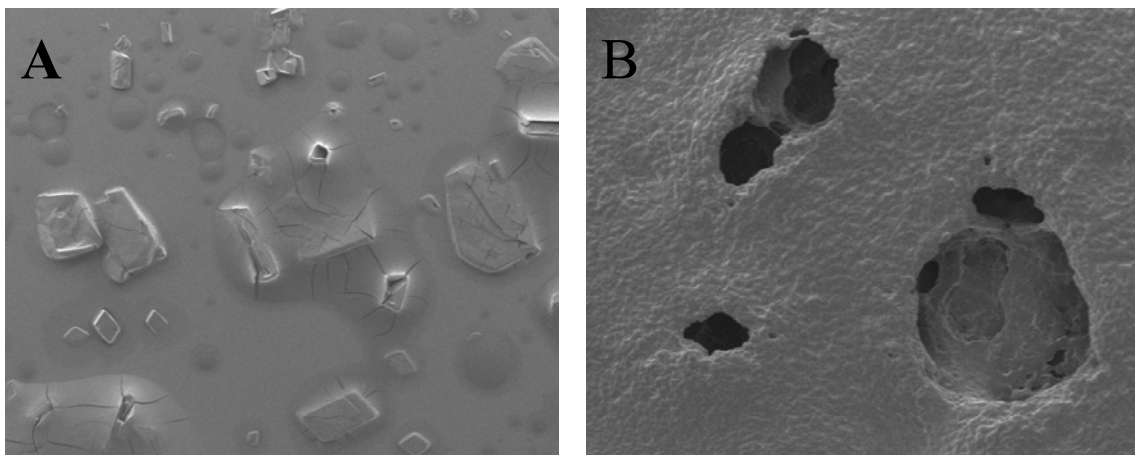


Figure 6.7 SEM micrographs of the surface of coated lenses. Both control lenses and drug combination lenses (DI+COL and DI+MMC) had smooth surfaces while the COL, colchicine only, (A) surface was rough and contained undissolved crystals in the dried state. Heparin + colchicine, HEP+COL (B), had a rough surface that contained pitting. (SEM 100X)

Particulate Evaluation: Since there was no cell accumulation on drug-eluting lenses and complications associated with drug-eluting coating are often observed on the capsule surrounding tissues, we have assumed that the degradation products (or particulate) from the drug-eluting coatings were responsible to the inflammatory reactions in surrounding tissues. To gather evidence to support this hypothesis, we

examined the accumulation of particles in solution for each of the drug loaded lenses used in the Phase I in vivo study. Briefly, lenses were soaked in BSS for 2 weeks at 37°C to mimic implantation conditions. After 2 weeks, BSS was analyzed for particulate as a result of coating breakdown. Deionized water was used as a background for all measurements.

Analysis of BSS alone revealed that BSS contains particles but all were less than 0.01 μm (Figure 6.8). Percent Channel represents the percentage of total particles at the specified size. Percent Passing represents the cumulative percent of total particles at or below the specified size. The drug-free coated lenses and uncoated IOL produced no particulate. All drug loaded lenses created particulate. The environmental conditions along with elevated levels of drug loading resulted in coating degradation and thus particulate production. DI+COL coated lenses produced particles. Less than 20% of the released particles from DI+COL coated lenses were greater than 1 μm (Figure 6.9). Approximately 90% of the particles produced by HEP+COL coated lenses were greater than 1 μm (Figure 6.10). Only about 50% of the particles produced by DI+MMC were greater than 1 μm (Figure 6.11). All the particles produced by the colchicine (COL) only lens were greater than 1 μm (Figure 6.12). Particle production and release by an IOL is not desirable and may lead to inflammatory responses in IOL surrounding tissues, such as lens capsule, and iris.

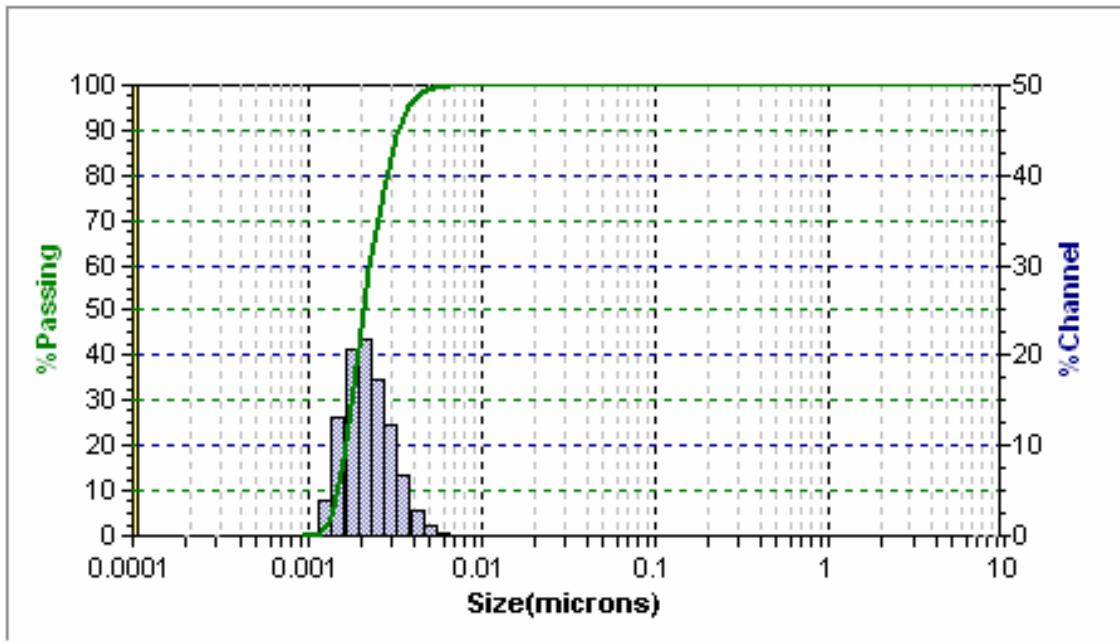


Figure 6.8 The size distribution of particles present in BSS. All of the particles produced were < 0.01 microns.

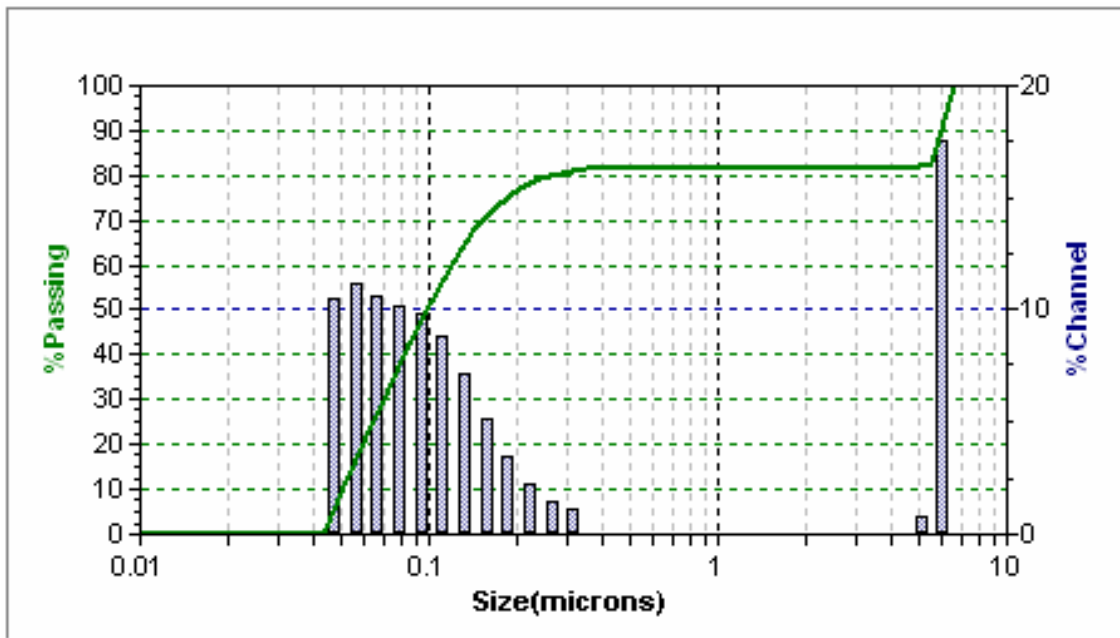


Figure 6.9 The size distribution of particles released from lenses loaded with diclofenac + colchicine. More than 80% (% Passing) of the particles produced were small in size (< 0.4 microns).

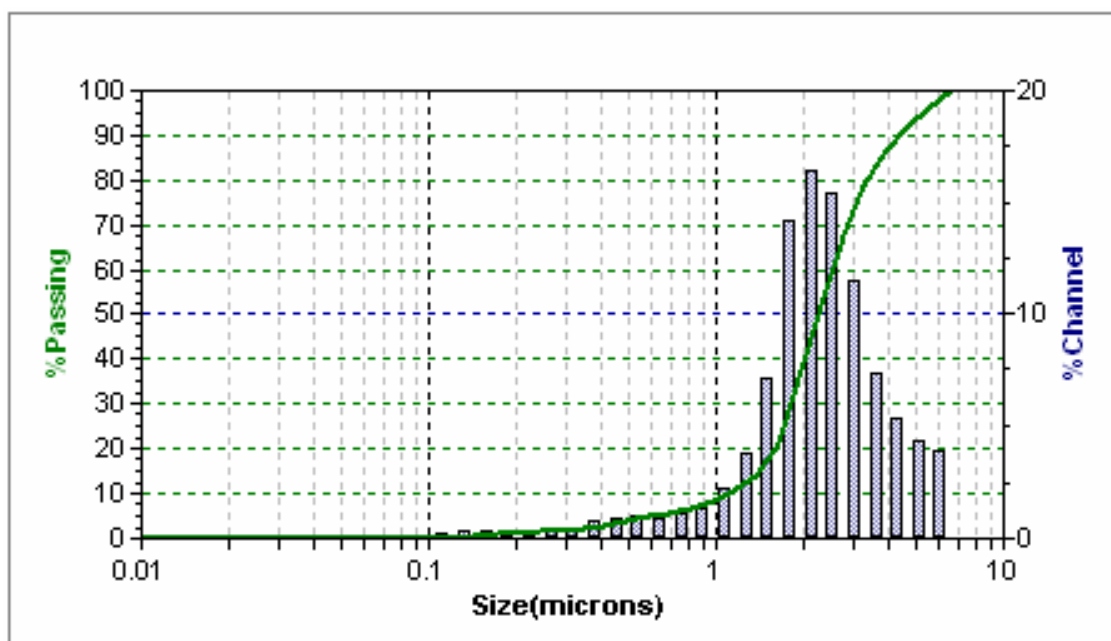


Figure 6.10 The size distribution of particles released from lenses loaded with heparin + colchicine. These conditions produced particulate with more than 90% of the particles >1.0 micron in size.

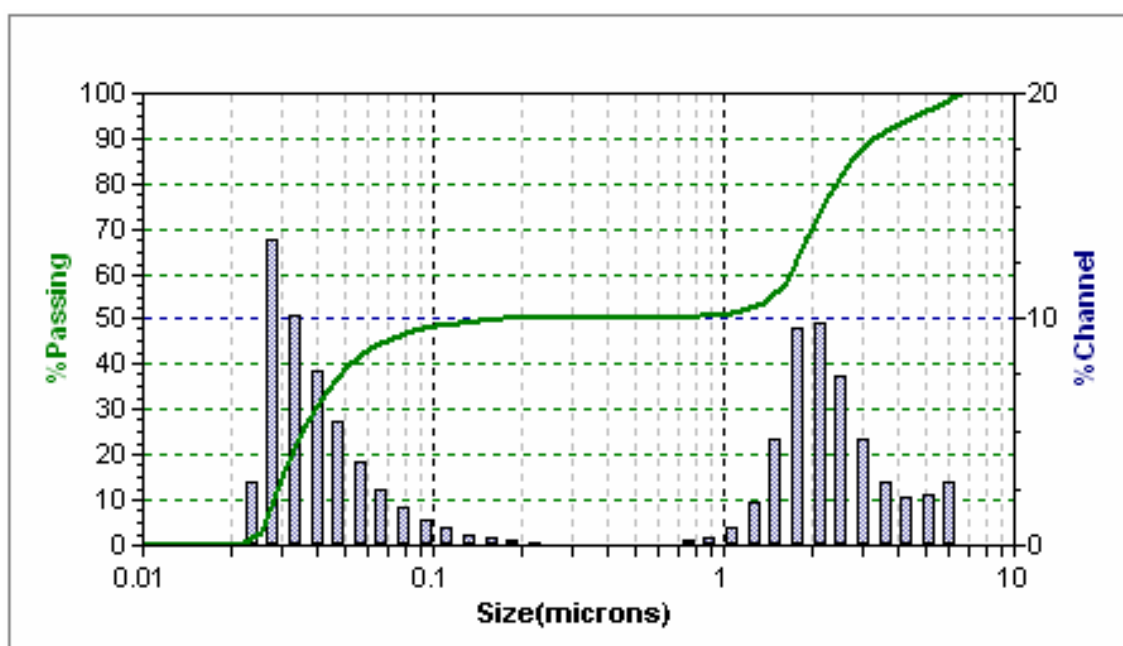


Figure 6.11 The size distribution of particles released from lenses loaded with diclofenac + MMC produced. These conditions produced particulate due to breakdown of the coating with approximately 50% of the particles >1.0 micron in size.

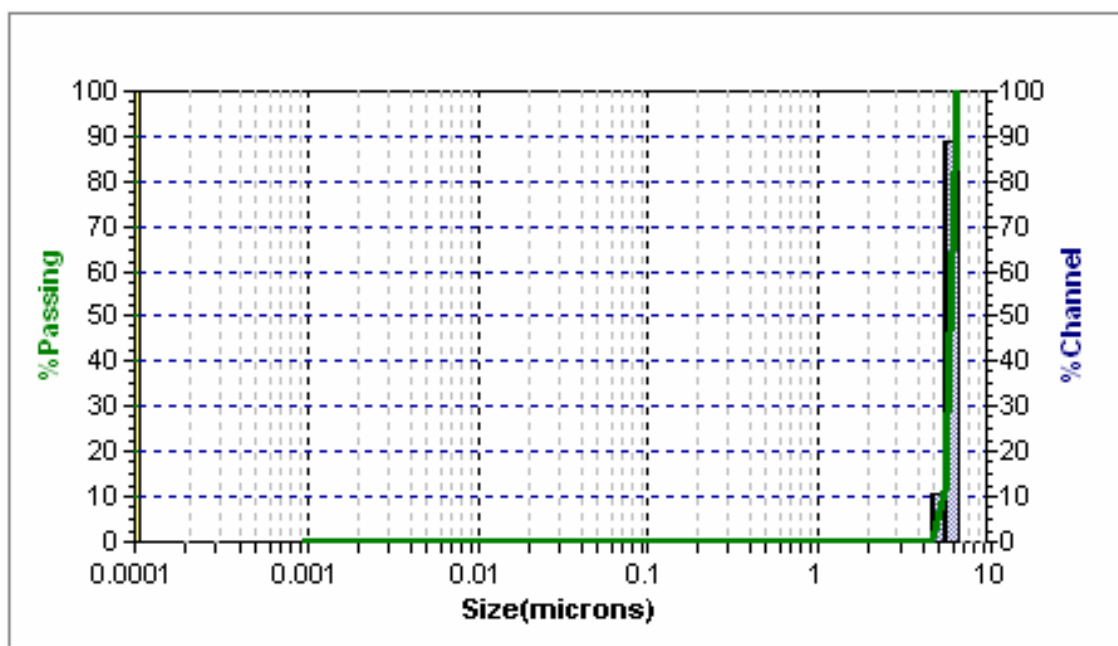


Figure 6.12 The size distribution of particles released from lenses loaded with colchicine only. These conditions produced particulate with all of the particles >1.0 micron in size.

Conclusion: Coating modification to reduce coating breakdown and associated inflammatory reactions. Results suggested that excessive drug loading weakened the integrity and stability of the drug-eluting coating. Such drawback can be resolved simply by reducing the drug loading concentrations. Indeed, our pilot study has shown that, by reducing drug loading concentrations, particle release from drug-eluting coatings could be substantially reduced. To test the versatility of this drug eluting system, lens coating systems were loaded with different drug concentrations and then tested in the Phase II and III study.

6.2 Phase II – Animal Implantation of Diclofenac Drug System

6.2.1 Introduction

To further improve the in vivo outcome of the drug eluting coating, we chose to only focus on diclofenac-eluting system and to improve coating stability by reducing drug loading concentration. The therapeutic effect of these coatings (with different drug eluting capacities) were investigated using rabbit implantation model as described earlier (section 6.2). Four AcrySof® MA60BM were coated for this investigation with diclofenac (DI) coating solutions of varying concentration, including concentrations of 42.8 mg/ml, 14.9 mg/ml, 5.2 mg/ml, or without diclofenac as coating control. All coated lenses were implanted for 2 weeks in rabbits before performing physiological and histological analyses.

6.2.2 Experimental Design

All procedures followed the same protocol as described in Section 6.1.2.

6.2.3 Results – Animal Study Phase II

Surface Roughness Evaluation: The optical surface of hydrated lenses was examined by SEM to evaluate surface characteristics or roughness due to each coating. Control lenses (drug-free coating) and coatings containing 5 mg/mL were smooth in nature (Figure 6.13A). However, as loading capacities were increased, the surface roughness also increased (Figure 6.13 B & C).

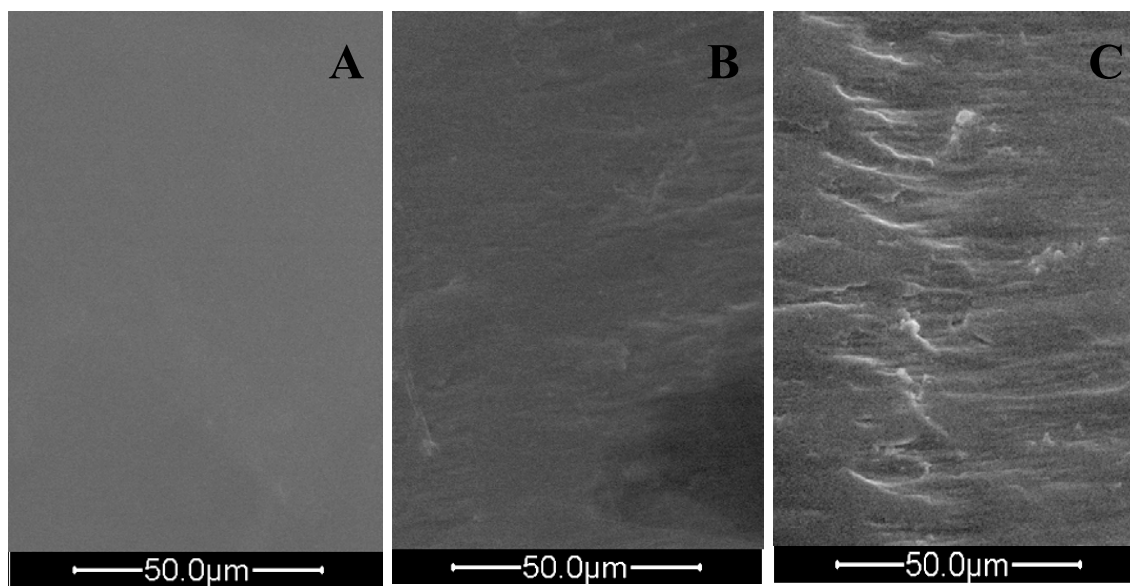


Figure 6.13 SEM micrographs of hydrated diclofenac coated lenses. Lenses were soaked in BSS at 37°C for 2 weeks. The control lenses and diclofenac loaded lenses with 5 mg/mL (A) had smooth surfaces. The surface roughness increased as loading capacities increased, (B) 15 mg/mL and (C) 40 mg/mL (500X).

Particulate Evaluation: No diclofenac loaded lenses with concentrations between 5 to 40 mg/mL created particulate. The signal for each of these concentrations was low indicating that only a small number of particles were detected. Figure 6.14 is a representative graph for all diclofenac coated lenses ranging in concentrations from 5 to 40 mg/mL.

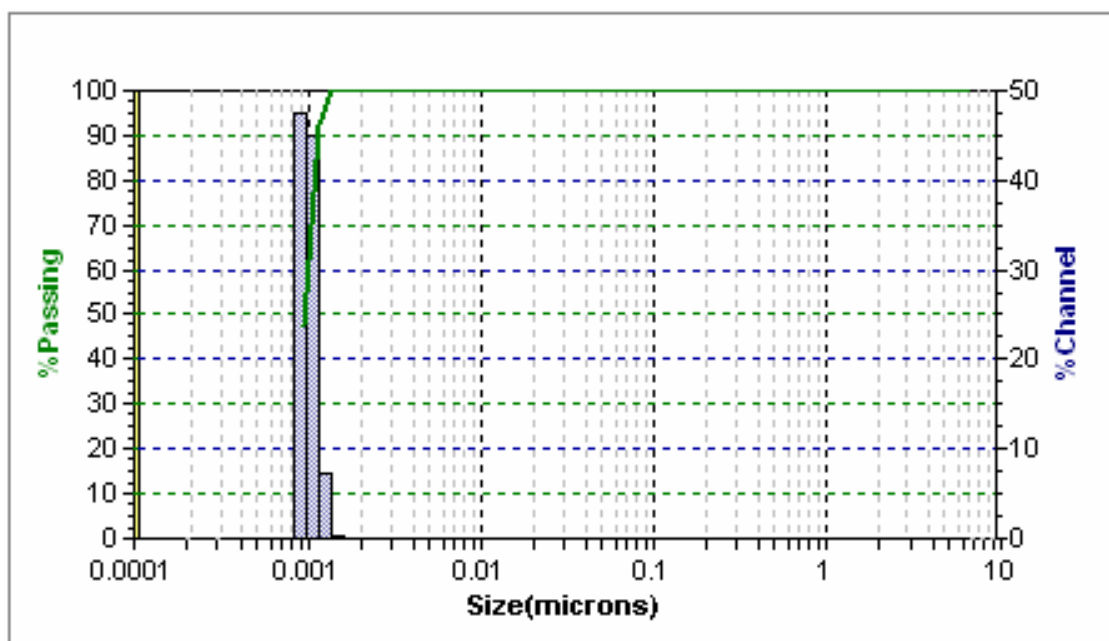


Figure 6.14 The size distribution of particles released from lenses loaded with diclofenac from 5 to 40 mg/mL coating solution. These conditions did not produce particulate. All particles were similar to BSS control (<0.01 μ m).

Histological Evaluation: The control group (drug-free coated IOL) revealed minimal intraocular inflammatory reaction and IOL surface deposits during the 2-week study. The diclofenac loaded lenses also revealed minimal intraocular inflammation and IOL surface deposits during the same time period.

Lenses from each rabbit were extracted, fixated, and stained after 2 weeks implantation. The number of adhered fibrotic cells on the surface of the IOL were counted (Leica microscope, 20X) after staining. The lens with coating containing 40mg/mL of diclofenac contained the highest number of adhered cells to the surface of the IOL (Figure 6.15). The number of adhered cells decreased along with lower diclofenac concentration (Figure 6.16). Fibrotic cells present on the surface of the

control IOL were elongated and healthy. Cells present on the surface of drug loaded lenses were rounded and did not show any signs of cellular activity. Rather unexpectedly, lenses with higher loading concentrations of diclofenac, 15 and 40 mg/ml, prompt prominent foreign body reactions. Although the mechanism governing such inverse responses has yet to be determined, we believe that higher concentration of diclofenac may be toxic to the surrounding cells and tissue.

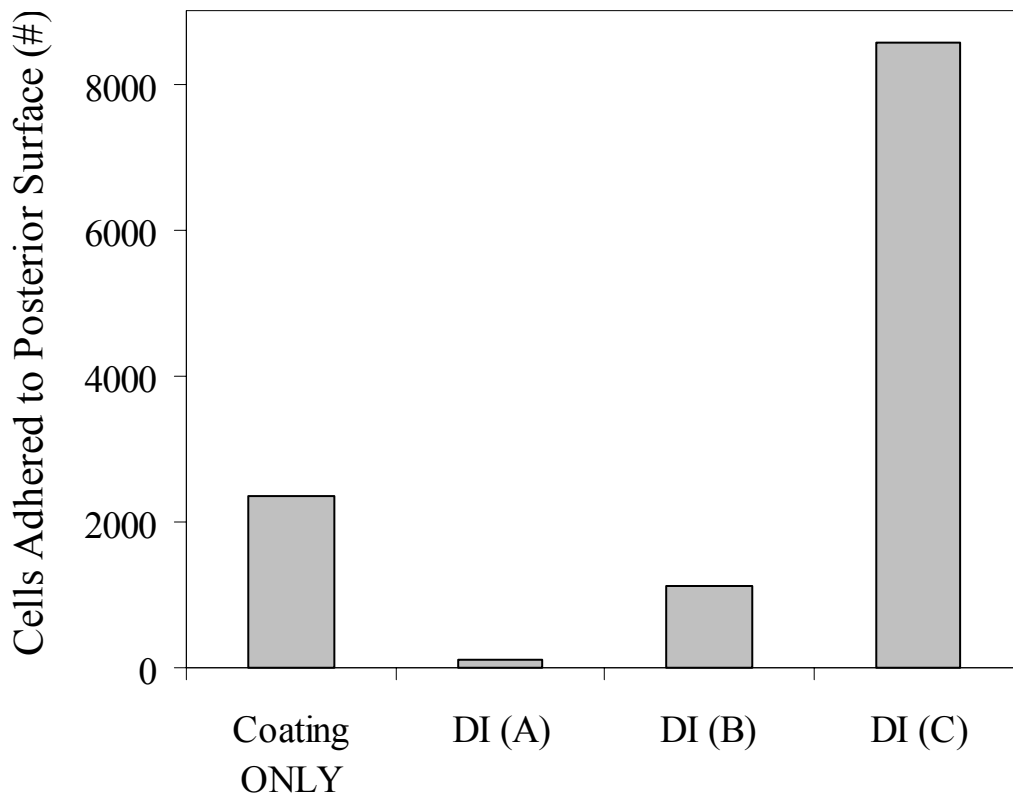


Figure 6.15 The loading concentrations of diclofenac (DI) considerably affected fibrotic cell accumulation on the posterior capsule. Low concentrations, DI (A) at 5.2 mg/mL, were sufficient to reduce the number of cells present on the surface of the IOL compared to the control (coating only) and other test lenses, DI (B) 14.9, and DI (C) 42.8 mg/mL coating solution concentration.

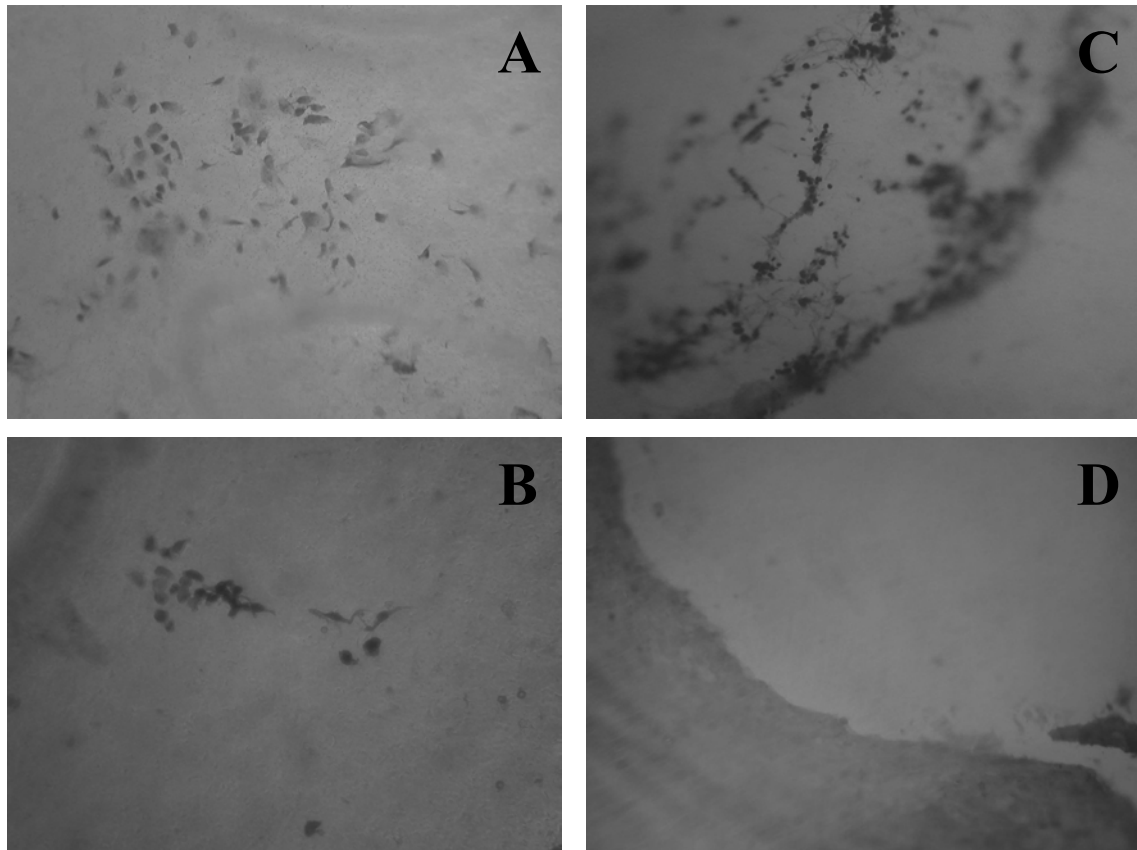


Figure 6.16 Adherent fibrotic cells on the surface of the lens after 14 days implantation. These pictures show regions on the posterior surface of the lens with the highest density of fibrotic cells growth and proliferation. The control lens has cell growth and migration on the posterior capsule. (A) Alcon MA60BM IOL + coating only. Drug delivery systems contained varying concentrations of diclofenac including 5 mg/mL (B), 15 mg/mL (C), and 40 mg/mL (D). The low concentration release (5 mg/mL) diclofenac effectively inhibited cell growth and migration as evident by a significantly reduced cell number compared to the control. At higher concentrations diclofenac did not effectively inhibit fibrotic cells adhesion to the surface of the IOL. (20X)

Histologic evaluation of the lens capsule was completed following lens extraction after 2-weeks implantation. As expected, higher concentration of diclofenac prompted inflammatory responses in corneal and iris tissues. In supporting of our hypothesis, no apparent lens capsule inflammation was associated with lower

concentrations of diclofenac (Figure 6.17 B&C). No inflammation was observed visually in rabbit eyes and no inflammatory cells were observed in histologic analysis of ocular tissue. Overall, we have excitingly discovered that coating with only 5 mg/ml diclofenac substantially reduced cell accumulation on IOL implants compared with IOL with or without drug eluting coating (Figure 6.17A).

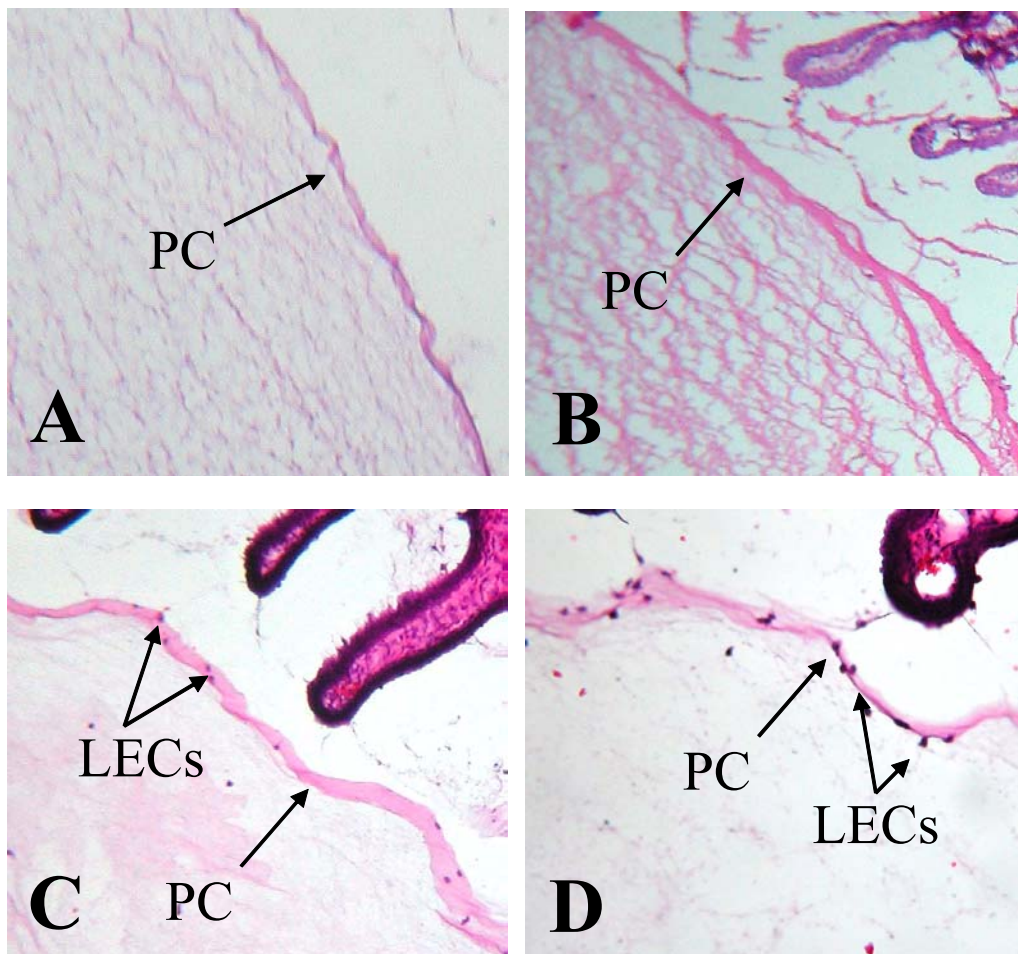


Figure 6.17 Cross section of posterior capsule for diclofenac loaded lenses. The posterior capsule (PC) for the control (A) and 5.2 mg/mL concentration diclofenac (B) had a thin PC with no adhered LECs. The PC was thickened and LECs adhered to the PC at both higher concentration levels, 14.9 mg/mL (C) & 42.8 mg/mL (D). (20X)

6.3 Phase III – Animal Implantation of Colchicine Drug System

6.3.1 Introduction

The results from in vitro studies and the first in vivo study have shown that colchicine is a potent cell migration and proliferation inhibitor. It is likely that colchicine-eluting coatings substantially diminish PCO formation. Our first series of studies have revealed that drug eluting coating effectively reduced cell adhesion and proliferation on IOL implants. However, we have also uncovered that high drug loading concentration may lead to coating breakdown and subsequent lens capsule inflammation. To further improve the in vivo outcome of the drug eluting coating, we chose to first create stable and smooth colchicine releasing coatings. The therapeutic effect of these coatings will be investigated using rabbit implantation model as described earlier (section 6.1). Four AcrySof® MA60BM were produced for this investigation. In this study, only a single LEC targeting drug, colchicine (COL), was evaluated at concentrations including 2.57 mg/mL, 10.53 mg/mL, and 30.27 mg/mL of coating solution. A drug-free coated IOL was included as a control. All lenses were implanted for 2 weeks in rabbits before performing physiological and histological analyses.

6.3.2 Experimental Design

All procedures followed the same protocol as described in Section 6.1.2.

6.3.3 Results – Animal Study Phase III

Surface Roughness Evaluation: The optical surface of hydrated colchicine coated lenses was examined by SEM to evaluate surface roughness due to each coating.

Control lenses (coating without drug) and coatings containing 2 to 30 mg/mL of colchicine were smooth in nature (Figure 6.18).

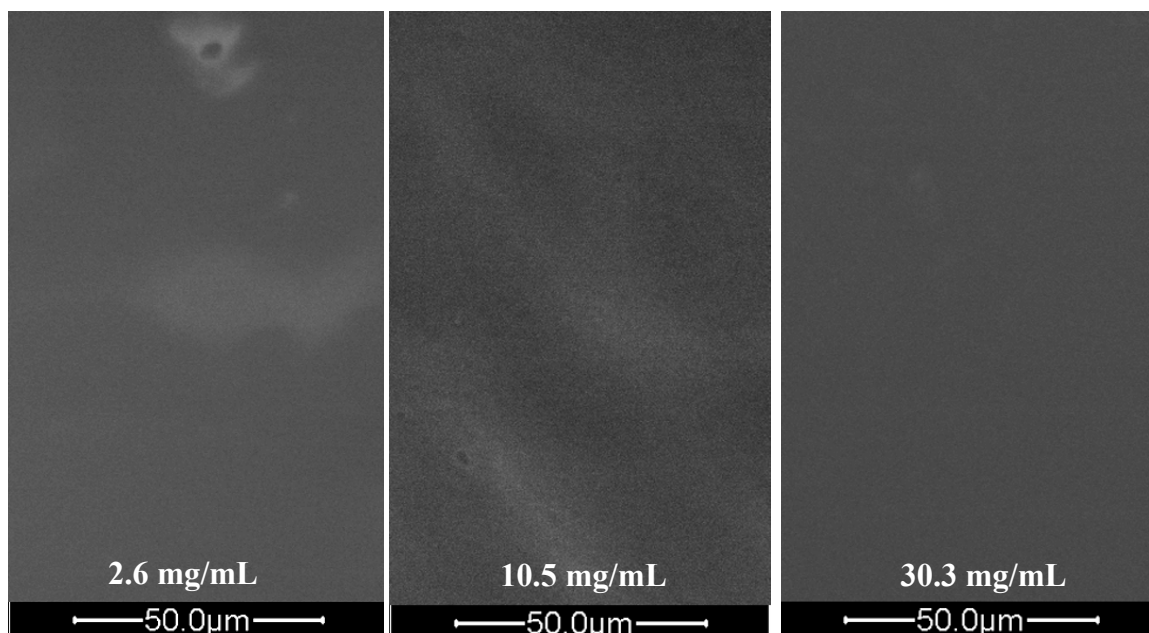


Figure 6.18 SEM micrographs of hydrated colchicine coated lenses. Lenses were soaked in BSS at 37°C for 2 weeks. The control lenses and diclofenac loaded lenses with 2 to 30 mg/mL had smooth surfaces. (SEM 500X)

Particulate Evaluation: Colchicine concentrations of 2.6 mg/mL, 10.5 mg/mL, and 30.3 mg/mL did not produce particulate. Figure 6.19 is a representative graph for particulate analysis for all colchicine concentrations ranging from 2.6 to 30.3 mg/mL. Thus, physiologic environmental conditions along with these levels of drug loading resulted in no coating degradation and particulate production after 2 weeks in vitro.

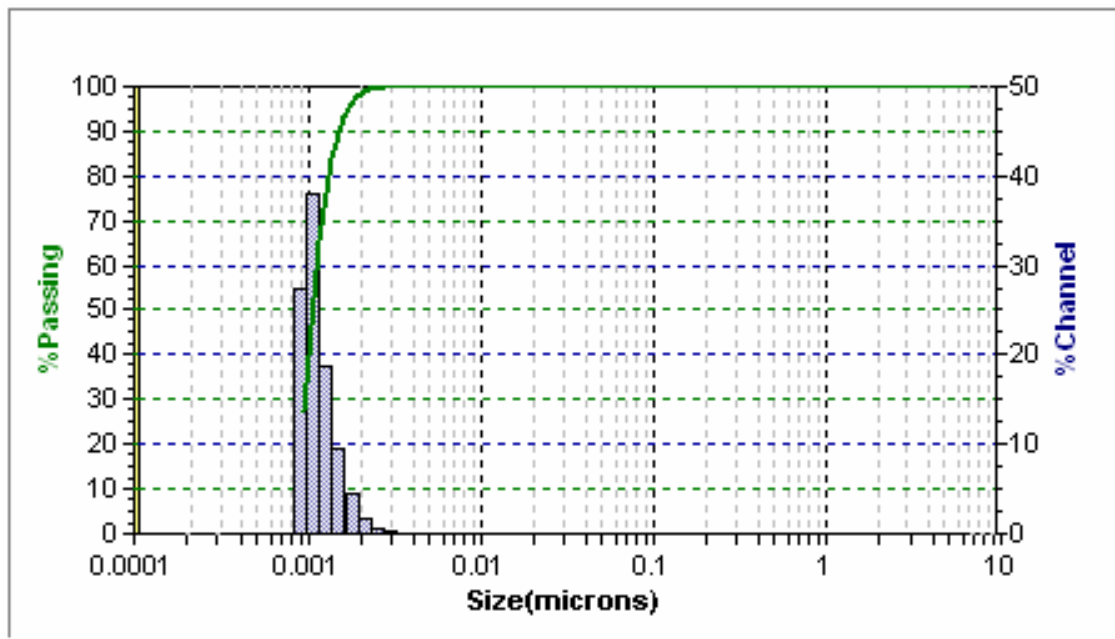


Figure 6.19 The size distribution of particles released from lenses loaded with colchicine from 2.6 to 30.3 mg/mL coating solution. These conditions did not produce particulate. All particles were similar to BSS control ($<0.01\mu\text{m}$).

Histologic Evaluation: The control IOL groups (drug-free coated IOL) revealed minimal intraocular inflammatory reaction and IOL surface deposits during the 2-week study. The colchicine loaded groups revealed minimal intraocular inflammatory reaction and IOL surface deposits during the 2-week study as well. No inflammation was observed visually in rabbit eyes and minimal inflammatory cells were observed in histologic analysis of ocular tissue in control lenses or lenses with colchicine loaded lenses.

Lenses from each rabbit were extracted, fixated, and stained after 2 weeks implantation. The number of adhered fibrotic cells on the surface of the IOL were

counted (Nikon optical microscope, 20X) after staining. The lens with coating containing 2.6mg/mL of colchicine contained the highest number of adhered fibrotic cells to the surface of the IOL. The number of adhered fibrotic cells decreased as colchicine concentration increased (Figure 6.20). Regions with the highest density of fibrotic cell growth and proliferation were captured on digital micrographs (20X) using an optical microscope (Figure 6.21). Digital micrographs of control lenses indicate that the cells are healthy as indicated by cellular characteristics, i.e. flattened and elongated. Drug loaded lenses that effectively reduced fibrotic cell growth and proliferation contained cells that were rounded and showed no signs of cellular activity. The results from this study have shown strong support that IOL coating with 10-30 mg/ml colchicines reduced IOL-mediated foreign body reactions and later PCO formation (Figure 6.22).

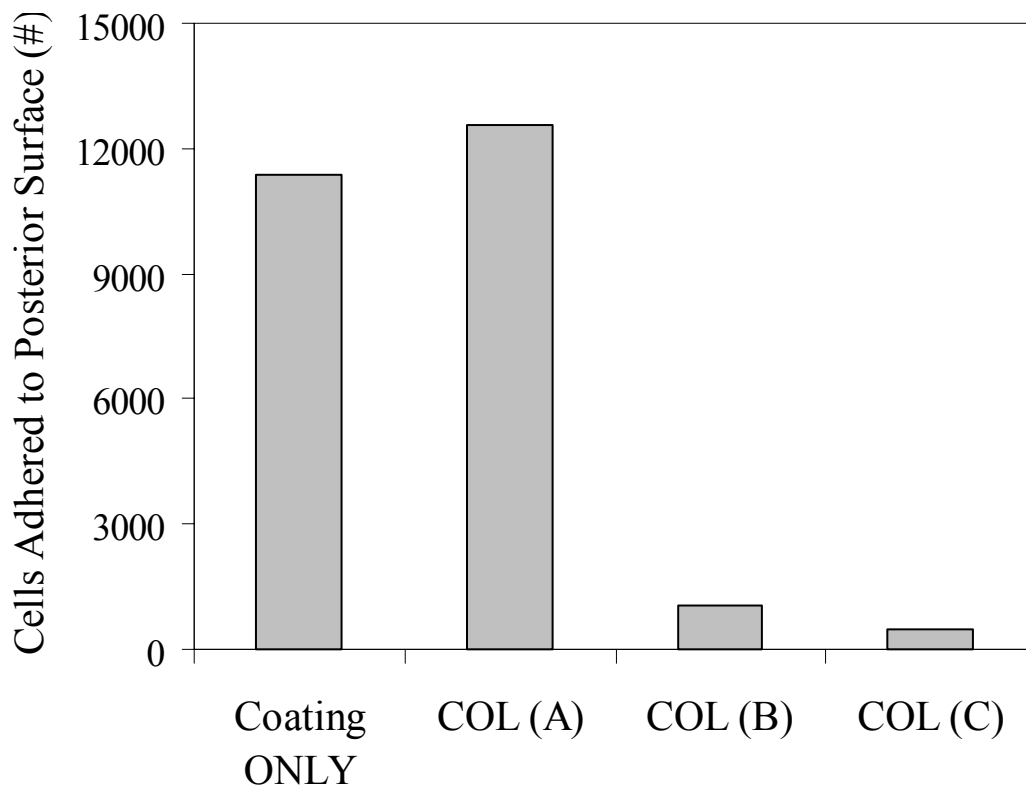


Figure 6.20 The loading concentrations of colchicine (COL) affected the degree of fibrotic cell adherence on the posterior capsule. Loading concentrations were based on coating solution concentrations including (A) 2.6, (B) 10.5, and (C) 30.3 mg/mL. High concentration release of colchicine reduced the number of fibrotic cells present of the IOL surface compared to the drug-free coated control. Fibrotic cells present on the surface of the control IOL were elongated and healthy. Cells present of the surface of drug loaded lenses shown here were rounded and did not show any signs of cellular activity (n=1).

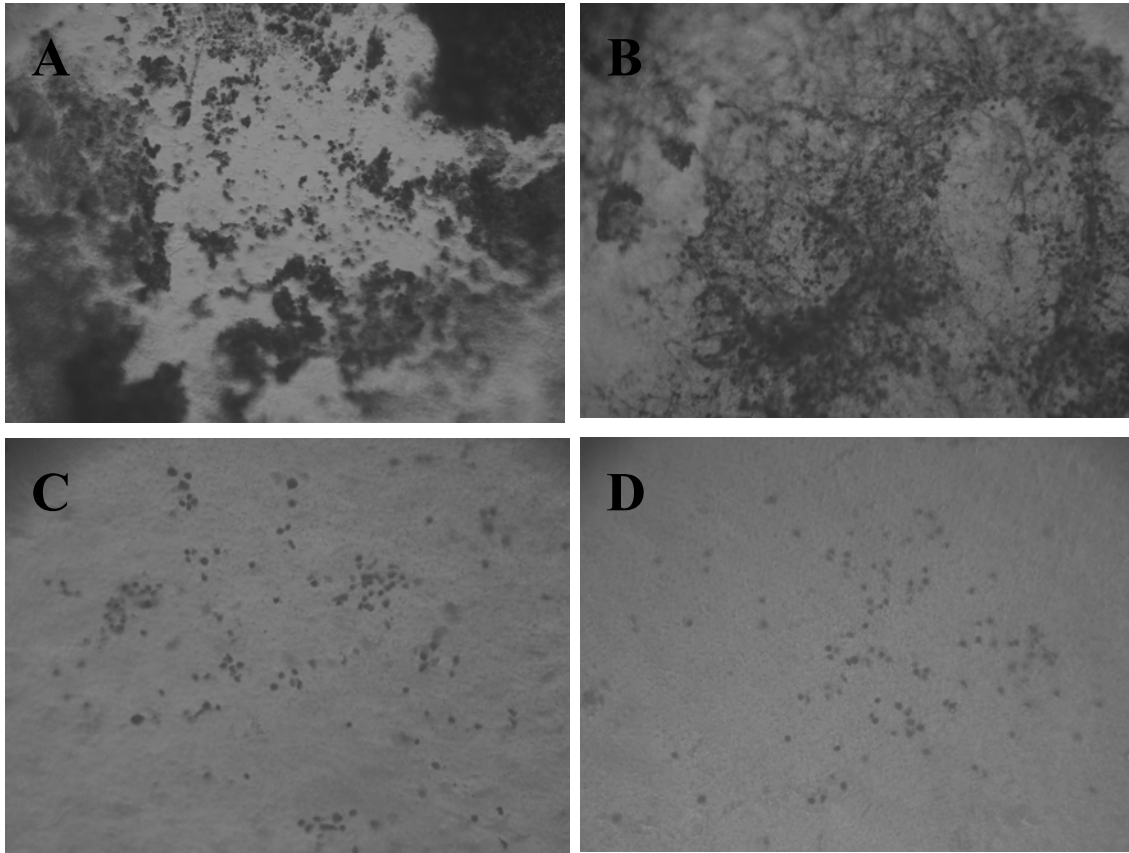


Figure 6.21 Adherent fibrotic cells on the surface of the lens after 14 days of implantation in New Zealand White rabbits. These pictures show regions on the posterior surface of the lens with the highest density of fibrotic cell growth and proliferation. The control lens, (A) Alcon MA60BM IOL + coating only, has cell growth and migration on the posterior capsule. Drug delivery systems contained varying concentrations of colchicine including 2.6 mg/mL (B), 10.5 mg/mL (C), and 30.3 mg/mL (D). The high concentration release (30 mg/mL) colchicine effectively inhibited cell growth and migration as evident by a significantly reduced cell number compared to the control. At lower concentrations diclofenac did not effectively inhibit fibrotic cells adhesion to the surface of the IOL (20X).

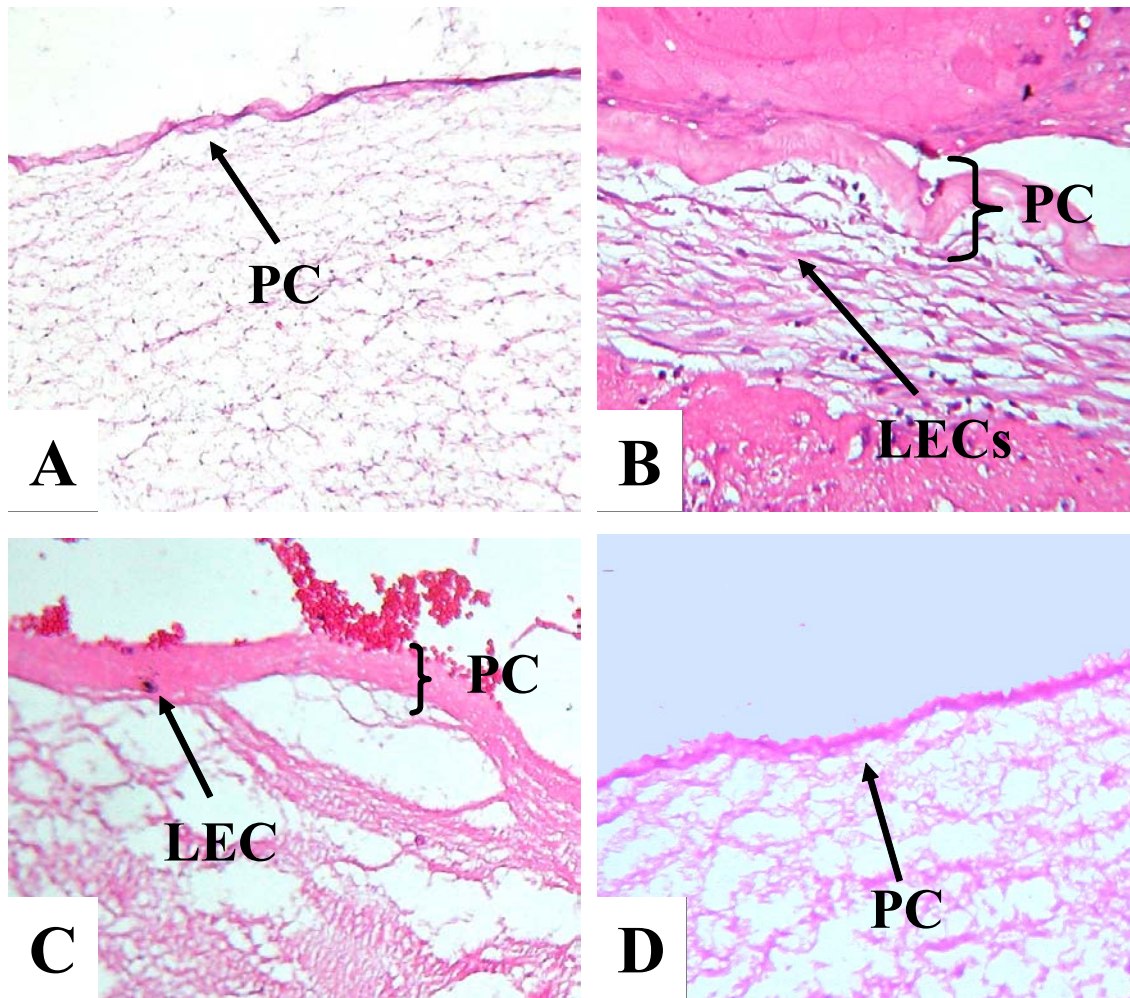


Figure 6.22 Cross section of posterior capsule for colchicine loaded lenses. The posterior capsule (PC) under normal conditions is thin (A). At the low concentrations of colchicine, 2.6 mg/mL (B) and 10.5 mg/mL (C), the posterior capsule was thickened. As the concentration was increased to 30.3 mg/mL (D), the number of LECs present on the lens decreased significantly thereby preventing the thickening of the posterior capsul. (20X)

CHAPTER 7

CONCLUSIONS AND PERSPECTIVE

Results from this study have demonstrated that intraocular lens coating may serve as a viable option as a drug delivery platform. The hydrogel coating used in this study effectively released a variety of drugs, including prospective drugs to combat PCO, for extended periods of time (> 2 weeks). However, in vivo studies indicated that the coating has limitations related to drug loading. When excessive drug was loaded into the coating, the coating integrity was weakened resulting in coating breakdown and particulate release. In order to achieve higher loading concentrations and improved hydrolytic stability, alternate coatings or other drug delivery platforms are required.

In vitro studies determined that specific drugs are capable of inhibiting inflammatory cell activation, LEC migration, and/or LEC proliferation at low concentrations. Results have also demonstrated that diclofenac (DI), colchicine (COL), and mitomycin-C (MMC) can be released from the aqueous based PU coating at minimum effective levels past 10 days. The release rates from the PU coating can be controlled by varying the crosslink density of the coating, the

hydrophilicity of the coating, coating thickness, dissolution rate of the drug, and molecular weight of the drug.

Depending on the properties of the drug, release was governed by ion-exchange phenomenon and/or diffusing out of the polymer matrix (coating). Upon implantation, the coating was hydrated by the surrounding medium (aqueous humor). Hydration caused the polymer matrix to swell and allowed drug to diffuse through the polymer and/or exchange ions with inorganic ions present in the medium. Both of these drug release mechanisms allowed drugs to be loaded onto a polymer matrix and then controllably released *in vivo* by diffusion or by exchange of ions from the salts present in surrounding medium.

In vivo studies demonstrated that the intraocular drug delivery system reduced IOL-associated foreign body reactions. Histological analysis provided evidence that cell adhesion to the IOL was significantly reduced compared to the control IOL. Histology also showed the effects of various drugs and drug concentration on ocular tissue. Results verified that optimal concentrations for each drug exist. When concentrations are not optimal, cellular responses are uninhibited, toxic environments may be produced, and other side effects may occur including chronic inflammation. Despite of early success, this drug eluting coating does have some drawbacks, including poor light transparency and weak stability when loaded with drugs. Further studies are needed to resolve these weaknesses.

Within the scope of this study, a variety of drugs demonstrated the ability to inhibit inflammation, LEC migration, and LEC proliferation at low concentrations. The

intraocular drug delivery system concept demonstrated that it was capable of releasing a variety of drugs for prolonged periods of time. Results provide first evidence to support that the intraocular drug delivery system can be engineered to reduce IOL-associated foreign body reactions and subsequent PCO formation processes. This concept is promising and provides a useful tool to combat not only PCO but also a variety of other eye diseases, including posterior eye diseases that are currently untreatable due to their location in the back of the eye.

APPENDIX A

DESIGNED EXPERIMENT #1 – 24 HOUR DRUG LOADING

Response: 24 hr release

ANOVA for Selected Factorial Model
 Analysis of variance table [Partial sum of squares]

Source	Sum of Squares	DF	Mean Square	F Value	Prob > F	
Model	1.09E-03	3	3.63E-04	253.83	0.0039	significant
A (Drug Loading)	8.34E-04	1	8.34E-04	582.27	0.0017	
B (Crosslinker)	1.85E-04	1	1.85E-04	129.04	0.0077	
AB	1.57E-04	1	1.57E-04	109.5	0.009	
Residual	2.86E-06	2	1.43E-06			
Cor Total	1.09E-03	5				

The Model F-value of 253.83 implies the model is significant. There is only a 0.39% chance that a "Model F-Value" this large could occur due to noise.

Values of "Prob > F" less than 0.0500 indicate model terms are significant. In this case A, B, AB are significant model terms.

Values greater than 0.1000 indicate the model terms are not significant. If there are many insignificant model terms (not counting those required to support hierarchy), model reduction may improve your model.

Std. Dev.	1.20E-03	R-Squared	0.9974
Mean	0.017	Adj R-Squared	0.9935
C.V.	6.86	Pred R-Squared	N/A
PRESS	N/A	Adeq Precision	37.643

Adeq Precision measures the signal to noise ratio. A ratio greater than 4 is desirable. Your ratio of 37.643 indicates an adequate signal. This model can be used to navigate the design space.

Coefficient Factor	Standard Estimate	95% CI DF	95% CI Error	Low	High	VIF
Intercept	0.022	1	5.18E-04	0.019	0.024	
A-Coating Incorporation	-0.013	1	5.18E-04	-0.015	-0.01	1
B-Xlinker	-5.89E-03	1	5.18E-04	-8.12E-03	-3.66E-03	1.13
AB	5.42E-03	1	5.18E-04	3.19E-03	7.65E-03	1.12

APPENDIX B

DESIGNED EXPERIMENT #1 – 48 HOUR DRUG LOADING

Response: 48 hr release

ANOVA for Selected Factorial Model

Analysis of variance table [Partial sum of squares]

Source	Sum of Squares	DF	Mean Square	F Value	Prob > F	
Model	2.94E-05	1	2.94E-05	22.89802	0.0087	significant
A (Drug Loading)	2.94E-05	1	2.94E-05	22.89802	0.0087	
Residual	5.13E-06	4	1.28E-06			
Cor Total	3.45E-05	5				

The Model F-value of 22.90 implies the model is significant. There is only a 0.87% chance that a "Model F-Value" this large could occur due to noise.

Values of "Prob > F" less than 0.0500 indicate model terms are significant. In this case A are significant model terms.

Values greater than 0.1000 indicate the model terms are not significant. If there are many insignificant model terms (not counting those required to support hierarchy), model reduction may improve your model.

Std. Dev.	0.001132	R-Squared	0.85129
Mean	0.005777	Adj R-Squared	0.814113
C.V.	19.60187	Pred R-Squared	0.706551
PRESS	1.01E-05	Adeq Precision	7.177781

The "Pred R-Squared" of 0.7066 is in reasonable agreement with the "Adj R-Squared" of 0.8141.

"Adeq Precision" measures the signal to noise ratio. A ratio greater than 4 is desirable. Your ratio of 7.178 indicates an adequate signal. This model can be used to navigate the design space.

Factor	Coefficient		Standard Error	95% CI		VIF
	Estimate	DF		Low	High	
Intercept	0.006559	1	0.00049	0.005197	0.00792	
A-Coating Incorporation	-0.00235	1	0.00049	-0.00371	-0.00098	1

APPENDIX C

DESIGNED EXPERIMENT #2 – DRUG RELEASE

Response: Total Drug Release - ANOVA for Selected Factorial Model
Analysis of variance table [Partial sum of squares]

Source	Sum of Squares	DF	Mean Square	F Value	Prob>F	
Model	1.808E-003	1	1.808E-003	18.96	0.0489	significant
PVP Content (C)	1.808E-003	1	1.808E-003	18.96	0.0489	
Residual	1.907E-004	2	9.536E-005			
Cor Total	1.999E-003	3				

The Model F-value of 18.96 implies the model is significant. There is only a 4.89% chance that a "Model F-Value" this large could occur due to noise. Values of "Prob > F" less than 0.0500 indicate model terms are significant. In this case C are significant model terms. Values greater than 0.1000 indicate the model terms are not significant. If there are many insignificant model terms (not counting those required to support hierarchy), model reduction may improve your model.

Std. Dev.	9.765E-003	R-Squared	0.9046
Mean	0.065	Adj R-Squared	0.8569
C.V.	15.11	Pred R-Squared	0.6184
PRESS	7.629E-004	Adeq Precision	6.158

The "Pred R-Squared" of 0.6184 is not as close to the "Adj R-Squared" of 0.8569 as one might normally expect. This may indicate a large block effect or a possible problem with your model and/or data. Things to consider are model reduction, response transformation, outliers, etc. "Adeq Precision" measures the signal to noise ratio. A ratio greater than 4 is desirable. Your ratio of 6.158 indicates an adequate signal. This model can be used to navigate the design space.

Factor	Coefficient Estimate	DF	Standard Error	95% CI Low	95% CI High	VIF
Intercept	0.065	1	4.883E-003	0.044	0.086	
C-PVP content	0.021	1	4.883E-003	2.541E-004	0.042	1.00

Final Equation in Terms of Actual Factors:

Total = 0.043345 + 2.12625E-003 * PVP content

Diagnostics Case Statistics

Std Order	Actual Value	Predicted Value	Residual	Leverage	Cook's Residual	Outlier Distance	t	Run Order
1	0.094	0.086	7.860E-003	0.500	1.138	0.648	1.356	3
2	0.078	0.086	-7.860E-003	0.500	-1.138	0.648	-1.356	4
3	0.038	0.043	-5.795E-003	0.500	-0.839	0.352	-0.737	2
4	0.049	0.043	5.795E-003	0.500	0.839	0.352	0.737	1

REFERENCES

- 1 Wenzel M, Reim M, Heinze M, Böcking A. Cellular invasion on the surface of intraocular lenses. In vivo cytological observations following lens implantation. *Graefes Arch Clin Exp Ophthalmol* 1988; 226: 449-454.
- 2 Okada K, Takahashi K, Sagawa H & Abe K. Evaluation of the images of specular microscopy of the cells on implanted intraocular lenses in vivo. *Cells & Materials*. 1991; 1: 119-128.
- 3 Spalton DJ, Shah SM & Kerr Muir MG. Specular microscope of the anterior intraocular lens surface. *Eye*. 1993; 7: 707-710.
- 4 Laurell C-G and Zetterström C. Effects of dexamethasone, diclofenac, or placebo on the inflammatory response after cataract surgery. *British Journal of Ophthalmology*. 2002;86:1380-1384.
- 5 Lois N, Dawson R, McKinnon AD, Forrester JV. A new model of posterior capsule opacification in rodents. *Invest. Ophthalmol. & Vis. Sci*. 2003; 44: 3450-3457.
- 6 Van Tenten Y, Schuitmaker JJ, De Groot V, Willekens B, VrensenGF, Tassignon MJ. Cell biological mechanisms underlying posterior capsule opacification : search for a therapy. *Bull. Soc. Belge Ophthalmol*. 2000; 278: 61-66.
- 7 Ratner B, et al. *Biomaterials Science*. Academic Press: New York, 1996.
- 8 Meacock WR, Spalton DJ, Stanford MR. Role of Cytokines in the pathogenesis of posterior capsule opacification. *Brit. J. Ophthalmol*. 2000; 84: 332-336.
- 9 Ohmi S, Uenoyama K. Experimental evaluation of posterior capsule opacification and intraocular lens decentration; comparison of intraocular lenses of 12.5 mm and 14.0 mm diameter. *J Cataract Refract Surg*. 1993;19:348-351.
- 10 Ravalico G, Tognetto D, Palomba M, et al. Capsulorhexis size and posterior capsule opacification. *J Cataract Refract Surg*. 1996;22:98-103.
- 11 Boulton M, Saxby L. Editorial: Adhesion of IOLs to the posterior capsule, *Br. J. Ophthalmol*. 1998; 82:468.
- 12 Garg A, Pandey SK, Chang D, Papopoulos P, Maloof A. *Advances In Ophthalmology*. Chapter 34 - Posterior capsule opacification: experimental and clinical studies and factors for prevention. 2005, pp. 1-786.
- 13 Apple DJ, Solomon KD, Tetz MR, et al. Posterior capsule opacification. *Surv. Ophthalmol*. 1992;37:73-116.

- 14 Boulton ME, Saxby L. Basic Science of the Lens: Secondary cataract, Ophthalmology. Mosby, St. Louis, MO (2003) 265-268.
- 15 Mansfield KJ, Cerra A, Chamberlain CG. FGF-2 counteracts loss of TGF β affected cells from rat lens explants: Implications for PCO. Molecular Vision. 2004; 10:521-532.
- 16 Kappelhof JP, Vrensen GFJM. The pathology of aftercataract. Acta Ophthalmol. 1992;70(Suppl):13-24.
- 17 Oharazawa H, Ibaraki N, Ohara K, Reddy VN. Inhibitory Effects of Arg-Gly-Asp (RGD) Peptide on Cell Attachment and Migration in a Human Lens Epithelial Cell Line. Ophthalmic Res. 2005; Jul-Aug 37(4):191-196.
- 18 Saika S. Relationship between posterior capsule opacification and intraocular lens biocompatibility. Prog. In Ret. & Eye Res. 2004; 23: 283-305.
- 19 Duncan G, Wormstone IM, Davies PD. The aging human lens: structure, growth, and physiological behaviour. Br J Ophthalmol. 1997; 81: 818-823.
- 20 Linnola R. The sandwich theory: A bioactivity based explanation for posterior capsule opacification after cataract surgery with intraocular lens implantation. Department of Ophthalmology, Department of Medical Biochemistry, University of Oulu, Finland (2000). J Cataract Refract Surg. 1997; 23: 1539-1542.
- 21 Liu CS, Wormstone IM, Duncan G, Marcantonio JM, Webb SF, Davies PD. Related Articles, Links A study of human lens cell growth in vitro. A model for posterior capsule opacification. Invest Ophthalmol Vis Sci. 1996; 37(5):906-14.
- 22 Okada K, Funahashi M, Iseki K, Ishii Y. Comparing the cell population on different intraocular lens materials in one eye. J Cataract Refract Surg. 1993; 19: 431-434.
- 23 Sawa M, Tsurimaki Y, Tsuru T, Shimizu H. New quantitative method to determine protein concentration and cell number in aqueous in vivo. Jpn J Ophthalmol. 1988; 32 (2): 132-142.
- 24 Ohara K, Okubo A, Miyazawa A, Miyamoto T, Sasaki H, Oshima F. Aqueous flare and cell measurements using laser in endogenous uveitis patients. Jpn J Ophthalmol. 1989; 33 (3): 265-270.
- 25 Yoshitomi T, Wong AS, Daher E, Sears SE. Aqueous flare measurement with laser flare-cell meter. Jpn J Ophthalmol. 1990; 34(1): 57-62.
- 26 Shah SM, Spalton DJ & Smith SE. Measurement of aqueous cells and flare in normal eyes. Br J Ophthalmol. 1001; 75: 348-352.
- 27 El-Maghraby AE, Marzouki A, Matleen TM, Soucek J, Karr MVD. Reproducibility and validity of laser flare/cell meter measurements of intraocular inflammation. J Cataract Refract Surg. 1993; 19: 52-55.
- 28 Miyake K. The significance of inflammatory reactions following cataract extraction and intraocular lens implantation. J Cataract Refract Surg. 1996, 22 (suppl 1): 759-763.

- 29 Nishi O, Nishi K, Fujiwara T, Shirasawa E, Ohmoto Y. Effects of cytokines on the proliferation of and collagen synthesis by human cataract lens epithelial cells. *Br. J. Ophthalmol.* 1996; 80(1): 63-68.
- 30 Varner S, Hupfer N, Buan J. Coatings: Sustained Drug Delivery for Retinal Disease. *Med. Dev & Diag. Ind.* July 2005, pp.64-70.
- 31 Peppas N. The structure of a highly crosslinked poly(2-hydroxyethyl methacrylate) hydrogels. *J Biomed Mater Res.* 1985, 19: 397-411.
- 32 Peppas L. Polymers in Controlled Drug Delivery. *Med Plastics and Biomat.* Nov 1997, pp. 34-40.
- 33 Wunder H. Fulfilling the IOL Injector Wish List. *Rev. of Ophthalmol.* 2004; 11(1): 3-4.
- 34 Burstein NC, Ding M, Pratt MV. Intraocular lens material evaluation by iris abrasion in vitro: A scanning electron microscope study. *J. Cataract Refract. Surg.* 1988; 14(5): 520-525.
- 35 Hofmeister FN, Yalon MS, Iida S, Goldberg MD. In vitro evaluation of iris chafe protection afforded by hydrophilic surface modification of PMMA IOLs. *J. Cataract Refract. Surg.* 1988; 14(5): 514-519.
- 36 Yalon M, Sheets JW, Reich S, Goldberg EP. Quantitative aspects of endothelium damage due to intraocular contacts: Effect of hydrophilic polymer graft coatings. *Int Cong. Ophthalmol.* 1983; 24: 273-276.
- 37 Lin T, Lu F, Conroy S, Sheu S, Su S, Tamg L. Antimicrobial Coatings: A Remedy for Medical Device Related Infections. *Medical Device Tech.* October 2001, 30-34.
- 38 ISO 10993-10:2002, Biological evaluation of medical devices -- Part 10: Tests for irritation and delayed-type hypersensitivity, pp. 1-49.
- 39 ISO 10993-6:1994, Biological evaluation of medical devices - Part 6: Tests for local effects after implantation, pp. 1-11.
- 40 Stager DR, Weakley DR, Hunter JS. Long-term rates of PCO following small incision foldable acrylic IOL implantation in children. *Journal of Pediatric Ophthalmology and Strabismus.* 2002; 39(2): 73-76.
- 41 Ismail MM, Alio JL, Ruiz JM. Prevention of secondary cataract by antimitotic drugs: experimental study. *Ophthalmic Res.* 1996; 28: 64-69.
- 42 Karon MD, Klyce KD. Effect of Inhibition of Inflammatory Mediators on Trauma Induced Stroma Edema. *Invest Ophthalmol Vis Sci.* 2003; 44(6): 2507-2511.
- 43 Kurosaka D, Nagamoto T. Inhibitory effect of TGF- β 2 in human aqueous humor on bovine lens epithelial cell proliferation. *Invest. Ophthalmol. Vis. Sci.* 1994; 35(9): 3408-3412.
- 44 Duncan G, Wormstone IM, Liu CS. Thapsigargin-coated intraocular lenses inhibit human lens cell growth. *Nature Med* 1997; 3: 958-960.
- 45 Yokoyama T. Interleukin in the aqueous humor in aphakic and pseudophakic eyes of rabbits. *Acta Soc Ophthalmol Jpn.* 1992; 96: 67-73.

- 46 Gordon-Thomson C. Differential cataractogenic potency of TGF- β 1, TGF- β 2, TGF- β 3 and their expression in the postnatal rat eye. *Invest. Ophthalmol. Vis. Sci.* 1998; 39: 1399-1409.
- 47 Hayashi N, Kato H. The change of immunohistochemical localization of basic fibroblast growth factor around the lens capsule after extracapsular extraction. *Acta Soc. Ophthalmol. Jpn.* 1991; 5: 621-624.
- 48 Malecaze F, Chollet P, Cavrois E, Vita N, Arne JL, Ferrara P. Role of interleukin-6 in the inflammatory response after cataract surgery. An experimental and clinical study. *Arch. Ophthalmol.* 1991; 109(12): 1681-1683.
- 49 Ruberti DW, Klyce SD, Smolek MK, Karon MD. Anomalous acute inflammatory response in rabbit corneal stroma. *Invest. Ophthalmol. Vis. Sci.* 2000; 41(9): 2523-2530.
- 50 Wallentin N, Wickstrom K, Lundberg C. Effect of cataract surgery on aqueous TGF-beta and lens epithelial cell proliferation. *Invest. Ophthalmol. Vis. Sci.* 1998; 39: 1410-1418.
- 51 Fischer GA, Parkinson TM, and Szlek MA. OcuPhor™ – The Future of Ocular Drug Delivery. 2000.
- 52 Inan UU, Ozturk F, Kaynak S, Kurt E, Emiroglu L, Ozer E, Ilker SS, Guler C. Prevention of posterior capsule opacification by intraoperative single-dose pharmacologic agents. *J Cataract Refract Surg.* 2001; Jul. 27(7): 1079-87.
- 53 Koraszewska-Matuszewska B. Heparin-surface-modified PMMA intraocular lenses in children in early and late follow-up. *Klin Oczna.* 2003; 105(5): 273-6.
- 54 Xie L, Sun J, Yao Z. Heparin drug delivery system for prevention of posterior capsular opacification in rabbit eyes. *Graefes Arch Clin Exp Ophthalmol.* 2003; 241(4): 309-13.
- 55 Chung H, Lim SJ, Kim HB, Effect of mitomycin-C on posterior capsule opacification in rabbit eyes. *J Cataract Refract Surg.* 2000; 26:1537-1542.
- 56 Haus CM, AL Galand. Mitomycin against posterior capsular opacification: an experimental study in rabbits. *Br J Ophthalmol.* 1996; Dec 80(12): 1087-1091.
- 57 Behar-Cohen FF, David T, D'Hermies F, Pouliquen YM, Buechler Y, Nova MP, Houston LL, Courtois Y. In vivo inhibition of lens regrowth by fibroblast growth factor 2-saporin. *Invest. Ophthalmol. Vis. Sci.* 1995; 36(12): 2434-2448.
- 58 Tetz MR, Ries MW, Lucas C, Stricker H, Volckeer HE. Inhibition of posterior capsule opacification by an intraocular-lens-bound sustained drug delivery system; an experimental animal study and literature review. *J Cataract Refract Surg.* 1996; 22(8): 1070-1078.
- 59 Palmade F, Sechoy-Chambon O, Regnouf de Vains JB, Coquelet C, Bonne C. Inhibition of cell adhesion to lens capsule by LCM 1910, an RGD-derived peptide. *J Ocular Pharm.* 1994; 10(4): 623-632.
- 60 Nishi O, Nishi K, Mano C, Ichihara M, Honda T, Saitoh I. Inhibition of migrating lens epithelial cells by blocking the adhesion molecule integrin: a preliminary report. *J Cataract Refract Surg.* 1997; 23(6): 860-5.

- 61 Fernandez V, Miryam A. Fragoso, Christian Billotte MD, Peggy Lamar, Marcia A. Orozco, Sander Dubovy MD. Efficacy of various drugs in the prevention of posterior capsule opacification: Experimental study of rabbit eyes. *J. Cataract Refract. Surg.* 2004; 30: 2598-2605.
- 62 Zhou J and Menko JS. The Role of Src Family Kinases in Cortical Cataract Formation. *Investigative Ophthalmology and Visual Science.* 2002; 43: 2293-2300.
- 63 Imoto Y, Ohguro N, Yoshida A, Tsujikawa M, Inoue Y, Tano Y. Effects of RGD peptides on cells derived from the human eye. *Jpn. J. Ophthalmol.* 2003; Sep-Oct 47(5): 444-53.
- 64 Sasabe T, Suwa Y, Kiritoshi A, Doi M, Yuasa T, Kishida K. Differential effects of fibronectin-derived oligopeptides on the attachment of rabbit lens epithelial cells in vitro. *Ophthalmic Res.* 1996; 28(4): 201-8.
- 65 Wong TT, Daniels JT, Crowston JG, Khaw PT. Related Articles, Links MMP inhibition prevents human lens epithelial cell migration and contraction of the lens capsule. *Br J Ophthalmol.* 2004; 88(7): 868-72.
- 66 Nishi O, Nishi K, Akaishi T & Shirasawa E. Detection of cell adhesion molecules in lens epithelial cells of human cataracts. *Invest Ophthalmol Vis Sci.* 1997; 38: 579-585.
- 67 Pyzdek T and Berger RW. *Quality Engineering Handbook.* New York: Marcel Dekker, Copyright 1992, pp 323-326.
- 68 ISO 10993-17:2002 Biological Evaluation of Medical Devices – Part 17: Establishment of allowable limits for leachable substances, pp1-25.
- 69 ISO 10993-5:1994, Biological evaluation of medical devices - Part 5: Tests for in vitro cytotoxicity, pp1-9.
- 70 FDA Report (Clark GS), Shelf Life of Medical Devices, April 1991, pp 4-16.
- 71 Karlgard CC, Wong NS, Jones LW, Moresoli C. In Vitro uptake and release of ocular pharmaceutical agents by silicon-containing and p-HEMA hydrogel contact lens materials. *Inter. J. of Pharmaceutics.* 2003; May 257(1-2): 141-151.
- 72 Wang Y, Challa P, Epstein DL, Yuan F. Controlled release of ethacrynic acid from poly(lactide-co-glycolide) films for glaucoma treatment. *Biomaterials.* 2004, Aug 25(18): 4279-4285.
- 73 Cunanan CH, Tarboux NM, Knight PM. Surface properties of intraocular lens materials and their influence on in vitro cell adhesion. *J Cataract Refract Surg.* 1991; 17(6): 767-773.
- 74 Popov SG, Villasmil R, Bernardi J, Grene E, Cardwell J, Popova T, Wu A, Alibek D, Bailey C, Alibek K. Effect of Bacillus anthracis lethal toxin on human peripheral blood mononuclear cells. *FEBS Letters, Volume 527, Issues 1-3, 11 September 2002; 211-215.*
- 75 Veva De Groot MD, Marie-José BR Tassignon MD, Gijs F.J.M. Vrensen. Effect of bag-in-the-lens implantation on posterior capsule opacification in human donor eyes and rabbit eyes. *Journal of Cataract & Refractive Surgery.* 2005; 31(2): 398-405.

- 76 Nishi O, Nishi K, Osakabe Y. Evaluation of posterior capsule opacification using a new posterior view method in rabbits. Single-piece acrylic versus 3-piece acrylic intraocular lens. *J Cataract Refract Surgery*. 2005; 31: 2369-2374.
- 77 Conroy S, Loh IH. Lubricious Coatings for Medical Devices. *Drug Delivery Systems and Sciences*. 2004, 3 (4); 89-92.
- 78 Jansen B, et al. Bacterial Adherence to Hydrophilic Polymer Coated Polyurethane Stent. *Gastro Endo*. 1993; 39: 670-673.
- 79 Swain E. Coatings: The Next Generation. *Med Dev & Diag Ind*. July 2004; 14-16.
- 80 Hoekstra D. Hyaluronan Modified Surfaces for Medical Devices. *Med Dev & Diag Ind*. Feb 1999, 28-30.

BIOGRAPHICAL INFORMATION

Brett Thomes performed his undergraduate work in Chemistry at Midwestern State University. He then obtained his Master's degree in Biomedical Engineering at the University of Texas at Arlington. He worked under the guidance and leadership of Dr. Robert Eberhart and Dr. Richard Timmons where he studied the influence of surface chemistry and surface roughness on biologic responses, specifically protein adsorption. His research received several honors including the Whitaker Foundation 1st Place Research Award at the Biomedical Engineering Conference (San Antonio, TX) and the Whitaker Foundation Excellence in Research Award at the Society for Biomaterials Conference (San Diego, CA). He then accepted a position within the medical device industry and continued to pursue a doctoral degree. His current interests are focused on ocular drug delivery systems to combat diseases located in the back of the eye. In collaboration with Alcon Laboratories he has proposed several patents related to ocular deliver drug systems.